

THE *CAENORHABDITIS ELEGANS* HOMOLOGUE OF HUNTINGTIN
INTERACTING PROTEIN 1 HAS MULTIPLE ROLES IN DEVELOPMENT

by

JODEY ALEXANDER PARKER

B. Sc., University of British Columbia in Association with the
University-College of the Cariboo, 1994

A THESIS SUBMITTED IN PARTIAL FULFILLMENT OF
THE REQUIREMENTS FOR THE DEGREE OF
DOCTOR OF PHILOSOPHY

in

THE FACULTY OF GRADUATE STUDIES

Department of Medical Genetics

Genetics Graduate Program

We accept this thesis as conforming
to the required standards

THE UNIVERSITY OF BRITISH COLUMBIA

March 2001

© Jodey Alexander Parker, 2001

In presenting this thesis in partial fulfilment of the requirements for an advanced degree at the University of British Columbia, I agree that the Library shall make it freely available for reference and study. I further agree that permission for extensive copying of this thesis for scholarly purposes may be granted by the head of my department or by his or her representatives. It is understood that copying or publication of this thesis for financial gain shall not be allowed without my written permission.

Department of Medical Genetics

The University of British Columbia
Vancouver, Canada

Date 7th of March, 2001

Abstract

Endocytosis is an essential process in all eukaryotes and is involved in biological processes such as nutrient uptake and neurotransmitter recycling. Mammalian cell culture and yeast genetic studies have implicated the *HIP1/SLA2* family of genes in linking the actin cytoskeleton to endocytosis. The contribution of the cytoskeleton to endocytic events is not well understood. Human *HIP1* is of medical importance as it has been shown to interact with huntingtin, and may be important to the etiology of Huntington disease. Analysis of this family of genes in a metazoan animal system, such as *C. elegans* or *Drosophila* is an area that has been largely unexplored. As endocytosis is a mechanism by which cells interact with their environments, the use of an animal system may be particularly informative as it may illustrate differences between unicellular and multicellular systems.

Through a combination of gene disruption and molecular characterization techniques, I have studied the function of *CeHIP1*, the *C. elegans* member of the *HIP1/SLA2* gene family. *CeHIP1* displays postembryonic, tissue-specific expression, and has several functions in the adult animal. *CeHIP1* has a role in maintaining proper morphology and function of the pharynx, the nematode feeding structure. *CeHIP1* is required for promoting fertilization; gene silencing results in reduced fecundity. The locus is dose sensitive. *CeHIP1* is haploinsufficient, and overexpression results in reduced viability and death of the animals.

C. elegans is an excellent model to interpret the function of the human homolog *HIP1*. Both *CeHIP1* and *HIP1* show restricted expression and display dose sensitive toxic effects, inferring a shared mode of action. This thesis describes the establishment of a simple animal model that may be used to delineate pathways common to both genes. These findings may reflect the situation in humans, and perhaps point out avenues of potential treatment for Huntington disease.

Table of Contents

Abstract	ii
Table of contents	iii
List of tables	viii
List of figures	ix
Dedication	xi
Acknowledgements	xii
Chapter I Introduction	1
1.1 <i>C. elegans</i> as a Model Animal System	1
1.1.1 The <i>C. elegans</i> Sequencing Projects	1
1.2 Huntington Disease, HIP1 and <i>C. elegans</i>	3
1.2.1 Huntington Disease	3
1.2.2 Significant Background <i>HIP1</i> , <i>SLA2</i> and <i>CeHIP1</i>	6
1.2.3 Yeast <i>SLA2</i>	7
1.2.4 Human <i>HIP1</i> and Mouse <i>HIP1R</i>	10
1.2.5 The Actin Cytoskeleton and Endocytosis	12
1.3 Forward and Reverse Genetics in <i>C. elegans</i>	15
1.4 Functional Approaches to Study <i>CeHIP1</i>	21
Chapter II Methods and Materials	22
2.1 Foreword	22
2.2 Nematode Strains and Culture Conditions	22
2.2.1 Transgenic Strains	22
2.2.2 Integration of Transgenic Arrays	23
2.3 Microscopy	23
2.4 Preparation of Cloned DNA	24
2.4.1 Plasmid and Cosmid Isolation from Bacteria	24
2.4.2 Plasmid isolation from <i>Saccharomyces cerevisiae</i>	24
2.5 Transformation	25

2.5.1 <i>E. coli</i> DH5 α	25
2.5.2 <i>E. coli</i> SURE cells	26
2.5.3 <i>E. coli</i> DH10B	26
2.5.4 <i>S. cerevisiae</i> Y190	27
2.5.4.1 Yeast Selection	28
2.6 DNA Sequencing	29
2.7 Electrophoresis	30
2.7.1 Agarose Gel Electrophoresis	30
2.7.2 Polyacrylamide Gel Electrophoresis	30
2.8 DNA Analysis	32
2.9 Polymerase Chain Reaction	32
2.10 Restriction Digests	32
2.11 Subcloning	33
2.11.1 Cloning of the <i>CeHIP1</i> cDNA	33
2.11.1.1 Preparing cDNA Clones	33
2.11.1.2 Cloning the Full Length <i>CeHIP1</i> cDNA	35
2.11.2 Construction of <i>CeHIP1</i> ::GFP Reporter	35
2.11.3 <i>CeHIP1</i> ::GST Fusion Protein	37
2.11.4 <i>CeHIP1</i> Overexpression Construct	37
2.11.5 RNA Interference Constructs	40
2.11.6 Yeast Two-Hybrid Constructs	40
2.12 PCR Mapping of Deficiencies	44
2.12.1 Preparation of Template DNA from Embryos	44
2.12.2 PCR Mapping of Deficiency Homozygotes	45
2.13 Site Selected Mutagenesis Screen	46
2.13.1 Growth and Synchronization for Mutagenesis	46
2.13.2 Mutagenesis	47
2.13.3 Library Plating	47
2.13.4 Library Harvest	48
2.13.5 PCR Screening	48
2.13.6 Identification of Deletion Candidates and Sib-Selection	49

2.13.7 Sib-Selection	50
2.14 RT-PCR	50
2.15 Protein Work	51
2.15.1 Expression and Protein Purification of CeHIP1	51
2.15.2 Antibody Production	52
2.15.3 Western Analysis	52
2.15.4 Immunocytochemistry	54
2.15.4.1 Whole Worm Fixation	54
2.15.4.2 Staining	56
2.15.4.3 Mounting	56
2.15.5 Dissection and Staining of Gonads	57
2.15.5.1 Gonad Dissection	57
2.15.5.2 Gonad Fixation	57
2.15.5.3 Antibody Staining of Dissected Gonads	58
2.15.5.4 Mounting	58
2.16 Overexpression Analysis	59
2.17 RNA Interference	60
2.17.1 RNAi Clones for <i>in vitro</i> Transcription	60
2.17.2 Preparation of Double Stranded RNA for Injection and Soaking	60
2.17.3 Injection of dsRNA	61
2.17.4 Soaking Animals with dsRNA	61
2.17.5 <i>in vivo</i> RNA Interference	62
2.17.6 Outcrossing of RNAi Animals	62
2.18 Yeast Two-Hybrid Analysis	63
2.19 Yeast Two-Hybrid Screen	63
Chapter III Results	65
3.1 CeHIP1 Gene Structure	65
3.2 Homology Studies	67
3.3 Expression of <i>CeHIP1</i>	77
3.3.1 RT-PCR	77

3.3.2 GFP Reporter	77
3.4 Protein Localization of CeHIP1	78
3.5 PCR Mapping of Deficiencies	83
3.6 Reverse Genetic Screen	91
3.7 Overexpression Analysis	91
3.8 RNA Interference Analysis	98
3.8.1 Fertilization Effects	101
3.8.2 Egg Laying Deficiency Observed after <i>CeHIP1</i> RNAi	106
3.8.3 CeHIP1 RNAi Deforms the Mature Pharynx	107
3.9 Testing for CeHIP1 Interaction with Human Huntingtin	113
3.10 Yeast Two-Hybrid Screen	113
3.10.1 Mutants Obtained	116
Chapter IV Discussion	117
4.1 Introduction	117
4.2 <i>CeHIP1</i> and the Nematode	117
4.2.1 <i>CeHIP1</i> and Fertilization	118
4.2.1.1 Anatomy of the Adult Gonad	118
4.2.1.2 The Spermatheca	120
4.2.1.3 Fertilization Errors	122
4.2.1.4 Receptor Mediated Endocytosis in the Oocyte	123
4.2.1.5 Sperm Depletion	124
4.2.1.6 Outcrossing Rescues the RNAi Phenotype; Therefore, Not a Sperm Defect	125
4.2.1.7 <i>CeHIP1</i> Promotes Fertilization in <i>C. elegans</i>	129
4.2.2 Egg Laying and <i>CeHIP1</i>	130
4.2.3 The Role of CeHIP1 in Pharynx Development and Function	132
4.2.3.1 CeHIP1 and the Cytoskeleton	134
4.2.3.2 Endocytosis and Pharynx Function	136
4.3 <i>CeHIP1</i> , A Dose Sensitive Gene?	138
4.3.1 <i>CeHIP1</i> and Haploinsufficiency	138

4.3.2 Overexpression of <i>CeHIP1</i>	139
4.4 <i>CeHIP1</i> and Interacting Proteins	141
4.4.1 Yeast Two-Hybrid Screen	141
4.4.1.1 T05C12.10 and <i>C. elegans</i> Hedgehog-Like Genes	141
4.4.1.2 F45E12.2 and RNA Turnover in <i>C. elegans</i>	144
4.5 Is <i>CeHIP1</i> the nematode homologue of human <i>HIP1</i> ?.....	145
4.6 Conclusion	146
4.7 Model	148
Bibliography	150

List of Tables

Table 3.1 Summation of Pairwise Sequence Alignment	73
Table 3.2 PCR Deficiency Mapping Data	93
Table 3.3 Comparison of RNA Interference Methods; Injection, Soaking and <i>in vivo</i>	102
Table 3.4 Outcrossing of CeHIP1 RNAi Hermaphrodites	103
Table 3.5 Additional Phenotypes of CeHIP1 RNAi	108

List of Figures

Figure 2.1 Cloning of pCeh350, pCeh351, and pCeh352	36
Figure 2.2 Cloning of the <i>CeHIP1</i> ::GFP Reporter Construct pCeh353.....	38
Figure 2.3 Cloning of the <i>CeHIP1</i> ::GST Fusion Construct pCeh365.....	39
Figure 2.4 Cloning of the RNAi Construct pCeh389	41
Figure 2.5 Construction of Clones for Yeast Two-Hybrid Mapping	43
Figure 3.1 <i>CeHIP1</i> Gene Structure	66
Figure 3.2 Predicted Protein Structure of CeHIP1	68
Figure 3.3 Predicted Hydrophobicity of CeHIP1	69
Figure 3.4 Stage Specific Expression of <i>CeHIP1</i>	70
Figure 3.5 Pairwise Sequence Alignment of CeHIP1 and Homologs	71-72
Figure 3.6 Predicted Coiled-Coil Domains	75
Figure 3.7 Pairwise Sequence Alignment of CeHIP1 and F08A8.6	76
Figure 3.8 The <i>C. elegans</i> Hermaphrodite Gonad	79
Figure 3.9 The <i>C. elegans</i> Male Gonad	80
Figure 3.10 <i>CeHIP1</i> Expression	81-82
Figure 3.11 Detection of CeHIP1 Protein	84
Figure 3.12 CeHIP1 Protein Localization in Developing Embryos	85-86
Figure 3.13 CeHIP1 Protein Localization in the Adult Hermaphrodite	87-88
Figure 3.14 CeHIP1 Protein Localization in the Adult Hermaphrodite and Male Gonad	89-90
Figure 3.15 Map of Deficiency Breakpoints in Relation to CeHIP1	92
Figure 3.16 PCR Mapping of <i>sDf110</i>	94
Figure 3.17 PCR Mapping of <i>nDf17</i>	94
Figure 3.18 PCR Mapping of <i>nDf20</i>	95
Figure 3.19 PCR Mapping of <i>nDf21</i>	95
Figure 3.20 PCR Mapping of <i>hDf21</i>	96
Figure 3.21 Reverse Genetic Screen Deletions	97
Figure 3.22 Overexpression of <i>CeHIP1</i>	99-100

Figure 3.23 The Effect of RNAi on CeHIP1 Protein	
Localization in the Gonad	104-105
Figure 3.24 The Effect of RNAi on Egg Laying	109-110
Figure 3.25 RNAi Effects on Pharyngeal Morphology	111-112
Figure 3.26 Two-Hybrid Analysis	114
Figure 3.27 Two-Hybrid Screen Positives	114
Figure 3.28 Mapping of the Two-Hybrid Interaction	115
Figure 3.29 Mapping of the Two-Hybrid Interaction	115
Figure 4.1 Depletion of CeHIP1 from the Gonad Results in the	
Production of Unfertilized Oocytes	127-129

Dedication

For my father, Robert L. Parker.

Acknowledgements

I wish to extend my gratitude to a number of people. Foremost, I thank Dr. Ann M. Rose for opening a door into a rich and rewarding world. Thank you for the opportunity to work with you in your laboratory. I thank my thesis committee, Dr. Peter Candido, Dr. Phil Hieter, and Dr. Steve Wood for keeping me on the right track once through the door. I would like to extend additional thanks to Dr. Steve Wood for the opportunity to teach as well as learn. I wish to thank Dr. Colin Thacker for a great many things, but mainly for his magnanimity and patience. I thank the members of the Rose laboratory, past and present for their support. I would like to extend thanks to Dr. Mairi MacKay for the opportunity to try things I had only read about. To my family, I extend thanks for their love and understanding. Lastly, I thank Leah DeBella. Thank you for the generosity, love and honesty you gave. My work was supported in part by a UBC Graduate Fellowship and the UCC Robert Frazier Memorial Fellowship.

Chapter I

Introduction

1.1 *C. elegans* as a Model Animal System

The *C. elegans* system has proven to be an amenable and successful model to study many aspects of biology. The nematode is a free living, self-fertilizing hermaphrodite, which can be easily grown and maintained in a laboratory setting (Brenner, 1974). The great power of the nematode system is its potential for genetic analysis, in part due to its rapid (3-day) life cycle, and small size (reviewed in Riddle, 1997). Additionally, the natural mode of *C. elegans* inbreeding by the self-fertilizing hermaphrodite, combined with the ability to cross hermaphrodites with males offers great advantages, as selfing or crossing can be manipulated at will. The animal's simple anatomy, transparent body, constancy in cell number and cell position has added to its usefulness as a model system. The complete cell lineage is known (Sulston and Horvitz, 1977) and the complete structure of the nervous system has been determined through serial section electron microscopy (White et al., 1986). Mutations in genes involved in virtually all aspects of development are allowing for the molecular genetic analysis of these processes at a very fine level.

1.1.1 The *C. elegans* Sequencing Projects

C. elegans is unique among animal systems as essentially its entire genome has been cloned into cosmid and yeast artificial chromosome contigs constituting the physical map of the genome (Coulson, 1988; Coulson, 1991; Coulson, 1995). The physical map

has been correlated with the genetic map at points where genetic loci have been cloned and ordered in relation to overlapping cosmids (Janke et al., 1997).

This resource allowed for an inquiry into the feasibility of obtaining the complete genomic sequence. The early success of the initial sequencing efforts led to the completion of the entire genomic sequence in 1998 (Consortium, 1998; Sulston et al., 1992; Wilson et al., 1994).

Examination of the sequence reveals that 42% of the predicted protein coding genes have matches outside of Nematoda. 36% of the predicted genes in *C. elegans* have significant matches in humans, including many genes involved in human disease. The acquisition of a sequenced genome has provided researchers with new opportunities. Researchers can peer into the *C. elegans* genome to find genes of particular interest to their studies. *C. elegans* offers an attractive place in which to study evolutionary conserved genes in a simple eukaryotic system (Consortium, 1998).

Comparative genomic approaches and multi-organism biology are valuable tools for genetic analysis. Connections across species between genes mutated in human disease states, and homologs in model organisms can be particularly powerful, as model organism gene function data and experimental approaches can help reveal the molecular mechanisms defective in disease (Bassett et al., 1997; Clark et al., 1999; Ploger et al., 2000). Such approaches have already proven informative for a number of human diseases. Studies of the *S. cerevisiae* *MEC1* and *TEL1* genes, for example have provided valuable insight into the function of the human *ATM* gene, (mutated in ataxia telangiectasia, Morrow et al., 1995). Both *C. elegans* and *Drosophila* have been used as models for the polyglutamine mediated neurodegeneration observed in a group of human

diseases including Huntington disease and the spinocerebellar ataxias (Faber, 1999; HDCRG., 1993; Kawaguchi et al., 1994; Satyal et al., 2000; Warrick et al., 1998; Warrick et al., 1999). Model organisms have made numerous contributions to the field of human disease research. As more of the human genome is sequenced and studied, the call upon the model organisms to generate insights will be even greater.

1.2 Huntington Disease, HIP1 and *C. elegans*

1.2.1 Huntington Disease

Huntington's chorea is one of a group of human neurodegenerative diseases caused by nucleotide triplet repeat expansion within the protein coding region of the gene (Andrew et al., 1997; Reddy et al., 1997; Ross et al., 1997). These diseases share the feature of a normal, non-pathological range of repeats, with the disease manifesting if the repeat expands above the normal range. Typically, this results in specific neuronal degeneration. It is probable that these diseases share a common pathological mechanism at the protein level. The expansion confers a dominant, toxic phenotype to these proteins. The larger the repeat, the more severe the disease, and the earlier the age of onset over successive generations. This phenomenon is called anticipation. Several investigations suggest that it is the expanded polyglutamine tract itself causing neurodegeneration. The introduction of polyglutamine tracts has been shown to cause neurodegeneration in transgenic mice, and cell death in transfected cells (Davies et al., 1997; Ikeda et al., 1996; Mangiarini et al., 1996; Paulson et al., 2000; Saudou et al., 1998).

Neuronal nuclear inclusions have recently been identified as a unifying feature in the pathology of all of these disease (Ross, 1997). Currently, it is unclear if the nuclear

inclusions cause the disease or are a component of the disease process (Sisodia et al., 1998). The inclusions are found preferentially in susceptible neurons and are linked to disease progression. A study of brains from HD patients reveals the presence of fibrils within the nuclear inclusion consistent with amyloid-like fibrils (DiFiglia et al., 1997). Individually introduced expanded polyglutamine repeats have been found to form insoluble amyloid-like fibrils as well. It is suggested that the aggregation of expanded polyglutamine repeats is the underlying cause of neurodegeneration in these diseases and the nucleus may be the primary site of action (Saudou et al., 1998; Sisodia et al., 1998).

However, these groups of diseases display an overlapping, yet distinct pattern of neuronal degeneration. Selective neuronal degeneration occurs despite the fact that the disease proteins are expressed widely in the brain, and throughout the body (Reddy and Housman, 1997; Ross, 1997). Additional factors may contribute to cell specific pathology. Interaction with a subset of proteins, which are temporally and/or spatially restricted, may confer cellular specificity (Matilla et al., 1997).

Indeed, recent investigations have shown the presence of nuclear inclusions is not sufficient to cause cell degeneration (Saudou et al., 1998; Warrick et al., 1999). Different cell types inherently differ in their sensitivity to the presence of expanded polyglutamine tracts. Again, this suggests that additional genes may be involved.

Several investigators have proposed that HD is caused by a toxic gain-of-function attributable to an abnormal protein-protein interaction modulated by the expanded polyglutamine tract (Barinaga et al., 1996; Ona et al., 1999; Saudou et al., 1998). Thus, the binding of distinct proteins to the expanded polyglutamine sequence could either bestow a new function on huntingtin, or alter its normal interactions with other proteins.

It is possible that the binding of a specific complement of proteins particular to certain cell types could confer a selective vulnerability to the effects of mutant huntingtin (Kalchman et al., 1997; Wanker et al., 1997).

Two groups have independently identified a protein that interacts with huntingtin (Kalchman et al., 1997; Wanker et al., 1997). The protein, designated HIP1, for **H**untingtin **I**nteracting **P**rotein **1**, shows considerable sequence identity to Sla2p, the gene product of *SLA2* (**S**ynthetic **L**ethal with **A**ctin binding protein 1 #**2**) in *Saccharomyces cerevisiae* (Holtzman, 1993). In *S. cerevisiae* Sla2p is known to be essential for the assembly and function of the cortical cytoskeleton (Li et al., 1995; Yang et al., 1999). HIP1 also shares significant identity with the protein encoded by the gene CeHIP1 of *Caenorhabditis elegans* (figure 3.5). A related gene has been isolated from mouse, mHIP1R (**M**ouse **H**IP1 **R**elated) and has been implicated in clathrin coated pit endocytic events in addition to its cytoskeletal role (Engqvist-Goldstein, 2000; Seki, 1998).

Immunohistochemistry, electron microscopy, and subcellular fractionations have demonstrated that huntingtin is primarily a cytoplasmic protein associated with vesicles and/or microtubules (Velier et al., 1998; Wood et al., 1996). This suggests that that it may be involved in cytoskeletal anchoring, transport of mitochondria, vesicles or other organelles in the cell.

HIP1 is enriched in the central nervous system where it colocalizes with the membrane fractions of human brain cells. An important observation is that the expanded polyglutamine tract disrupts the interaction between huntingtin and HIP1 . The restricted expression of *HIP1*, along with its localization pattern, limits its interaction with huntingtin to the central nervous system, and specifically, to the membrane. This

interaction, along with HIP1's homology to Sla2p and CeHIP1 suggests that the huntingtin-HIP1 interaction may be essential for the normal function of membrane cytoskeleton of brain cells (Kalchman et al., 1997). Additionally, the role of HIP1, and homologues, may be evolutionary conserved and important to all eukaryotes.

1.2.2 Significant Background *HIP1*, *SLA2* and *CeHIP1*

CeHIP1 is a member of a growing family of genes that includes human *HIP1*, human and mouse *HIP1R*, yeast *SLA2*, and the putative *Drosophila* protein CG10972 (Adams et al., 2000; Holtzman et al., 1993; Kalchman et al., 1997; Seki et al., 1998). These proteins show identity to one another, and they share a similar arrangement of three predicted coiled-coil regions, as well as a C-terminal region similar to the C-terminus of the mammalian membrane associated protein talin (Hemmings, 1996; Yang et al., 1999). Talin contains at least three actin binding domains, one of which, amino acids 2269-2541, shares homology to a domain possessed by the family of CeHIP1 related proteins (Hemmings et al., 1996). This domain is an F-actin binding motif, the I/LWEQ module and has been shown to bind filamentous actin *in vitro* (McCann and Craig, 1997). Analysis of these genes in their respective systems has outlined a role for this family.

CeHIP1 and homologs possess another motif, the ENTH (Epsin N-terminal homology) domain (Kay, 1999). This protein segment of approximately 140 amino acids, usually starting within the first 20 residues of the protein has been found in all eukaryotes. Although many of the proteins with this sequence share little homology

outside of the ENTH domain, many of the proteins are involved in endocytosis and/or regulation of cytoskeletal organization (Kay, 1999).

The rat protein Epsin is known to bind to the EH (Eps15 Homology) domains of Eps15, a substrate for the epidermal growth factor tyrosine kinase with three EH domains (Tebar et al., 1996). Eps15 is involved in clathrin-mediated endocytosis. Eps15 localization has been observed in nerve terminals where clathrin-mediated endocytosis of synaptic vesicles takes place (Benmerah et al., 1998; Chen et al., 1998). Thus, proteins with an ENTH domain have been placed amongst the milieu of proteins involved in clathrin-mediated endocytic events.

1.2.3 Yeast *SLA2*

Studies in yeast have shown that *SLA2* is essential for correct organization of the cortical actin cytoskeleton (Holtzman et al., 1993). *SLA2* (also known as *END4* and *MOP2*) is also required for endocytosis and the accumulation and maintenance of a plasma membrane ATPase at the cell surface (Na et al., 1995; Raths et al., 1993). Yeast cells lacking Sla2p display a temperature sensitive growth defect, being unable to grow at higher temperatures (Yang et al., 1999). The cells exhibit a disorganized actin cytoskeleton, their cell surface is disorganized and their cell surface growth is depolarized (Holtzman et al., 1993; Yang et al., 1999). Normally, cortical actin patches are spatially restricted to growing domains within the cell cortex. *SLA2* null mutants no longer show this, instead actin patches are distributed evenly across the surface of the mother and the bud. Lastly, *SLA2* mutants accumulate post-Golgi vesicles, possess an abnormally thick cell wall, and do not undergo the wild-type bipolar budding pattern.

Many of these defects are observed in mutants affecting the cortical actin cytoskeleton (Holtzman et al., 1993; Na et al., 1995; Raths et al., 1993).

Deletion mutations of *SLA2* are synthetically lethal with null alleles of several genes encoding components of the cortical actin cytoskeleton, *ABP1*, *SRV2*, *SAC6*, and *GCSI*. *ABP1* encodes a protein containing a C-terminal Src homology 3 domain and an N-terminal ADF homology domain (Drubin et al., 1988; Lappalainen et al., 1997). *SRV2* codes for a protein that binds to actin monomers as well as to adenylyl cyclase, a component of the Yeast Ras signaling pathway (Lila et al., 1997). *SAC6* encodes the actin filament-bundling protein fimbrin (Holtzman et al., 1993). *GCSI* is a GTPase-activating protein for Arf proteins in yeast that appear to have a direct effect on actin dynamics (Blade et al., 1999). The interactions of these genes suggest that Abp1p, Gcs1p, Sla2p, Sac6p, and Srv2p promote cytoskeletal dynamics (Yang et al., 1999).

Sla2p is a component of the cortical actin cytoskeleton. Sla2p localizes to a subset of cortical actin patches, as well as to cortical patches that are free of actin. This pattern is in contrast to other actin binding proteins, such as Abp1p or cofilin, which are present in all actin patches, but absent from patches devoid of actin. Additionally, treatment of cells with the actin depolymerizing drug latrunculin A (latA) displayed a cytoplasmic distribution of Abp1p and cofilin, while Sla2p maintained cortical localization, and exhibited correct polarization in ~ 20% of the treated cells. These data suggest that Sla2p distribution is not wholly dependent on the F-actin binding domain (Yang et al., 1999).

The introduction of different *SLA2* deletion mutants into a null background has outlined a role for distinct regions of the protein. Sla2p appears to have a high level of

redundancy. N or C terminal deletions (separate, not both) of Sla2p do not greatly perturb functional activity, as localization to cortical patches is maintained. Both the N- and C-terminal domains of Sla2p contain a cortical patch localization signal, and it is likely this localization is responsible for viability. Additionally, the N-terminus of Sla2p, containing the ENTH domain, appears to localize to the cortex independently of actin. This domain displays cortical localization in cells lacking filamentous actin (Yang et al., 1999). Sla2p deletion mutants lacking the central coiled-coil domain exhibited no functional activity; the cytoskeleton was disorganized, but Sla2p was still localized at the periphery. The central coiled-coil domain is thought to bind other proteins and is believed to mediate Sla2p dimerization (Lupas, 1991; Yang et al., 1999). There is evidence for Sla2p existing in the cytoplasm in an inactive state, and through a series of unidentified signals activates Sla2p and promotes its localization to the cortex (Yang et al., 1999).

It is worth noting that overexpression of the Sla2p talin-like domain results in death in *SLA2* deletion cells. The cells display a disorganized cytoskeleton, and the filamentous actin of the cell appears to form large, cable-like structures (Yang et al., 1999). This may represent a titration of available filamentous actin to the F-actin binding module of Sla2p.

This data sketches a complex cellular role for Sla2p; it has many functions in maintaining cortical actin cytoskeleton dynamics and when Sla2p is perturbed, the result is one of numerous defects to cell functioning.

1.2.4 Human *HIP1* and Mouse *HIP1R*

Work from higher animal systems has suggested additional functions for the Sla2p related proteins. HIP1 was initially identified as a protein that interacted with human huntingtin. The strength of the interaction is inversely related to the size of the polymorphic polyglutamine tract of huntingtin. Thus, mutant huntingtin with a large polyglutamine repeat (greater than 35 repeats) interacts weakly with HIP1. The conserved central putative coiled coil domain of HIP1 mediates this interaction (Kalchman et al., 1997).

Thus, a model linking polyglutamine length, the pathogenesis of HD, and the interaction of huntingtin with HIP1 requires that their association be crucial for normal cellular function. Theoretically, the altered association of huntingtin with HIP1, as effected through the increased polyglutamine tracts, could lead to a disruption of biochemical events at the membrane causing premature cell death, and ultimately the clinical manifestations of HD (Kalchman et al., 1997).

The function of HIP1 is unknown, but its characterization has shown that it is enriched in the central nervous system and testes. HIP1 shows overlap with the areas of the brain that undergo neurodegeneration in HD (Kalchman et al., 1997).

The identification of related gene products, HIP1R, and mouse HIP1 Related (mHIP1R), has led to the discovery of a link between the actin cytoskeleton and components of the endocytic machinery (Engqvist-Goldstein et al., 2000; Seki et al., 1998). mHIP1R can bind F-actin *in vitro* and colocalizes with F-actin *in vivo*, and this interaction is mediated through the I/LWEQ module. mHIP1R shows punctate immunolocalization and is enriched at the cell cortex and in the perinuclear region

(Engqvist-Goldstein, 2000). Additionally, mHIP1R colocalizes with markers for receptor-mediated endocytosis. First, mHIP1R is observed to colocalize with the coat protein clathrin, which is involved in budding of vesicles from the plasma membrane and the *trans* Golgi network (Hirst, 1998). mHIP1R and clathrin showed a similar subcellular distribution and were enriched at the cortex and perinuclear region. Colocalization was also observed for mHIP1R and the adaptor protein AP2, which is involved in budding from the plasma membrane during clathrin-mediated endocytosis (Hirst, 1998). The two proteins could be observed at the cell cortex, but AP-2 was absent from the perinuclear region. The last marker tested was transferrin, a component of endocytic vesicles (Hirst, 1998). mHIP1R colocalized with transferrin in early endocytic compartments.

The colocalization of mHIP1R with components of the endocytic machinery is dependent on the N-terminal region, containing the ENTH domain, and the central coiled-coil domain. Expression of either the N-terminal or the central coiled-coil domain alone resulted in cytosolic, non-vesicular staining. Expression of constructs containing the talin-like domain with either the N-terminal or the central coiled-coil region resulted in colocalization with F-actin (Engqvist-Goldstein et al., 2000).

1.2.5 The Actin Cytoskeleton and Endocytosis

Thus, from studies of this gene family, a network of physical and genetic interactions involving cortical patch proteins, kinases and components of clathrin-coated pit endocytosis is beginning to emerge.

Both receptor-bound ligands and extracellular fluid enter animal cells through clathrin-coated pits (Mellman, 1996). The clathrin cage is composed of clathrin heavy and light chains and forms repeated triskelions that self-assemble into planar lattices. This structure is associated with clathrin adaptor complexes called AP2, which are associated with clustered transmembrane receptors. The planar lattices are thought to round up to form pits, which pinch off to form coated vesicles (Hirst, 1998). Dynamin, another pit-associated protein, is required for pinching off clathrin-coated vesicles from the plasma membrane (de Camilli et al., 1995).

A combination of mammalian biochemistry and yeast genetics has furthered our understanding of endocytic trafficking (Rothman et al., 1996; Schekman et al., 1996). Endocytosis has been extensively studied through biochemical methods, mostly using physical association and copurification techniques (Mellman, 1996). Progress has been made using *in vitro* functional assays, such as early endosome fusion, but many parts of the pathway have not been reconstituted (Mukherjee et al., 1997). Genetic analysis, mainly from yeast, has made important contributions to the understanding of endocytosis, including the identification of connections between the endocytic pathway and the actin cytoskeleton (Drubin et al., 1988; Engqvist-Goldstein et al., 2000; Wendland et al., 1998; Yang et al., 1999). Genetic analysis in metazoan animals such as *C. elegans* and *Drosophila* has not been explored fully as of yet. As endocytosis is a mechanism that

allows a cell to interact with its environment, important aspects of endocytosis may differ between unicellular and multicellular organisms. One example is lipoprotein uptake, such as LDL or yolk endocytosis, which is an adaptation required for nutrient uptake and cellular homeostasis within multicellular organisms (Grant et al., 1999). Additional examples include growth factor receptor regulation during development, synaptic vesicle recycling in the nervous system, and antigen processing in the immune system (Mellman, 1996).

Genetic analysis in *Drosophila* and *C. elegans* has provided insights into endocytic events. The *Drosophila* dynamin homologue *shibire* mutants, which were originally identified because of their generally impaired nervous system, demonstrated the importance of dynamin in pinching off clathrin-coated vesicles (de Camilli et al., 1995). Likewise, the study of general synaptic function genetically in *C. elegans* led to the discovery of the role of synaptotagmin in synaptic vesicle recycling (Jorgensen et al., 1995; Nonet et al., 1993). Most recently, a role for rme-2 (receptor mediated endocytosis), a member of the LDL receptor superfamily in receptor mediated endocytosis has been outlined for yolk uptake in the *C. elegans* oocyte (Grant et al., 1999).

The contribution of the actin cytoskeleton, and accessory proteins to endocytosis is not known. There are numerous steps at which one can envisage their participation. The cytoskeletal components may localize the endocytic machinery to areas of the plasma membrane by physically restraining the machinery, or by directly associating with the components. The actin cytoskeleton may deform or invaginate the plasma membrane, which would aid the endocytic machinery in pinching off the plasma membrane

(Qualmann et al., 2000). Alternatively, the cortical cytoskeleton may need to be removed to allow endocytosis to proceed. The actin cytoskeleton is a rigid structure that inhibits membrane traffic, which could be overcome by localized actin turnover (Trifaro, 1993). The cytoskeleton may help drive detached endocytic vesicles through the cytoplasm, a theory supported by the visualization of various vesicle structures with actin comet tails (Merrifield et al., 1999).

Thus, there are numerous ways in which the cytoskeleton could participate in endocytosis. The cytoskeletal contributions need not be mutually exclusive, or be common to all cell types and participate in all forms of vesicle formation (Qualmann et al., 2000).

mHIP1R has been shown to colocalize with components of the endocytic machinery (clathrin and AP2) and has been shown to bind F-actin. Thus, mHIP1R may represent a link between F-actin and clathrin-coated endocytic structures. This may promote proper spatial organization of endocytosis, or actin dependent movement of newly formed vesicles, or both. (Qualmann et al., 2000). Perhaps CeHIP1 is involved in this process.

Further understanding into the role of *HIP1* in the normal and disease states in mammalian cells can be derived from studies of its yeast homologue, *SLA2*, its *C. elegans* homolog, *CeHIP1*, and from the mouse *mHIP1R*. Although the yeast and cell culture systems are excellent in which to study the respective gene's cellular function, *C. elegans* could provide insights into its potential developmental and tissue specificity. Even though the cell biology of the *CeHIP1* family of genes is likely to be conserved, *CeHIP1*'s role may be dependent on when and where it is found in the developing animal.

Huntingtin has been shown to be essential for development in mice as the mouse huntingtin knockout is embryonic lethal, and is required through adulthood (Dragatsis et al., 2000; Nasir et al., 1995). Thus, it is suggested that *HIP1* may have a developmental role as well. Developmental questions are well suited to the *C. elegans* system, where several important issues can be addressed. What is the null mutation of *CeHIP1*? At what time, and where in development is the gene expressed? What interacting partners exist for CeHIP1?

I have used a combination of gene disruption and molecular characterization techniques to study the role of *CeHIP1* in the context of animal development. This approach has allowed for an examination of *CeHIP1*'s role in the nematode. This, in conjunction with the cellular and molecular findings from the aforementioned studies has allowed for a description of the function of *CeHIP1* in a simple animal system. This approach has implicated yet more unanticipated pathways, and may provide insights into the etiology of Huntington disease.

1.3 Forward and Reverse Genetics in *C. elegans*

Genetic research can be thought to be of two schools, forward and reverse genetics. The directionality refers to whether one is moving from a phenotype to an associated sequence (forward) or from a sequence to an associated phenotype (reverse). Classical or forward genetics requires no prior knowledge of the gene or the gene product. It relies on the identification of genes based on phenotype. The phenotype can then be mapped and sequence correlated to it. The development of the second approach was contingent on the advent of sequencing technologies and the growing amounts of

sequence made available by the genomic and cDNA sequencing projects. Reverse genetics moves from a sequence of interest to the production of a mutant phenotype associated with said sequence.

Forward genetic approaches laid the groundwork, demonstrating that specific sequence could give rise to a certain phenotype. The sequencing projects then demonstrated that there exist many sequences that are similar to well characterized genes, but had no mutants associated with them. Thus there has been a strong need to develop technologies that will allow one to proceed from sequence to phenotype. Both forward and reverse genetic procedures are available to researchers; the usage depends largely on the question one is asking.

The reverse genetic techniques available to the nematode system are not as robust as that in other organisms. At the present time, there exists no method to generate a targeted mutation in the *C. elegans*. Homologous recombination based gene targeting systems have been highly successful in yeast and mouse systems, and it has recently been reported that the approach had been extended to *Drosophila melanogaster* (Niedenthal et al., 1999; Rong et al., 2000; Winzeler et al., 1999). It is hopeful that this method will soon be available to the nematode system.

Reverse genetics in the worm consists of random mutagenesis followed by complementation to transgenic animals, site-selected mutagenesis and RNA interference (RNAi) (Fire et al., 1998; Janke et al., 1997; Moulder et al., 1998; Zwaal et al., 1993).

Correlation of the physical and genetic maps is one method to ascribe phenotype to sequence. A successful application of this has come from screens for essential genes followed by transgenic rescue of the phenotype (Janke et al., 1997). As the gene

sequence is known, a transgenic animal carrying an extra copy of the gene can be constructed. The transgenic strain can then be tested for complementation against mutations in the vicinity.

Another method consists of random mutagenesis of a population of animals followed by PCR screening to identify chromosomal rearrangements in the desired gene. At present there are two variations on the PCR based screen. The first makes use of transposon insertion and deletion to produce rearrangements (Ketting et al., 1997; Plasterk et al., 1999; Zwaal et al., 1993). Transposons are mobile genetic elements that integrate at various regions on chromosomes. When transposons are mobilized, they can insert into a gene, which may cause a mutation. Alternatively, a frameshift mutation can result through imperfect excision of the transposon, creating a small deletion or insertion in the gene. This rearrangement can be detected and followed by PCR. Primers flanking the gene of interest produce a discrete band in a wild-type background. Insertion or excision of a transposon will result in a respective increase or decrease in band size.

The PCR based screen is sensitive enough to allow for large populations of animals to be assayed. Upon identification of a potential rearrangement, it is selected for from the siblings of the animals used in the assay through successive rounds of PCR and subdividing the population from whence it came. Ultimately, successful sibling selection results in the isolation of a single worm bearing the chromosomal rearrangement (Zwaal et al., 1993).

This method is not without caveats however, which have to do with the behavior of transposons. Transposon insertion is nonrandom as they will insert into AT rich sequence more frequently (Ketting et al., 1997; Plasterk et al., 1999). As most genes are

GC rich this means that transposons often insert into noncoding regions. Additionally, if a transposon does insert into a gene, it can be spliced out of the message as if it were an intron (Rushforth et al., 1993). The major problem with this method is that if the transposon inserts into a noncoding region of the gene and cannot be forced to undergo imperfect excision, no mutation of the gene is created. This procedure is labor intensive with no guarantee of a mutant phenotype even if a single worm bearing a PCR defined chromosomal rearrangement has been isolated.

The second approach is a modification of the first. Transposons are replaced by chemical mutagenesis (Jansen et al., 1997; Moulder et al., 1998). In this approach oligonucleotides specific to the gene of interest are synthesized to generate a product of 3-4 kb. Nested PCR is used to screen mutagenized populations of animals for PCR products that are smaller than wild type, implying that a region of DNA between the primers has been deleted. As PCR is a sensitive technique, smaller products can be detected amidst wild type. Smaller products will be favored over larger ones through successive rounds of amplification. Thus, deletion bands can be followed and selected for until a single animal is identified. The obvious advantage of this approach over the transposon-based method is that animals isolated will bear a deletion in the gene of interest.

The choice of mutagen is very important and several considerations must be made. The type of lesion induced by the mutagen is of utmost importance. Single nucleotide substitutions, small deletions, or chromosomal rearrangements can be generated with different mutagens. The frequency of mutation is also important; if the frequency is too high, the production of accessory, or second site, mutations can

complicate the recovery and analysis of the desired mutant. Of course, if the frequency is too low, then the number of genomes that must be screened to recover a mutant may become prohibitive. For the PCR based screens, the mutagen must generate deletions small enough to fall between the primer sets, but large enough to be distinguished from wild type. The mutagen most often used in this procedure is ultraviolet light in the presence of trimethylpsoralen (UV-TMP). TMP is a DNA cross-linking agent which is activated by ultraviolet light (Cinibo et al., 1985). The cross-links are thought to be repaired by sequential nucleotide excision and recombinational repair. An error in this process can result in a deletion mutant. UV-TMP mutagenesis followed by inefficient repair generates mutations of various sizes, but they fall into three categories: very large deletions in excess of hundreds of kilobases, medium size deletions between 500 and 3000 nucleotides and small deletions ranging from 50 to 500 nucleotides (Gengyo-Ando et al., 2000; Yandell et al., 1994 and Dr. Erin Gilchrist, personal communication). This method has been used to generate numerous *C. elegans* deletion mutants (Dr. Don Moerman, personal communication).

RNAi is a relatively new technique that is being used widely to study gene function in *C. elegans* (Fire et al., 1998). The introduction of double-stranded RNA into *C. elegans* often results in sequence specific gene silencing. In many instances RNAi results in a phenocopy of a null mutation in the targeted gene (Fire et al., 1998; Ketting et al., 1999).

There are several methods to deliver dsRNA into the worm. An early method consisted of synthesizing dsRNA *in vitro* and either introducing it into the worm through microinjection, or by soaking the animals in a dsRNA solution (Fire, 1998). Two

additional methods have been described recently. Worms can be fed bacteria expressing sense and antisense RNA under the control of an inducible promoter. The worms ingest the dsRNA along with the bacteria (Timmons et al., 1998). In the last approach, a transgenic strain of worms is created that contains a transgene that can produce dsRNA under the control of an inducible promoter (Tavernarakis et al., 2000).

The methods are not equivalent in disrupting endogenous gene function. There is considerable anecdotal evidence suggesting that genes respond better to different delivery methods. There is evidence that RNAi phenotypes may differ from mutations in the same gene (Fire et al., 1998; Frase et al., 2000). The effectiveness of RNAi may be dependent on the spatial and temporal action of the gene of interest (Tavernarakis et al., 2000). Genes that are active early are particularly susceptible to RNAi, and the injection of dsRNA is very effective. Late acting genes, especially neuronally expressed genes, are refractory to RNAi for as of yet undetermined reasons (Fraser, 2000). The use of transgenes to generate RNAi *in vivo* has been successful in generating phenotypes for many, but not all, genes that had been otherwise resistant to RNAi from other delivery methods. While RNAi can be a powerful and forthright approach to determine gene function, the main disadvantage is that it is not a true genetic method. RNAi functions to deplete endogenous message, and this situation does not always recapitulate a null mutation. The effects of RNAi are transient, and do not often persist beyond the first generation.

1.4 Functional Approaches to Study *CeHIP1*

With this information at hand, I will outline the approach I have taken to study the function of *CeHIP1* in *C. elegans*. When I initiated the study of *CeHIP1*, RNAi had not been described. Studies of *SLA2* described defects in the cortical actin cytoskeleton and endocytic events. It was difficult to predict how a *CeHIP1* loss of function would manifest itself in *C. elegans*.

A reverse genetic approach was undertaken to study the function of *CeHIP1*. Site selected mutagenesis screens of *CeHIP1*, following the UV-TMP protocol, in concert with the examination of preexisting mutants, were conducted in hopes of identifying a mutation of the *CeHIP1* locus (Moulder et al., 1998).

Molecular characterization of *CeHIP1* was performed. Experiments were designed to study the temporal and spatial characteristics of *CeHIP1*, including gene expression and protein localization. These experiments were highly successful and provided valuable information about the role of *CeHIP1* in an animal system. Also, a screen was performed to identify potential interacting proteins of *CeHIP1*. This too was successful as it identified potential pathways in which *CeHIP1* may function outside of what had been described from other systems.

The advent of RNAi ultimately allowed for the study of *CeHIP1* function. With this technique, I developed a system that identified multiple roles for *CeHIP1* in the nematode. The information provided within describes the function of an evolutionarily conserved gene with importance to human disease in a simple eukaryotic system. It is hoped that the understanding of *CeHIP1* will provide insights into the function of the related gene *HIP1*, and into the etiology of Huntington disease.

CHAPTER II

Methods and Materials

2.1 Foreword

The *C. elegans* research community is a cooperative and generous group. There are several resources available to all members (ACeDB, and the CGC) that were invaluable aids in my studies. Additional resources were gifts kindly donated by individual researchers.

2.2 Nematode Strains and Culture Conditions

Caenorhabditis elegans strains were maintained on petri plates containing nematode growth medium (NGM) streaked with *Escherichia coli* OP50 as a food source (Brenner, 1974). The genetic nomenclature used follows that of (Horvitz, 1979). The wild-type N2 strain and mutant strains used were obtained from our laboratory or the *C. elegans* Genetic Stock Center unless otherwise noted.

2.2.1 Transgenic Strains

Heritable lines of transgenic worms carrying various constructs were created by injecting the constructs along with pCeh361, which contains a wild type rescuing copy of *dpy-5* into CB907 *dpy-5* (*e907*) hermaphrodites following transformation methods described elsewhere (Fire, 1986; Mello, 1991). Strains made and injection conditions used: marker plasmid pCeh361 was injected at a concentration of 75 ng/ μ l. Test plasmids pCeh353, pCeh389, and pCeh391 were injected at various concentrations until stable integrants were obtained. Typically, I would start at a concentration of 20 ng/ μ l,

for a final concentration of 100 ng/ μ l with the marker plasmid. If no transformants could be obtained, the concentration of test plasmid was dropped from 10 to 5 and sometimes to 1 ng/ μ l until transformants were obtained. The final concentration of plasmid DNA was adjusted to 100 ng/ μ l with pBluescript SK+ DNA (Stratagene).

2.2.2 Integration of Transgenic Arrays

Arrays were integrated by exposing 30-40 young adult hermaphrodites to 3500 rads from a ^{60}Co source. Animals were let grow to starvation, upon which pieces of agar were cut out of the petri dishes to new plates. Numerous (500 to 1000) animals carrying the wild type marker were picked individually to new plates and the segregation patterns of their progeny were observed. Animals giving rise to 100% wild type progeny were kept as candidates for successful integration. Strains were outcrossed several times, and assayed either through PCR, GFP fluorescence, or both.

2.3 Microscopy

Microscopy was conducted at the Biosciences Electron Microscopy Facility at the University of British Columbia. Light microscopy was conducted on a Zeiss Axioscope, and recorded on a DVC Spot Camera. Confocal microscopy was performed on a Zeiss Axioscope with the Bio-Rad Radiance Plus system.

2.4 Preparation of Cloned DNA

2.4.1 Plasmid and Cosmid Isolation from Bacteria

Preparation of DNA follows that of Sambrook et al. (1989). Briefly: 1.5 ml of an overnight culture was transferred to a microfuge tube and spun at 13,000 rpm for 1 minute. The supernatant was aspirated and the pellet resuspended in 100 μ l of ice cold Solution I (50 mM glucose, 25 mM TrisCl (pH 8.0), and 10 mM ethylenediaminetetracetic acid (EDTA) pH 8.0). To this was added 200 μ l Solution II (0.2 M NaOH, and 1% SDS). The tube was gently inverted several times and incubated on ice for 5 minutes. 150 μ l of cold Solution III (3 M potassium acetate, 5 M glacial acetic acid) was added, the tube gently inverted and incubated on ice for 5 minutes. The tube was then spun at 13,000 rpm for 5 minutes. The supernatant was transferred to a fresh tube containing 900 μ l cold 95% ethanol, and spun at 13,000 rpm for 5 minutes. The supernatant was aspirated, leaving behind a pellet, which was washed once with 150 μ l of cold 70% ethanol. The pellet was air dried and resuspended in 20 μ l TE (pH 8.0) with RNase A (25 μ g/ml) and stored at -20°C.

DNA for microinjection was purified with a Qiagen Spin Miniprep Kit following the manufacturer's protocol.

2.4.2 Plasmid isolation from *Saccharomyces cerevisiae*

A 5 ml culture (with appropriate selection) was inoculated with a single colony and grown overnight at 30°C. The cells were pelleted in a microfuge (13,000 rpm), and 200 μ l of lysis solution (2% Triton X-100, 1% SDS, 100 mM NaCl, 10 mM Tris pH 8.0, and 1.0 mM EDTA) was added. To this was added 200 μ l phenol/chloroform and 0.3 g

of 425-600 micron diameter glass beads (Sigma). The mixture was vortexed for 5–10 minutes, and placed in a microfuge and spun at 13,000 rpm for 5 minutes. The supernatant was removed to a fresh tube and the DNA was precipitated with 500 μ l 95% EtOH and 10 μ l of 7.5 mM ammonium acetate. The supernatant was removed and the pellet resuspended in 20 μ l dH₂O. 1 μ l was used for subsequent transformations into electrocompetent DH10B cells.

2.5 Transformation

Strains used include: *Escherichia coli* strains DH5 α , DH10B (GIBCO-BRL), and *Epicurian coli* SURE (Stratagene). The *S. cerevisiae* strain Y190 was used in all yeast experiments.

2.5.1 *E. coli* DH5 α

Chemical transformation competent DH5 α cells were thawed on ice, and 50 μ l aliquots were transferred to pre-chilled 15 ml tubes. An appropriate amount of the ligation mix was added to each tube, gently swirled, and incubated for 30 minutes on ice. The tubes were heat-shocked for 45 seconds at 37°C, and quickly returned to ice for 2 minutes. 400 μ l of LB media was added to each tube and each tube was incubated, with shaking for 60 minutes at 37°C. 120 μ l of the transformed competent cells were transferred onto LB plates with the appropriate selection agents (Ampicillin at 30 μ g/ml, or Kanamycin at 50 μ g/ml) and let grow overnight at 37°C.

Colonies that appeared were picked individually into 2ml LB with the appropriate antibiotic and grown overnight at 37°C. Negative controls included transforming with

vector alone and positive controls consisted of transforming with a known concentration of plasmid DNA. DNA was prepared following as described above.

2.5.2 *E. coli* SURE cells

Chemical transformation competent *E. coli* SURE cells are used to clone DNA with problematic secondary structure, such as inverted repeats (Stratagene). Cell aliquots were thawed on ice and gently mixed. 100 μ l of the competent cells was transferred to prechilled 15 ml tubes. 1.7 μ l 1.25 M β -mercaptoethanol was added to the cells. The cells were placed on ice gently swirled every 2 minutes over the next 10 minutes. Approximately 50 ng of DNA was added to the cells and gently mixed. The mixture was incubated on ice for 30 minutes. The cells were heatshocked at 42°C for 30 seconds and returned to ice for 2 minutes. 900 μ l of preheated (37°C) was added to the cells and incubated at 37°C with shaking for 60 minutes. 200 μ l of the transformation mix was plated onto LB plates with the appropriate selection.

2.5.3 *E. coli* DH10B

Electrocompetent *E. coli* DH10B cells were used to recover plasmids from minipreparation from yeast cells. Transformation was done using a BioRad Micropulser Electroporation Apparatus (BioRad).

The electrocompetent cells were thawed on ice. A fresh 1.5 ml microfuge tube and a 0.2 cm electroporation cuvette were also placed on ice. 40 μ l of the competent cells was mixed with 1-2 μ l of DNA in a cold microfuge tube. The solution was mixed well and incubated on ice for 1 minute. The micropulser was set to Ec2, the setting for

the 0.2 cm cuvette. The mixture was transferred to a cold cuvette, and the suspension was tapped to the bottom. The cuvette was placed in the electroporation apparatus and pulsed once. 1 ml of SOC medium was added to the cuvette. The cells were gently resuspended with a Pasteur pipette and transferred to a 15 ml polypropylene tube and incubated with shaking at 37°C for 1 hour. 100-200 µl of the transformation mix was plated on selective medium.

2.5.4 *S. cerevisiae* Y190

The yeast strain Y190 was used for transformations and assays. Yeast transformations were performed using a modified lithium acetate transformation protocol (Gietz and Schiestl, 1995).

5 ml of liquid YPAD was inoculated with a single yeast colony, and grown overnight, with shaking at 30°C. The growth of the culture was measured (its optical density measured) and used to inoculate 50 ml of warm YPAD to a cell density of $OD_{600} = 0.05$. The culture was incubated at 30°C with shaking until it reached a density of $OD_{600} = 0.2-0.3$. The culture was harvested in a sterile 50 ml centrifuge tube at 5,000 rpm for 5 minutes. The supernatant was poured off, and the cells resuspended in 25 ml of sterile dH₂O and centrifuged again. The supernatant was poured off and the cells were resuspended in 1.0 ml 100 mM lithium acetate and transferred to a 1.5 ml microfuge tube. The cells were pelleted at top speed for 15 seconds, and the lithium acetate was removed with a pipette. The cells were resuspended in a final volume of 500 µl of 100 mM lithium acetate. A 1.0 ml sample of salmon sperm carrier DNA (2.0 mg/ml, Sigma, S3126) was boiled for 5 minutes, and quickly chilled in ice water. The cell suspension

was vortexed and distributed in 50 μ l aliquots and stored on ice. The cells were pelleted and the lithium acetate removed. The transformation mix consists of 240 μ l PEG (50% w/v), 36 μ l 1.0 M lithium acetate, 25 μ l salmon sperm DNA (2.0 mg/ml), and 50 μ l water and plasmid DNA (0.1–10 μ g). The ingredients were added in the order listed. The tubes were vortexed vigorously until the pellet had been completely mixed. The tubes were then incubated at 30°C for 30 minutes. The samples were then heat-shocked in a water bath at 42°C for 20 – 25 minutes, and then placed in a microfuge and spun down at 6,000 rpm for 15 seconds. The transformation mix was removed with a pipette and 1.0 ml of sterile dH₂O was added and the pellet was resuspended by gently pipetting up and down. Between 100-200 μ l of the transformation mix was plated onto the appropriate synthetic dropout (SD) plates. The plates were incubated at 30°C for 2–4 days.

2.5.4.1 Yeast Selection

Synthetic dropout is a minimal media used in yeast transformations to select and test for specific phenotypes. SD medium is prepared by combining a minimal SD base (nitrogen base and a carbon source) with a stock of dropout solution that contains a specific mixture of amino acids and nucleosides. SD medium is prepared as follows: 6.7 g Yeast nitrogen base without amino acids, 20 g Agar (for plates only), 850 ml H₂O, 100 ml of the appropriate sterile 10 \times dropout solution or the required amount of DO Supplement powder (CSM –HIS-LEU-TRP, BIO 101, Inc.). Adjust pH to 5.8 if necessary, and autoclave. Allow medium to cool to ~ 55°C before adding 3-AT, or X-gal. Add the appropriate sterile carbon source, usually dextrose (glucose) to 2%. Adjust final volume to 1 L.

The three selection markers used in this study were tryptophan, leucine, and histidine. pGBT9 GAL4 binding domain vectors contain the TRP1 marker, allowing for selection on SD media missing tryptophan (SD – TRP + LEU + HIS). The pACT2 and pGAD10 GAL4 activation domain vectors contain the LEU2 marker, which allows for selection on media without leucine (SD + TRP – LEU + HIS). Selection for transformants containing both plasmids, pGBT9 with either pACT2 or pGAD10 was done with media missing tryptophan and leucine (SD – TRP – LEU + HIS).

The yeast two-hybrid screen relies on the activation of the HIS3 (or lacZ) reporter gene to allow for growth on media missing histidine. If the two fusion proteins, the GAL4 binding domain fusion protein and the activation domain fusion protein, interact, the HIS3 gene will be activated through the reconstitution of a functional GAL4 protein. Thus, potential interacting proteins can be identified as transformants able to grow on media without tryptophan, leucine and histidine (SD – TRP – LEU – HIS).

2.6 DNA Sequencing

DNA to be sequenced was prepared by various methods depending on the source. A typical sequencing reaction consisted of: template DNA (250-500 ng), 8.0 µl terminator premix (PCR buffer, dinucleotide triphosphates (dNTPs), and DNA polymerase), 3.2 pmol primer, and dH₂O to 20 µl. The thermal cycling program used was: 25 cycles of 96°C for 30 seconds, 50°C for 15 seconds, 60°C for 4 minutes, followed by incubation at 4°C. DNA was precipitated in ethanol and dried in a vacuum centrifuge. Sequencing was carried out with an automated sequencer (Applied Biosystems) at the Nucleic Acids Protein Services Unit, University of British Columbia.

2.7 Electrophoresis

2.7.1 Agarose Gel Electrophoresis

Agarose gel electrophoresis was used to determine the size of restriction fragments, PCR products and estimate the concentration of DNA samples. Gel concentrations ranged from 0.6-1.5 % w:v agarose in 0.5_x TBE electrophoresis buffer (1_x TBE: 0.045M Tris, 0.045M boric acid, 0.001M EDTA pH8.0) with 0.1 µg/ml ethidium bromide. Samples were loaded with a one-sixth volume of 6_x loading buffer (40% w:v sucrose in water, 0.25% bromophenol blue, 0.25% xylene cyanol). The mixed samples were loaded with a pipette into wells of the agarose gel. Electrophoresis was performed at 80-120V for one to two hours in 0.5_x TBE running buffer containing 0.1 µg/ml ethidium bromide. An ultraviolet transilluminator (300nm wavelength) was used to visualize the DNA. Size and concentration estimates were made by comparison to known molecular weight and concentration standards run alongside the samples

2.7.2 Polyacrylamide Gel Electrophoresis

Polyacrylamide electrophoresis was used to for the analysis of proteins. 8 – 10% polyacrylamide gels were made by combining 30% acrylamide mix (29.2% acrylamide and 0.8% *N, N'* - methylene-bis-acrylamide), 1.5 M Tris pH 8.8, 10% sodium dodecyl sulfate (SDS), 10% ammonium persulfate (APS), and *N, N, N', N'*, tetramethylethylenediamine (TEMED) and dH₂O to get a final concentration of 8-10% polyacrylamide, 0.38 M Tris pH 8.8, 0.1% SDS, 0.1% APS, and 0.8% TEMED. This gel, the resolving gel, was cast using the BioRad Gel Cast system. Briefly, the mixture was poured between two glass plates separated by a spacer. A volume of isopropanol was

overlain to promote solidification of the gel. Once set, the isopropanol was washed out and the stack was poured. The stack was made by combining 30% acrylamide mix, 1.0 M Tris pH 6.8, 10% SDS, 10% APS, and TEMED and dH₂O to get a final concentration of 5% polyacrylamide, 0.125 M Tris pH 6.8, 0.1% SDS, 0.1% APS, and 0.01% TEMED, and pouring over top of the running gel. A comb was inserted into the stack and the gel was allowed to solidify before use. After the gel had polymerized, it was placed in a vertical electrophoresis chamber and filled with 1× running buffer (10× Laemmli Running buffer: 30.3 g Tris base, 144.2 g glycine, 10 g SDS, pH to 8.3, and volume to 1 L).

Protein samples were loaded with an equal volume of 2× sample buffer (62.5 mM Tris pH 6.8, 2% SDS, and 10% glycerol) along with the appropriate molecular weight marker. The samples were run at 80-90 V through the stack, and 110-120 V through the resolving gel. The gel was run until the marker dyes had migrated to the bottom of the resolving gel. Separation was visualized with a staining solution (0.25% Brilliant Blue G, Sigma, 50% methanol, and 10% acetic acid). The gel was stained for 10-15 minutes before being washed with a destaining solution (7% glacial acetic acid, and 5% methanol). The gel was destained until the desired resolution was obtained. Gels were dried by mounting onto Whatman filter paper and dried for approximately 45 minutes in a vacuum gel drier at 80°C.

2.8 DNA Analysis

Analysis of DNA sequence was conducted with the following computer programs: DNA Strider, Amplify, BLAST (ncbi.nlm.nih.org), ClustalW (Thompson, 1994), www.sgi.com/chembio/resources/clustalw/parallel_clustalw.html), Boxshade (Huffman and Baron, www.isrec.isb-sib.ch/pub/), COILS (Lupas, 1991), at <http://dot.imgen.bcm.tmc.edu:9331/>) ACeDB (**A C. elegans Database**, documentation, code, and data available from anonymous FTP servers at lirmm.lirmm.fr, cele.mrc-lmb.cam.ac.uk and ncbi.nlm.nih.gov), and WormBase (www.wormbase.org).

2.9 Polymerase Chain Reaction

PCR was optimized on single worms. A typical reaction consisted of: 5 μ l template DNA, 2.5 μ l 10_x PCR buffer, 2.5 μ l 25 mM MgCl₂, 4 μ l 1.25 mM dNTPs (Pharmacia), 100 ng forward primer, 100 ng reverse primer, 2.5 Units *Taq* DNA polymerase (Qiagen), and dH₂O to 25 μ l. Thermal profiles for all amplification was: 40 seconds at 94°C, followed by 30 cycles of 30 seconds at 94°C, 30 seconds at primers averaged T_m (54-64°C), 2 minutes at 72°C, followed by a final extension of 7 minutes at 72°C, and cooling and holding at 4°C. To estimate melting temperature (T_m) for an oligo, the following formula was used: $T_m = (2^\circ\text{C} \times (A+T)) + (4^\circ\text{C} \times (G+C))$.

2.10 Restriction Digests

Restriction digests were used to check the integrity of plasmid clones, to provide DNA for molecular cloning procedures, and to provide template for RNA transcription experiments. Restriction enzymes were obtained from either Gibco-BRL or New

England Biolabs. The amount of DNA digested was dependent on the application. The buffers used were those recommended by the manufacturer. All restriction digests were carried out for at least one hour at the appropriate temperature with at least a two-fold excess of enzyme.

2.11 Subcloning

2.11.1 Cloning of the CeHIP1 cDNA

EST clone yk5h12, which encodes the near full length CeHIP1 coding region, was obtained from Yuji Kohara (National Institute of Genetics, Japan). Isolation of cDNA clones is presented below:

2.11.1.1 Preparing cDNA Clones

A 2 ml culture of XL-1 Blue MRF' (Stratagene) cells was grown overnight in LB supplemented with 0.2% maltose and 10 mM MgSO₄. The next day, 5 ml of supplemented LB was inoculated with 0.1 ml of the overnight culture and grown to an OD₆₀₀ = 0.5. The culture was then stored at 4°C. Phage stocks were diluted in suspension media (SM, 100 mM NaCl, 10 mM MgSO₄, 50 mM Tris-Cl, pH 7.5) to concentrations of 1/100, 1/1,000, and 1/10,000. 200 µl of the XL1 Blue MRF' cells was added to each dilution and incubated at 37°C for 15 minutes. 3.5 ml of NZY top agar was added to each tube and plated on NZY plates (NZY, 0.5 L, 5 g NZ amine, 2.5 g NaCl, 2.5 g bacto-yeast extract, and 1 g MgSO₄ × 7 H₂O, with 3.5 g agarose for the NZY top agar). The plates were incubated at 37°C overnight. The next day the plates were examined for the presence of plaques. Individual plaques were cored with a Pasteur

pipette and dispersed in 1.0 ml of SM. To this was added two drops of chloroform, and the mixture was stored at 4°C.

To prepare for phage excision 2 ml overnight cultures of XL-1 Blue MRF' and XLOLR (pRF', Stratagene) were grown in supplemented LB. The next day separate 25 ml of LB was inoculated with 0.5 ml of the overnight cultures and grown until $OD_{600} = 1.0$, and then stored at 4°C. In a 50 ml tube was added 200 μ l XL1 Blue MRF' cells, 250 μ l of the phage stock, and 1.0 μ l ExAssist Helper Phage (Stratagene). The mixture was incubated at 37°C for 15 minutes. To this was added 3.0 ml of LB, and the mixture was further incubated at 37°C for 2.5 hours to overnight. The tube was then heated at 70°C for 15 minutes to kill the cells, and centrifuged at 4,000g for 15 minutes to pellet the debris. The supernatant, which contains the excised filamentous phagemid, was transferred to a sterile tube and stored at 4°C. 200 μ l of the XLOLR cells were transferred into 1.7 ml microfuge tubes. To these was added 10 μ l and 100 μ l aliquots of the excised phagemids, and the mixture was incubated at 37°C for 15 minutes. 50 μ l of each mixture was plated onto LB ampicillin plates and incubated overnight at 37°C.

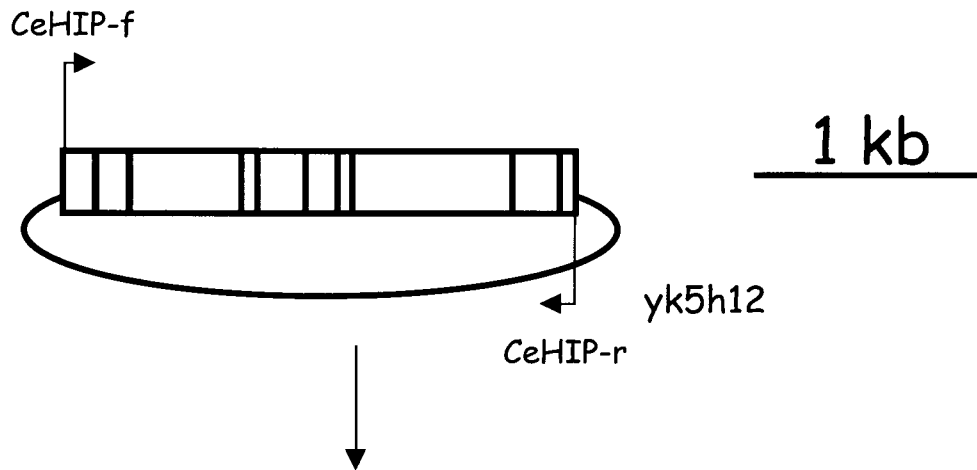
The next day, individual colonies were picked and streaked onto new plates and again incubated overnight at 37°C. Several of the resultant colonies were picked into 2 ml LB ampicillin cultures and grown overnight at 37°C. DNA was prepared as described elsewhere and used to transform DH5 α cells (also described elsewhere). Restriction digests and sequencing of miniprepared DNA was conducted to confirm the identity and integrity of the clones.

2.11.1.2 Cloning the Full Length CeHIP1 cDNA

Clone yk5h12 is 8 bp short of the full length CeHIP1 message at its 5' end. Oligonucleotides (provided by Dr. M Hayden, University of British Columbia) were synthesized to amplify the full length *CeHIP1* cDNA off of yk5h12 and add in the missing 5' end. Specifically, PCR was done using CeHIP-f 5' gagcccggggatggatcatcgtgctcaagcgcgaggtatt (*SmaI* site underlined) and CeHIP-r 5' gccactactggatccttaaaaactaaccttgctgcaac (*BamHI* site underlined) with a long range PCR kit (Expand Long Template PCR System, Boehringer Mannheim). The 2.9 kb fragment was gel purified (QiaQuick Gel Extraction Kit, Qiagen, Germany) and digested with *SmaI* and *BamHI*. The fragment was cloned into pBluescript-SK using *SmaI* and *BamHI* ligation sites following standard molecular biology protocols (Sambrook et al. 1989). A typical ligation reaction consisted of 1× T4 DNA ligase buffer, 50-100 ng vector DNA, 100-200 ng insert DNA, 400 Units T4 DNA ligase, and dH₂O to 10 µl. The mixture was incubated overnight at 4°C, and transformed into the appropriate competent cells. This clone, named pCeh352, was sequenced on both strands to confirm its identity (figure 2.1).

2.11.2 Construction of CeHIP1::GFP Reporter

Oligonucleotides KRp 244 5' cgctgcagttctcctctctgcccatttc (*PstI* site underlined) and KRp 245 5' ccggggatccgcttgagcagcatgatccat (*BamHI* site underlined) were synthesized to amplify the putative CeHIP1 promoter region and some coding elements (from -1067 To +18, with the initiation of transcription site being +1). This fragment was amplified with Pfu Turbo (Stratagene) and cloned in frame with the pPD95.70 GFP



Long range PCR

CeHIP-f 5' gagcccggggatggatcatcgtgctcaagcgcgaggtatt
(*SmaI* site underlined)

CeHIP-r 5' gccactactggatccttaaaaactaaccttggtcgcaac
(*BamHI* site underlined)

Digestion with *BamHI* and *SmaI*

Ligation into pGBT9
[*BamHI*, *SmaI*]
Clone pCeh350

Ligation into pACT2
[*BamHI*, *SmaI*]
Clone pCeh351

Ligation into pBSSK
[*BamHI*, *SmaI*]
Clone pCeh352

Figure 2.1 Cloning of pCeh350, pCeh351, and pCeh352.

genomic transformation vector (provided by Dr. Andy Fire, Carnegie Institute of Washington, Baltimore, MD). The resulting clone was named pCeh353 (figure 2.2).

2.11.3 CeHIP1::GST Fusion Protein

A portion of the CeHIP1 cDNA, from clone pCeh352, was amplified with oligonucleotides KRp300 5' gcggatccgcagaattgaaagcaacggcag (*Bam*HI site underlined) and KRp301 5' tcgcccgggtgattggcgtgtgattctcg (*Sma*I site underlined) with Pfu Turbo polymerase. The 357 nucleotide fragment (which corresponds to nucleotides 1224 to 1560 of the CeHIP1 coding region and amino acids 408 to 520 of the polypeptide) was purified and digested with *Bam*HI and *Sma*I, gel purified and ligated in frame into the multiple cloning site of pGEX-4T-1 (GST Gene Fusion System, Pharmacia Biotech). The pGEX-4T-1 vector generates recombinant proteins with a carboxy-terminal GST tag. The resulting clone was named pCeh365 (figure 2.3).

2.11.4 CeHIP1 Overexpression Construct

Clone pCeh391 was constructed by amplifying the full length CeHIP1 cDNA with primers KRp355 5' gcttaggctagcatggatcatcgtgctcaagcg (*Nhe*I site underlined), and KRp356 5' cggggtacccttgttcgcaaccaactgagcc (*Kpn*I site underlined), with Pfu Turbo polymerase. The PCR product was digested with *Nhe*I and *Kpn*I, gel purified and ligated into the corresponding sites of the heat shock vector pPD49.78 (provided by Dr. Andy Fire).

2.11.5 RNA Interference Constructs

Clone pCeh352 was digested *Bam*HI and *Eco*47III, which cuts twice within the *CeHIP1* coding region. The resulting 3443 base pair fragment was gel purified and religated. The resulting clone, named pCeh372, contains the first 1309 base pairs of the *CeHIP1* cDNA.

In vivo RNA interference constructs were cloned in a two step process. First, oligonucleotides CeHIP-f and KRp328 5' cgtggtacctcggaatctggaacgatgac (*Kpn*I site underlined) were used to amplify a 732 bp fragment of the *CeHIP1* cDNA off pCeh352 using Pfu Turbo polymerase. The fragment was purified and cloned into the *Sma*I and *Kpn*I ligation sites of the heat shock promoter 16.2 vector pPD49.78.

The resulting clone was named pCeh386. Secondly, to produce an inverted repeat of the *CeHIP1* cDNA, pCeh386 was digested with *Sma*I and *Kpn*I to remove the 732 nucleotide fragment, which was then subcloned into a fresh pCeh386 that had been cut with *Kpn*I and *Eco*RV, and transformed with SURE cells (Stratagene). The resulting clone contained an inverted repeat of the 732 nucleotide *CeHIP1* cDNA, and was named pCeh389. The integrity of the clone was confirmed through multiple restriction digests (figure 2.4).

2.11.6 Yeast Two-Hybrid Constructs

The full length *CeHIP1* cDNA was amplified by long range PCR with CeHIP-f and CeHIP-r, gel purified, digested with *Bam*HI and *Sma*I and cloned into the multiple cloning site of the yeast two-hybrid binding domain pGBT9 vector (Clontech). The resulting clone was sequenced to confirm its identity and named pCeh350.

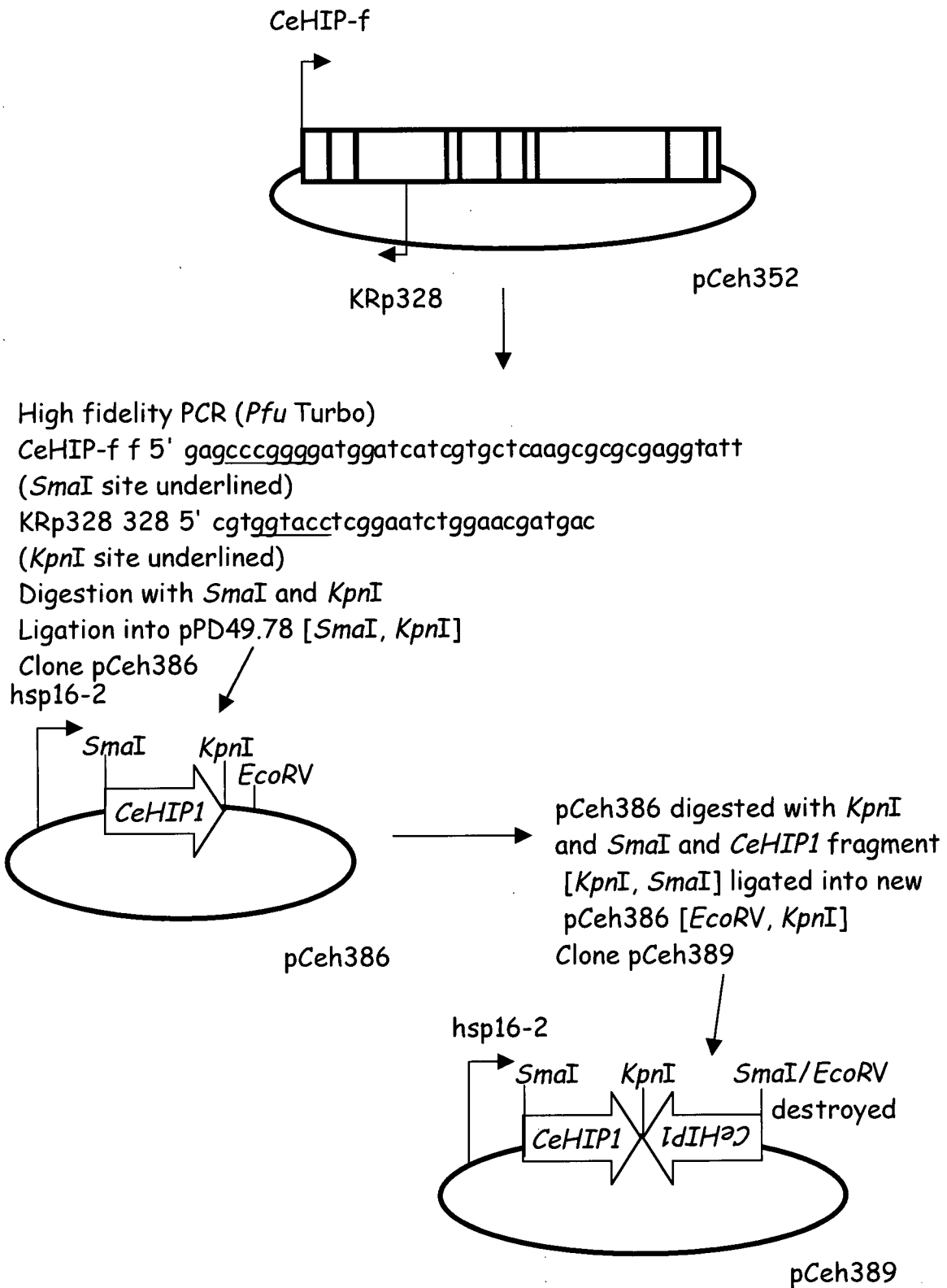


Figure 2.4 Cloning of the RNAi Construct pCeh389.

The CeHIP1 cDNA was subcloned into the yeast two-hybrid activation domain vector pACT2 (Clontech), at the *Bam*HI and *Sma*I sites. The resulting clone was sequenced to confirm its identity and named pCeh351.

Clones used to map the protein-protein interactions of CeHIP1 were generated through restriction digests and subsequent religation of pCeh350.

Clone pCeh374 was made by digesting pCeh350 with *Sma*I and *Sty*I, which removes the first 1628 nucleotides of the 2779 nucleotide *CeHIP1* cDNA. The protruding 5' end left by digestion with *Sty*I was filled in with 1 Unit of the large fragment of DNA Polymerase I, or the Klenow fragment, along with 0.5 mM dNTPs, and incubated at room temperature for 30 minutes. The large fragment (~ 7.1 kb) was gel purified, to which was added DNA ligase, and the ligated circular vector was transformed into DH5 α cells (methods described previously) (figure 2.5).

Clone pCeh375 was generated through digestion of pCeh350 with *Bam*HI and *Sty*I, which removed the last 1151 nucleotides of the *CeHIP1* cDNA. Protruding 5' ends were filled as described, and the larger fragment (~ 6.6 kb) was gel purified, religated, and transformed into DH5 α cells.

Dr. Michael Hayden kindly provided human huntingtin and HIP1 clones. Clones include 16pGBT9, which contains the coding sequence for the first 540 amino acids of human huntingtin with 16 glutamine repeats, ligated at the *Sma*I site of the GAL4-DNA-binding domain of the yeast two-hybrid vector pGBT9. The HIP1 clone contained nucleotides 714 to 1871 of the full length *HIP1* cDNA cloned into the GAL4 activation domain of the yeast two-hybrid vector pGAD10.

2.12 PCR Mapping of Deficiencies

2.12.1 Preparation of Template DNA from Embryos

Animals homozygous for the deficiencies used in this experiment were embryonic lethals. Heterozygous adult hermaphrodites were allowed to lay eggs for 12-16 hours and removed to a new plate. The embryos were let hatch for 12-16 hours at 20°C. Animals that failed to hatch were presumed to be homozygous for their respective deficiency, and were used in the subsequent PCR mapping experiments.

Arrested embryos were transferred to an area of the plate without bacteria, to which was added 3-4 μ l of chitinase solution (20 mg/ml chitinase, Sigma, 50 mM NaCl, 70 mM KCl, 2.5 mM MgCl₂, and 2.5 mM CaCl₂). The eggs were let sit for 5 minutes, or until the solution had absorbed into the agar.

Single eggs were picked with a piece of fishing line that had been cut to be of a length smaller than a microfuge tube. The fishing line was cut with blunt scissors to provide a rough, frayed end, which facilitates egg transfer. A pair of tweezers was used to pick up the fishing line. Transfer was observed under the dissecting microscope. The fishing line and single egg were transferred into a microfuge tube containing 5 μ l lysis buffer (1_x PCR buffer, Qiagen, 1.5 mM MgCl₂, and 60 μ g/ml Proteinase K, Gibco-BRL). Mineral oil was added along the length of the fishing line to help wash the egg into the lysis buffer. The samples were briefly spun at full speed in the microfuge, and placed at -70°C for 10-15 minutes. The samples were placed in thermocycler (Perkin Elmer-Cetus DNA Thermal Cycler), and the eggs were digested at 65°C for 60 minutes, followed by inactivation of the enzyme at 95°C for 15 minutes. The lysed embryos were stored at -

70°C. To prepare template DNA from single worms, the chitinase digestion was omitted, and animals were transferred to the lysis solution with a worm pick.

2.12.2 PCR Mapping of Deficiency Homozygotes

Two primer sets were used in each PCR for deficiency mapping experiments. All reactions were run in duplicate with multiple samples. Mapping experiments consisted of PCR with test primers, and positive and negative controls in all combinations. Positive controls were primer sets used to amplify DNA from LGI that should not be deleted as the deficiencies being studied mapped to LGIII. Negative controls were primer sets amplifying DNA predicted to be deleted by genetic mapping experiments. Test primers that produced no PCR product, along with the appropriate controls, indicated that the deficiency in question deleted the DNA from which the test oligonucleotides were designed. Amplification of the test primers demonstrated that the deficiency did not delete the DNA in question.

Oligonucleotides used in the mapping experiments include: KRp 47 5' attctatccgaatcctccga, and KRp94 5' ggttcgatacttctggcgt, which amplify a 275 nucleotide fragment corresponding to the *bli-4* (LGI) coding region, KRp112 5' ctgcatgttctgggtcc, and KRp113 5'caggcgtcttctcagtgcg, which amplify a 360 nucleotide fragment corresponding to the *C. elegans rad-3* homologue, (LGI), KRp176 5' cccaatgccaataacttgg, and KRp177 5' gtctggtcactcaatgattc, which amplify a 270 nucleotide fragment corresponding to the *dpy-19* (F22B7.10, LGIII) coding region, KRp 178 5' gtcactagatggacgatctg, and KRp179 5' cggcaatatatcacatgagg which amplify a 674 nucleotide fragment corresponding to the *sma-2* (ZK370.2, LGIII) coding region, KRp

300 and KRp301 which amplify a 976 nucleotide fragment corresponding to *CeHIP1* (LGIII), and KRp347 5' gcaggatctggaggacttc, and KRp348 5' cggcataggcattgaagtaa, which amplify a 442 nucleotide fragment corresponding to *unc-32* (ZK637.10, LGIII) coding region.

2.13 Site Selected Mutagenesis Screen

This methods follows that described by Moulder and Barstead (<http://snmc01.omrf.uokhsc.edu/revgen/RevGen.html>, 1997).

2.13.1 Growth and Synchronization for Mutagenesis

N2 worms were grown on 5-10 150mm rich NGM (RNGM, equivalent to 3_ NGM) agarose plates until a large population of gravid adults was obtained. The animals were washed off of the plate with M9 buffer (22 mM KH₂PO₄, 22 mM Na₂HPO₄, 85 mM NaCl, 1 mM MgSO₄), and briefly spun in a clinical centrifuge (1100 rpm, 5 minutes). To the worms was added 10 volumes of basic hypochlorite (0.25 mM KOH, 1-1.5% hypochlorite, made fresh), and incubated at room temperature for 10-15 minutes with occasional mixing. The extracted eggs were washed 4-5 times with 10 volumes of M9 buffer. The eggs were distributed over 15-20 RNGM plates seeded with *E. coli*. The animals were let grow until the majority was at the late L4 or young adult stage (approximately 52 hours at 20°C).

2.13.2 Mutagenesis

To the suspension of worms in M9 was added an equal volume of M9 containing 4, 5', 8-trimethylpsoralen (Sigma) at 60 $\mu\text{g/ml}$ (from a stock at 3 mg/ml in dimethyl sulfoxide). The worm suspension was incubated for 15 minutes, in the dark at room temperature. The worms were then transferred, in the dark, to a sterile 15 cm petri dish and the suspension was irradiated with 360 nm UV light for 90 seconds at 340 $\mu\text{ W/cm}^2$ with gentle shaking. The UV source was assembled from a Blak Ray UVL-21 clamped to a ring stand and calibrated to the desired dosage. The mutagenized worms were collected by washing with M9 and distributed over 10-15 RNGM plates seeded with *E. coli*. and allowed to grow for 24 hours in the dark at 20°C. The F1 eggs were collected by treating the worms with basic hypochlorite, as previously described. The eggs were allowed to hatch overnight on a RNGM plate without *E. coli*.

2.13.3 Library Plating

The worms were collected with M9 buffer and an estimate of the number of worms was made from spotting several volumes of the suspension onto plates and counting. The worm suspension was adjusted to make a concentration of 500 worms/0.25 ml. The worms were then distributed in aliquots of 500 worms over 1152 60 mm OP50 seeded RNGM plates using a repeating pipettor. The plates were stored in groups of 96, and allowed to grow at 20°C for 5 days.

2.13.4 Library Harvest

The plates were numbered in groups of 96 and placed in stacks of 6. To each plates in the stack was added 1.5 ml of sterile dH₂O containing streptomycin (100 µg/ml, Sigma) and mycostatin (12.5 µg/ml, Sigma). The plates were gently rocked to dislodge the worms, and 200 µl of the suspension was transferred to a well of a deep, 96 well microtiter plate (DyNa Block 1000 deep well microplates, Midwest Scientific) containing 200 µl of lysis solution (2_ PCR buffer, 3 mM MgCl₂, and 200 µg/ml Proteinase K ,Gibco-BRL). The worm plates were stored at 10°C to slow development. The blocks were sealed with a flexible mat lid (Flexible mat lid, 96 well, Midwest Scientific), and taped down to prevent mixing between wells. The worms were frozen at -70°C for 20-30 minutes. The blocks were incubated, with occasional mixing, overnight at 65°C. The blocks were spun down in a clinical centrifuge equipped with bucket carriers at 1,100 rpm for 30 seconds. A 50 µl aliquot from the well of each block was transferred to a single 0.2 ml PCR tube, arranged in strips of 12. The tubes were capped and incubated at 94°C for 20 minutes to inactivate the Proteinase K. The blocks and template DNA were stored at -70°C.

2.13.5 PCR Screening

Nested PCR was used to screen for deletions of *CeHIP1*. The primer sets used to screen for deletions were approximately 3000-3500 nucleotides apart. Oligonucleotides include KRp157 5' gaggtattcgttcgagctca, KRp163 5' agccagaaccttcttgact, KRp164 5' gtgccaagtcatatctcctc, KRp165 5' ctgacaagagtccttctgtc, KRp228 5' tcatagtcaggctcctcca, KRp229 5' catttcttcttcttcgcag, KRp230 5' agagccacaacaagcgagtc, KRp233 5'

aaccgagagagcgtccaatc. The PCR reactions were done in 96 well PCR trays (MJ Research) sealed with dimpled rubber mats (Perkin Elmer).

First Round PCR: Each reaction was 25 μ l in volume and contained: 5 μ l template DNA, 2.5 μ l MgCl₂, 4 μ l 1.25 mM dNTPs, 100 ng forward outside primer, 100 ng reverse outside primer, 2.5 Units *Taq* DNA polymerase, and dH₂O to 25 μ l.

Thermocycling conditions were: 2 minutes at 94°C, followed by 30 cycles of 40 seconds at 94°C, 30 seconds at 58°C, 2 minutes at 72°C, followed by a final extension of 7 minutes at 72°C, and cooling and holding at 4°C.

Second Round PCR: Each reaction was 25 μ l in volume and contained: 2.5 μ l MgCl₂, 4 μ l 1.25 mM dNTPs, 100 ng forward inside primer, 100 ng reverse inside primer, 2.5 Units *Taq* DNA polymerase, and dH₂O to 25 μ l. Template DNA for second round amplification was transferred from the first round reaction using a 96-pin replicator (Boekel Replicator). The volume transferred was not considered significant.

2.13.6 Identification of Deletion Candidates and Sib-Selection

1,152 nested PCR reactions were conducted and visualized through standard gel electrophoresis configured for the analysis of samples in microtiter arrays. Equipment used included: 12 channel pipettors (Eppendorf) and an electrophoresis system capable of handling 200 samples at a time (Owl Scientific).

Samples that show bands smaller than wild type were selected for further analysis. Five PCR's were set up for each putative deletion. If the same size band resampled, it was considered a valid candidate and sib selection was initiated.

2.13.7 Sib-Selection

Plates that had given putative deletion candidates were taken from the 10°C incubator, and a portion of the population was distributed over 96 new 60mm RNGM plates seeded with *E. coli* at a concentration of 50 worms/plate. The plates were let grow for 4-5 days at 20°C and the population was harvested, template DNA prepared, and PCR screening conducted as described previously. No candidates resampled after the first round of selection. Several of the putative deletion bands were sequenced, which confirmed they were indeed deletions of *CeHIP1*.

2.14 RT-PCR

Developmental stage specific RNA (obtained from V. Vijayaratnam) was used to make first strand cDNA (RT-PCR Kit, Life Technologies). The procedure is as follows: 1.3 µl of RNA (1.5 µg/µl), 1.0 µl of 10 µM adaptor primer KRp75 5'-ggccacgcgctgactagtagtacttttttttttttttttttt, and dH₂O to 15.5 µl was added to a microfuge tube. The mixture was placed at 70°C for 10 minutes, on ice for 1 minute, and quickly spun down in a microfuge. Next was added 2.5 µl of 10 × PCR buffer, 2.5 µl of 25 mM MgCl₂, 1.0 µl of 10 mM dNTP mix, and 2.5 µl of 0.1 M DTT, to a total of 24 µl. The tube was gently mixed, briefly microfuged, and incubated at 42°C for 1 minute. To the tube was added 1.0 µl of Reverse Transcriptase (5 Units/µl). The tube was then incubated at 42°C for 50 minutes. The tube was placed at 70°C for 15 minutes, and then briefly spun down. The tube was placed at 37°C for several minutes, to which was added 1.0 µl of RNase mix, and the mixture was incubated at 37°C for 30 minutes. The tube was spun down and stored at -20°C.

PCR amplification was performed with either oligonucleotide KRp59 5' ataagaatcgggccggggtttaaccagttactca (splice leader sequence SL2 underlined) or KRp60 5' ataagaatcgggccggggtttaattaccaagtttg (splice leader sequence SL1 underlined) with the CeHIP1 specific primer KRp155 5' gaggtattcgttcgagctca. The results were visualized with standard agarose gel electrophoresis techniques.

2.15 Protein Work

2.15.1 Expression and Protein Purification of CeHIP1

pCeh365 was transformed into DH5 α cells and cultured in 500 ml LB medium with 50 μ g/ml ampicillin, and soluble protein was expressed following induction of log phase cells with 0.5 mM isopropyl-1-thio- β -D-galactopyranoside (IPTG). Bacterial cell pellets were suspended in 5 ml lysis buffer (50 mM Tris pH 7.5, 150 mM NaCl, 1% Triton X-100) with 2 mg/ml lysozyme, 0.2 mg/ml DNase I, 2 mM phenylmethylsulfonyl fluoride (Sigma), and 2 μ g/ml leupeptin (Sigma). The suspension was incubated on ice for 30 minute, and then sonicated for 20 seconds, 3 times. The cell lysate was then centrifuged at 12,000 \times g for 10 minutes. The supernatant was transferred to a fresh tube and stored at -70°C. The supernatant was transferred to a fresh tube containing a 200 μ l bed volume of activated glutathione-sepharose beads (Pharmacia). The tube was incubated for 1 hour at 4°C with rocking. The tube was centrifuged at 1,600 rpm for 5 min. The flow through was set aside and the beads were washed with 1 \times PBS, and centrifuged as previous, for a total of 3 washes. Half of the bed volume (100 μ l) of 20 mM glutathione was added to the beads and bound fusion protein, which was gently mixed and incubated at RT for 15 min. The mixture was spun at 500 \times g for 3 minutes.

The elutant was transferred to a fresh tube. A total of 3 elutants was collected into one tube. To visualize the relative fusion protein content, SDS-PAGE was performed using samples of the uninduced and induced cultures, soluble and insoluble fractions, the flow through, the beads and the elutant. The fusion protein was concentrated with a Centriprep-10 centrifugal concentrator (Centriprep). The concentration of the protein was measured with the Bradford Assay, and by comparing to concentration standards through SDS-PAGE.

2.15.2 Antibody Production

Purified recombinant protein was used to raise polyclonal antisera in rabbits (Covance, Pennsylvania). Polyclonal antibody BC33 was the one used in all experiments to study the protein localization of CeHIP1. Prior to use the antisera was treated with a bacterial acetone powder, using a strain expressing the pGEX-4T-1 vector alone (Miller, 1995).

2.15.3 Western Analysis

The antibodies were tested for specificity by immunoblot analysis against the fusion protein. Bacterial lysate filters were prepared by separating the proteins on 10% SDS-PAGE gels and transferred to a nitrocellulose membrane by electroblotting at 2.5 mA for 60 min. Transfer was confirmed by staining the gel with Brilliant Blue G (Sigma) and a portion of the filter with Ponceau S (Sigma). Membranes were probed with antibodies BC33 and chaperonin antibody (kindly provided by Dr. Candido, University of British Columbia), 1/10,000 dilution, followed by secondary antibodies at

1:10,000 dilution (donkey anti-rabbit horseradish peroxidase-conjugated secondary antibody, Promega). Protein-antibody complexes were detected by enhanced chemiluminescence system (ECL, Amersham Pharmacia Biotech), or Super Signal Chemiluminescent System (Pierce).

Whole worm filters were prepared as follows: 5 plates of N2 worms were grown for 2-3 days, until a mixed population was established. The worms were washed off of the plates with M9 into 200 ml S medium (1 litre S basal, with 10 ml 1 M potassium citrate pH 6, 10 ml trace metals solution, 1 M CaCl₂, 1 M MgSO₄; S basal: 0.1 M NaCl, 0.05 M potassium phosphate pH 6, 5 mg cholesterol; trace metals solution: 5 mM disodium EDTA, 2.5 mM FeSO₄ × 7H₂O, 1 mM MnCl₂ × 4H₂O, 1 mM ZnSO₄ × 7H₂O, 0.1 mM CuSO₄ × 5H₂O) with 4 g of C600 bacterial pellet in a 500 ml fluted flask. The worms were let grow for 5-6 days. The worms were poured into a 250 ml graduated cylinder and let settle overnight at 4 °C. The supernatant was removed leaving approximately 10-15 ml that was transferred to a 15 ml tube. The worms were spun for 5 min at 2,000 rpm in a clinical benchtop centrifuge. The supernatant was removed and 3 ml cold dH₂O was added to the pellet. The worms were spun as described and the supernatant removed. 10 ml of 40% sucrose was added to the pellet, and gently mixed. The worms were spun for 6 min at 2,000 rpm, and the top layer of worms was carefully removed to a fresh tube containing 10 ml 40% sucrose, and spun as before. The upper phase was removed to a fresh tube containing 10 ml of 0.1 M NaCl, and spun for 5 min at 2,000 rpm. This wash was repeated once. The pellet was transferred in 50 µl aliquots to microfuge tubes to which was added 50 µl 3× SDS sample buffer (New England BioLabs), 50 µl M9, and 30 µl 425-600 micron diameter glass beads. The samples were

frozen in ethanol/dry ice, and stored at -70°C . An aliquot was thawed, vortexed and incubated at 90°C for 10 min. The sample was spun down at 13,200 rpm for 1 minute, and incubated at 100°C . The sample was loaded onto a 9% SDS-PAGE gel for protein separation. The protein was transferred to a nitrocellulose filter by electroblotting at 70 mA, ON at 4°C . The efficiency of the transfer was monitored through the use of prestained markers, staining of the gel with Brilliant Blue G, and a portion of the filter with Ponceau S. The membrane was probed with BC33 preimmune, BC33 antisera, BC33 antisera that had been depleted with the bacterial acetone powder, and the chaperonin antibody, all at 1/1,000 dilution. The depleted BC33 antibody detected a single 100 kDa band, approximately the size of the predicted 104 kDa CeHIP1 protein. This band was not present in the preimmune. The signal was cleaned up considerably after treatment with the bacterial acetone powder.

2.15.4 Immunocytochemistry

Staining of whole worms is a modification of Finney, 1990 and Miller, 1995.

2.15.4.1 Whole Worm Fixation

3 to 4 100 mm NGM plates seeded with OP50 were used to grow worms until the plates were full, but not starved or crowded. The worms were washed off the plates with M9 buffer into a 15 ml sterile tube. The worms were briefly spun down at 1,100 rpm for 30 seconds. The supernatant was removed and 7 ml of 4% sucrose was added to the worm pellet. The worms were gently rocked at room temperature for 30-45 minutes to remove bacteria from their guts. The worms were briefly spun down as described, and

transferred to a 1.7 ml microfuge tube. The worms were spun down and liquid removed to a final volume of 0.5 ml. The worms were chilled on ice for 10 minutes. To the worms was added ice cold 2× Ruvkun fixation buffer (160 mM KCL, 40 mM NaCl, 20 mM disodium ethylene glycol bis (β -aminoethyl ether)-*N, N'*-tetracetic acid (Na₂EGTA), 10 mM spermidine-HCL, 30 mM Na, 1,4-piperazinediethanesulfonic acid (Pipes), pH 7.4 and 50% methanol) to a final concentration of 1×. 16% paraformaldehyde was added to a final concentration of 2%. The worms were mixed well and frozen in dry ice/ethanol. The worms were thawed under a stream of tap water, and subsequently refrozen. A total of 4 freeze/thaw cycles was used. Worms were incubated on ice for 30 minutes with occasional mixing after the final thaw. The worms were then washed twice with Tris-Triton buffer (TTB, 100 mM Tris-HCl, pH 7,4, 15 Triton X-100, or Nonidet P-40, and 1 mM EDTA). Worms were incubated overnight in TTB with 1% β -mercaptoethanol at 37°C on a rocker platform. The worms were then washed with 1× BO₃ (diluted fresh from 20× BO₃ Buffer, 1 M H₃BO₃, 0.5 M NaOH, and pH adjusted to 9.5) 0.01% Triton, and then incubated in 1× BO₃, 0.01% Triton, 10 mM dithiothreitol (DTT) for 15 minutes at room temperature with gentle agitation. The worms were then washed with 1× BO₃, 0.01% Triton and incubated in 1× BO₃, 0.01% Triton, 0.3% H₂O₂ for 15 minutes at room temperature. The lids of the microfuge tubes were sealed with lid closures to ensure that any escaping oxygen did not cause the lids to pop open. The worms were then washed with 1× BO₃, 0.01% Triton and once with AbB (1× PBS, 0.1% bovine serum albumin, 0.5% Triton X-100 or Nonidet P-40, 0.05% sodium azide, and 1 mM EDTA) buffer for 15 minutes. The fixed animals were stored in AbA (1× PBS, 1% bovine serum albumin,

0.5% Triton X-100 or Nonidet P-40, 0.05% sodium azide, and 1 mM EDTA) buffer, at 4°C for up to a month.

2.15.4.2 Staining

A 25 µl aliquot of worms was transferred with a wide bore pipette to a new microfuge tube. Antibody was diluted in AbA (antibodies used: BC33 1/200, HSP25 1/250) to a final volume of 100 µl. The samples were wrapped in foil and incubated overnight at 4°C on a rocking platform. The worms were pelleted and washed with several changes of AbB for 15 minutes at RT. Three 30 minute washes with AbB were followed by a 1.5 hour wash, all at room temperature. The samples were rinsed once AbA, and an appropriate dilution of secondary antibody was added (1/200) in 100 µl of AbA. The secondary antibody used was FITC-conjugated AffiniPure Donkey Anti-Rabbit IgG (Jackson Laboratories). The samples were wrapped in foil and incubated overnight at 4°C on a rocking platform. The worms were pelleted and washed with AbB as described above. At this point either 4', 6-diamidino-2-phenylindole (DAPI, Sigma) was added (to a final concentration of 2 µg/ml), or Propidium Iodide (Sigma) was added (final concentration of 1 µg/ml, with 100 µg/ml RNaseA in 1× PBS). Care was taken to minimize the sample exposure to light.

2.15.4.3 Mounting

2% agarose pads on slides were prepared (Mello, 1995). Equal volumes of the sample and 2× mounting media (20 mM Tris-HCl, pH 8.0, 0.2 M 1,4-diazabicyclo-2,2,2-octance (DABCO), 90% glycerol) were mixed in a microfuge tube, and 10 µl was

transferred to the agarose pad. A coverslip was gently overlaid, and after settling, was sealed with nail polish.

The worms were observed by either light or confocal microscopy (Biosciences Electron Microscopy Facility, University of British Columbia).

2.15.5 Dissection and Staining of Gonads

Dissection and staining of gonads follows that of Francis, 1995.

2.15.5.1 Gonad Dissection

200-300 late L4 and adult N2 hermaphrodites were transferred to an unseeded NGM plate. The worms were suspended in 1-3 ml of 1× PBS/0.2 M levamisole (Sigma) and transferred to a 5 cm diameter watchglass. The heads of the worms were cut off with two 25-gauge syringe needles. The worms were decapitated by placing their heads between the syringe tips and moving them in a scissor-like motion. Excess liquid was removed with a Pasteur pipette.

2.15.5.2 Gonad Fixation

The dissected gonads were fixed in a methanol/formaldehyde solution, made by mixing 10 ml of 16% paraformaldehyde, 3.3 ml of 0.1 M K_2HPO_4 (pH 7.2), and 40 ml methanol. The solution was stored at -20°C until use. The dissected gonads were transferred to a glass tube, or a siliconized microfuge tube (Sigmacote, Sigma). The tube was spun at 1,100 rpm for 2 minutes and the supernatant removed. The gonads were washed once with 1× PBS.

2.15.5.3 Antibody Staining of Dissected Gonads

The fixed gonads were incubated in AbB for several hours at 4°C, and incubated with the primary antibody (BC33) at a concentration of 1:500 in AbA overnight at 4°C. The gonads were then washed 3 times with 1× PBS, 0.1% Tween-20 with a 5 minute incubation time. The gonads were incubated with secondary antibody (as above) at a concentration of 1:250 in AbA overnight at 4°C. The gonads were then washed for 5 minutes, 3 times with 1× PBS, 0.1% Tween-20. The gonads were incubated with 1× PBS, 0.1% Tween-20 containing 1 µg/ml propidium iodide and 100 µg/ml RNaseA.

2.15.5.4 Mounting

The gonads were washed 1× PBS, 0.1% Tween-20 and an equal volume of mounting media was added to the tube. The gonads were drawn out with a wide bore pipette and transferred onto a 2% agarose pad on a slide. After the gonads had settled, a finely drawn hair was used to push the gonads and carcasses away from one another. A coverslip was overlain and let settle by gravity. A few moments were allowed for evaporation of the liquid on the slide (to improve image resolution) before the coverslip was sealed with nail polish.

2.16 Overexpression Analysis

Germ line transformation was used to produce a transgenic strain carrying clone pCeh391 (and the *dpy-5* marker, pCeh361) as an extrachromosomal array. pCeh391 contains the *CeHIP1* cDNA behind the heatshock promoter hsp16-2. There exist a number of heat inducible loci in *C. elegans*. The genes encoding the 16 kDa heat shock polypeptides are found at two loci. Locus A contains the 16-1 and 16-48 genes, while locus B contains the 16-2 and 16-41 genes. The two loci are differentially regulated with locus B producing up to seven fold more mRNA during heat induction than locus A (Jones, 1989). While induction of the heat shock genes occurs throughout the animal, the two loci display spatially distinct expression. The 16-1/16-48 genes show greater expression in the muscle and hypodermis, while the 16-2/16-41 genes have increased expression in intestine and pharyngeal tissue (Stringham, 1992). As *CeHIP1* was found to be expressed in the pharynx, the hsp 16-2 promoter was chosen for *CeHIP1* overexpression and RNA interference experiments. To analyze the effect of increased *CeHIP1* expression, transgenic L4 animals were heatshocked for 60 minutes at 30°C. Animals were allowed to recover for 12-24 hours and examined for a phenotype. 15-20 animals were used per trial, and 7 trials were scored for phenotypes.

2.17 RNA Interference

Several approaches were used to deliver dsRNA into *C. elegans*.

2.17.1 RNAi Clones for *in vitro* Transcription

To prepare template for transcription, two separate reactions were set up. In the first, pCeh372 was cut with *Pst*I to linearize the plasmid, and RNA was transcribed with T3 polymerase. The second aliquot of pCeh372 was digested with *Xba*I to linearize the plasmid, and complementary RNA was transcribed with T7 polymerase.

2.17.2 Preparation of Double Stranded RNA for Injection and Soaking

The RNA transcription reaction was as follows: 1 µg of cut template DNA, 5 µl 5× transcription buffer, 1.0 µl each of 10 mM rATP, rCTP, rGTP, and rUTP, 1.0 µl 0.75 M DTT, 1.0 µl of T3 or T7 polymerase (5 Units/µl), and diethyl pyrocarbonate (Sigma) treated dH₂O to 25 µl. The mixture was incubated at 37°C for 30 minutes. To each reaction was added 1.0 µl of Dextran T-500 (20 mg/ml), 75 µl dH₂O. The DNA was purified through phenol/chloroform extraction and precipitated in ethanol. The pellet was resuspended in 10 µl of RNase-free TE pH 7.4. 1.0 µl of each reaction was run on a standard TAE agarose gel to determine their relative concentrations.

To make dsRNA, equal volumes (5.0 µl) of sense ssRNA, antisense ssRNA, and 3× Injection buffer (3×IM: 20 mM KPO₄ pH 7.5, 3 mM K citrate pH 7.5, and 2% PEG 6000) were mixed together and incubated at 68°C for 10 minutes, and then shifted to 37°C for 30 minutes. 1.0 µl of the template, each ssRNA and the dsRNA was run on a 1.0% TAE agarose gel to examine the efficacy of the synthesis.

2.17.3 Injection of dsRNA

dsRNA was injected into the distal arm of the gonads of young adult N2 hermaphrodites after the method of Mello, 1991. The animals were let recover overnight and were subsequently transferred every 16-20 hours and their progeny examined for phenotypes. Typically, 10-20 animals were injected with a specific dsRNA for each trial. At least 4 trials were conducted for each dsRNA to be tested. Injected dsRNAs include *CeHIP1* dsRNA made from pCeh372 and *dpy-5* dsRNA made from pCeh377.

Clone pCeh377 was used as a positive control in these experiments. It contains the complete coding region for the *dpy-5* gene. The *dpy-5* phenotype is readily observable in maturing animals. The negative control was the administration of the injection buffer alone.

2.17.4 Soaking Animals with dsRNA

20–30 L4 animals to be treated with dsRNA were picked into a microfuge tube containing 10 μ l of DEPC treated dH₂O, and spun in a microfuge at 1,000 rpm for 1 minute. The majority of the dH₂O was removed and the 5 μ l of the appropriate dsRNA solution was added to the tube. The worms were placed at 20°C overnight. The next day the animals were transferred individually to seeded NGM plates. The worms were transferred every 16-20 hours and their progeny examined for any defects. This would be considered a single trial, and at least 4 trials would be conducted for each dsRNA tested. ssRNAs used included: *CeHIP1* prepared from pCeh372 and *dpy-5* prepared from pCeh377.

2.17.5 *in vivo* RNA Interference

Several transgenic strains were established carrying clone pCeh389 as a transgene. Strain KR3761 (carrying pCeh389, with the *dpy-5* marker pCeh361, as an extrachromosomal array) and strain KR3792 (with the array integrated into the genome) was used for the *in vivo* RNAi studies.

In vivo RNA interference experiments were conducted as outlined elsewhere (Tavernarakis, 2000). Specifically, L1 to L3 stage hermaphrodites were heat shocked at 35°C for 4 hours. After heat shock, animals were allowed to recover overnight at 20°C, and transferred every day and assayed for various defects.

2.17.6 Outcrossing of RNAi Animals

Animals to be used in mating experiments were allowed to recover overnight and subsequently transferred to a plate with the appropriate male strain: heatshocked and non-heatshocked N2 males or KR3792 males. L1 to L3 animals were heat shocked at 35°C for 4 hours and allowed to recover at 20°C until the males reached sexual maturity (when they could be easily distinguished from hermaphrodites in the population). A typical trial would consist of placing 15-20 RNAi treated animals with an excess of males (~ 3 males for every hermaphrodite) over several NGM dot plates and allowing for mating overnight at 20°C. Hermaphrodites would be transferred individually to new NGM plates and subsequently transferred every 16–24 hours and scored for the unfertilized oocyte phenotype.

2.18 Yeast Two-Hybrid Analysis

To determine if CeHIP1 protein could interact with human huntingtin, a two-hybrid approach was taken. The human huntingtin clone, 16pGBT9, was transformed into yeast Y190 cells to produce strain AP1. Clone pCeh351 (CeHIP1 in pACT2) was transformed into AP1 producing strain AP6. Strain AP6 was grown on SD – TRP –LEU –HIS plates to test for protein-protein interaction. The positive control was yeast strain AP3 (16pGBT9 and the clone carrying human HIP1, HIP1pGAD10). Negative controls included yeast strains AP5 (pCeh351, and pGBT9 vector), AP4 (HD16pGBT9 and pGAD10), AP5 (CeHIP1pACT2 and pGBT9).

2.19 Yeast Two-Hybrid Screen

The yeast strain Y190 was used for all transformations and assays. Yeast transformations were performed using a modified lithium acetate transformation protocol.

Y190 competent cells were transformed with pCeh350 (CeHIP1 in pGBT9). The resulting strain was named AP7. A *C. elegans* cDNA library cloned into pACT2 (kindly provided by Dr. Barstead, Oklahoma Medical Research Foundation) was transformed into AP1. The transformants were plated on sixty 150 mm SC media plates deficient in tryptophan, leucine, and histidine. The herbicide 3-amino-triazole (3-AT) was used to limit the number of false His⁺ positives. The transformants were placed at 30°C for 5 days and β -galactosidase filter assays were performed on all colonies found. Primary His⁺/ β -galactosidase clones were replated and assayed again for His⁺ and the ability to turn blue with the filter assay.

The β -galactosidase chromogenic filter assays were conducted by transferring the yeast colonies onto Whatman filters. To lyse the cells the filters were submerged for 20 seconds in liquid nitrogen. The filters were dried at room temperature for at least 5 minutes and placed onto filter papers presoaked with Z-buffer (100 mM NaPO₄ pH 7.0, 10 mM KCl, 1 mM MgSO₄) supplemented with 50 mM 2-mercaptoethanol and 0.07 mg/ml 5-bromo-4-chloro-3-indolyl β -D-galactoside. Filters were placed at 37°C for up to 8 hours.

Colonies that turned blue were streaked on fresh plates, and let grow at 30°C for 2–5 days. Individual colonies were picked into liquid media and let grow overnight at 30°C. Plasmid DNA was isolated and prepared as described elsewhere.

Chapter III

Results

3.1 *CeHIP1* Gene Structure

The gene structure of *CeHIP1* was determined to allow for subsequent study through a combination of gene disruption and molecular characterization techniques. The physical map location of *CeHIP1* is ZK370.3, on chromosome III. *CeHIP1* spans 4808 nucleotides of genomic DNA. It codes for a 2798 nucleotide transcript that is *trans* spliced to the splice leader sequence SL1 (figures 3.1 and 3.4). For the construction of a green fluorescent protein (GFP) transcriptional reporter, it was necessary to learn if *CeHIP1* possessed its own regulatory elements.

trans splicing is the process by which an identical short leader sequence is spliced onto the 5' end of multiple mRNAs. Some transcription in *C. elegans* is polycistronic, with many open reading frames being transcribed into a single large transcript. *trans* splicing is responsible for separating the long polycistronic transcripts into monocistronic units. Genes that are first in the unit are usually *trans* spliced to the SL1 sequence, with the genes making up the remainder of the polycistronic unit being *trans* spliced to the SL2 sequence. Thus, *trans* splicing to SL1 is usually indicative of a gene possessing its own promoter region directly upstream (Blumenthal, 1988; Evans, 2000; Krause, 1987). This was important to know, as it allowed for analysis of the region directly upstream from *CeHIP1* to be the putative promoter region.

The putative *CeHIP1* promoter region contains two potential PHA-4 binding sites: TGTTTGC at -898 nucleotides, and TGTTTGT at -290 nucleotides (Gaudet and Mango, personal communication, figure 2.2).

PHA-4 is a transcription factor of the forkhead/HNF3 variety, and is expressed in all pharyngeal cells (Horner, 1998; Kalb, 1998). The identification of the possible CeHIP1 promoter region allowed for the construction of a promoter-GFP reporter construct predicted to display pharyngeal expression.

3.2 Homology Studies

The translated CeHIP1 protein is 927 amino acids in length and has a molecular weight of approximately 104 kDa (figures 3.2 and 3.11). Comparison of CeHIP1 to proteins from other species identified regions that are conserved through evolution and are presumed to have shared, important functions. CeHIP1 shows similarity to human HIP1, mouse HIP1R, and yeast Sla2p (table 3.1, figure 3.5).

Computer based analysis of CeHIP1 reveals several distinct domains in the family of CeHIP1 proteins. This group of proteins also share identity with the mammalian cytoskeletal protein talin. Talin is a mammalian cytoskeletal protein found in focal adhesions, protein assemblies mediating interactions between the actin cytoskeleton and the extracellular environment (Burrige, 1983; Hemmings, 1996). The carboxy terminus of each of these proteins contains an actin-binding motif, the I/LWEQ module, which has been shown to bind F-actin *in vitro* (McCann, 1997; McCann, 1999). CeHIP1, and the related proteins have another sequence in common, the ENTH (**E**psin **N**-terminal **h**omology) domain (Kay, 1999). This protein sequence has been found in many eukaryotes, including plants, fungi and animals. The majority of proteins with ENTH

Kyte-Doolittle Hydropathy

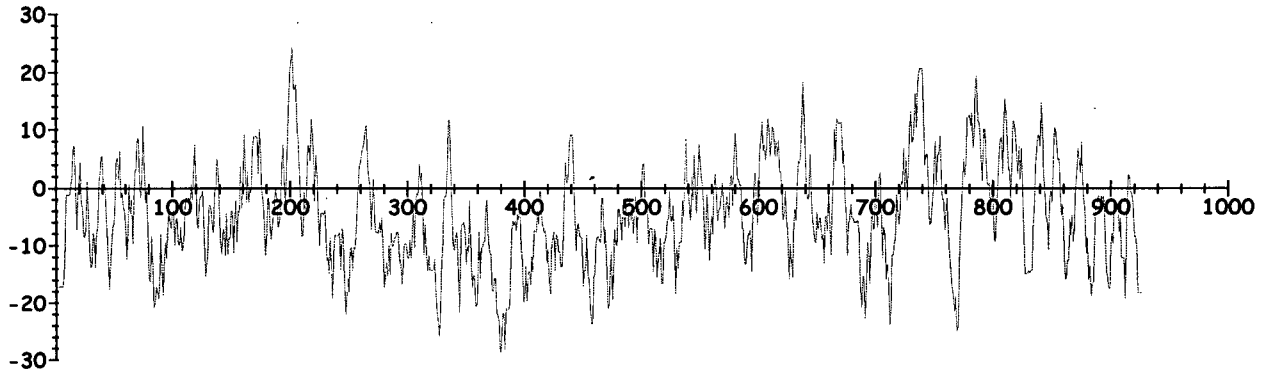


Figure 3.3 Predicted Hydrophobicity of CeHIP1.

The hydropathy of CeHIP1 was predicted using Gene Runner Software based on Kyte, 1982. The X-axis measures the length of the CeHIP1 protein (927 amino acids). The Y-axis is a measure of the relative hydrophobicity of the protein over a discrete interval (Kyte, 1982). This information was used to locate hydrophilic and potentially antigenic areas of CeHIP1. Amino acids 408 to 520 appeared to be hydrophilic and non-homologous to any predicted *C. elegans* proteins. This region was used to raise the polyclonal CeHIP1 antibody.

	HIP1	mHIP1R	Sla2p
CeHIP1	31/49	31/48	21/42

Table 3.1 Summation of Pairwise Sequence Alignment.

The percent identity and similarity of the homologs with CeHIP1 is listed. The first number refers to percent identity, the second refers to percent similarity. HIP1, human Huntingtin Interacting Protein 1. mHIP1R, mouse HIP1 Related protein. Sla2p, yeast homolog of CeHIP1.

domains appear to have functions in endocytosis and regulation of cytoskeleton organization (Kay, 1999). CeHIP1 related proteins possess potential coiled-coil domains, which may be important for protein-protein interaction (Lupas, 1991; Lupas, 1997).

CeHIP1 also shows similarity to the putative ORF F08A8.6 in *C. elegans*. F08A8.6 spans 2486 nucleotides of genomic DNA, with a 1089 nucleotide transcript, and coding for a 362 amino acid protein. Pairwise sequence analysis of CeHIP1 and F08A8.6 reveals that F08A8.6 matches up with the first third of CeHIP1 (figure 3.7). It was important to determine if F08A8.6 was an active gene, as it may have had redundant functions which would complicate analysis of CeHIP1. Additionally, it was important to design a polyclonal antibody that would recognize a non-homologous region of CeHIP1 in the event that F08A8.6 was functional. However, there are no ESTs mapping to F08A8.6, and RT-PCR with mixed stage RNA detects no transcript. It is probable that F08A8.6 is a pseudogene.

This information was used to design pCeh365, a CeHIP1 fusion construct outside of the region of homology to F08A8.6. pCeh365 corresponds to residues 408-520 of the CeHIP1 protein, a region that is non-homologous to any protein in *C. elegans*. Hydropathy analysis of the segment predicts it to be hydrophilic, and thus may promote antigenicity in raising an antibody (figure 3.3).

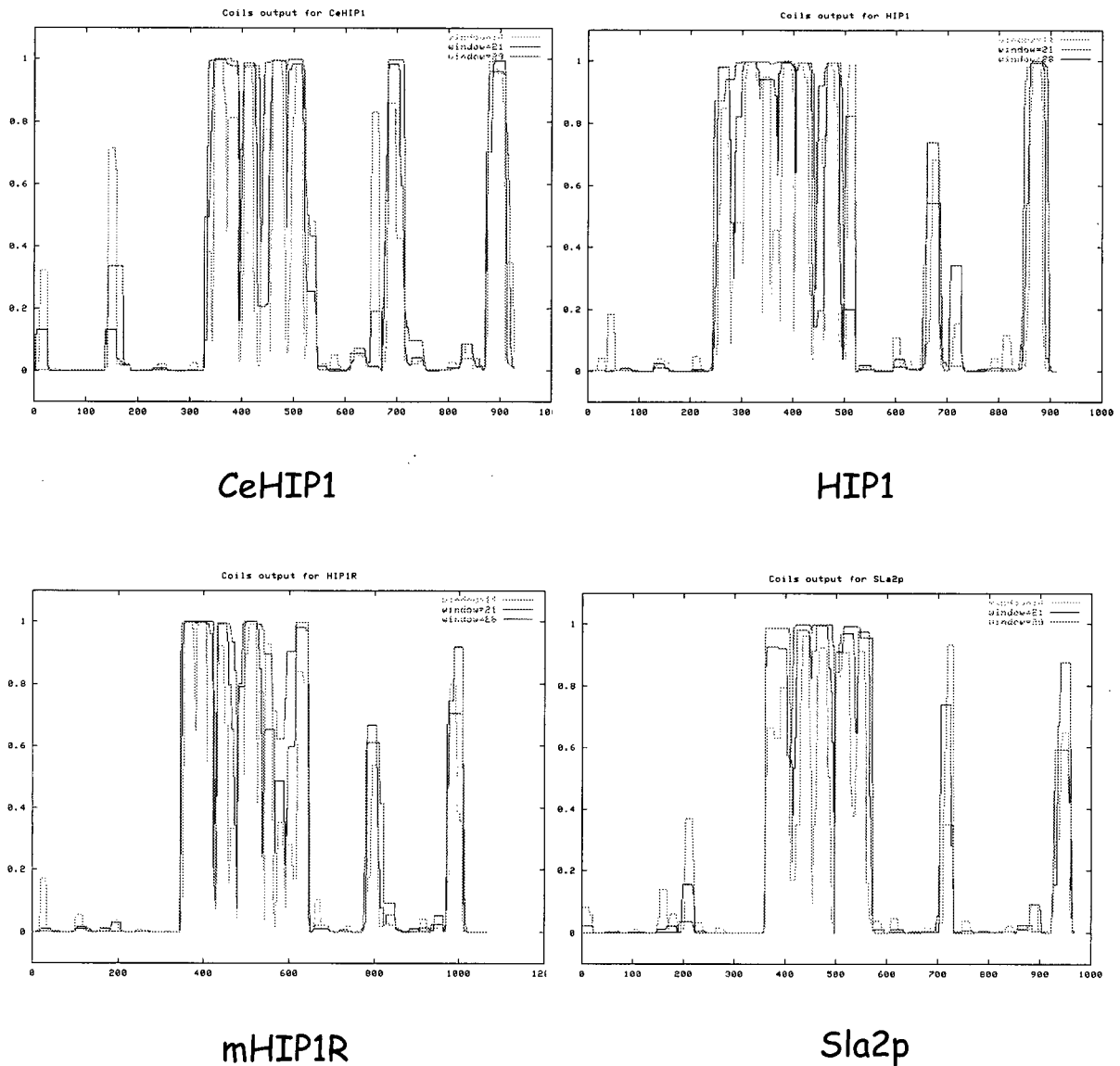


Figure 3.6 Predicted Coiled-Coil Domains.

The COILS program (Lupas et al. 1991) was used to predict potential coiled-coil domains of CeHIP1 and its homologs in humans (HIP1), mouse (mHIP1R), and yeast (Sla2p). The probability of coiled coil formation is plotted as function of the amino acid position in the protein.

3.3 Expression of *CeHIP1*

Several approaches were used to determine the spatial and temporal localization of *CeHIP1* in the nematode.

3.3.1 RT-PCR

RT-PCR experiments reveal that *CeHIP1* is expressed from the first larval stage into adulthood. Transcription could not be detected in embryos (figure 3.4).

3.3.2 GFP Reporter

The *CeHIP1* promoter::GFP reporter, pCeh353, was used to construct several transgenic strains. Fluorescence was detected in the pharynx of fully formed young larvae ready to hatch, and persisted through all successive stages. Fluorescence was also be detected in late larval development during the L4 stage, in the spermatheca, vulva and anal depressor muscles. These structures maintained fluorescence through adulthood (figures 3.8, 3.9, and 3.10).

To see if *CeHIP1* was expressed in male specific structures, the GFP reporter was crossed into KR1088 *dpy-5 (e61) him-1 (e879)* background, and animals from this cross were examined for fluorescence. The *him-1 (e879)* mutation produces males at a frequency greater than the wild type frequency of 1:1000. Hermaphrodites from the newly constructed strain displayed fluorescence identical to previously constructed *CeHIP1*::GFP strains. Males displayed fluorescence in the pharynx, as well as the vas deferens and cloaca (figure 3.10).

3.4 Protein Localization of CeHIP1

With GFP reporter constructs, transcription does not always equal protein localization, and the reporter may not be expressed exactly like the endogenous gene. Most transgenes are silenced in the *C. elegans* germline, which could potentially mask a site of gene action. I produced a polyclonal antibody to study the spatial and temporal localization of CeHIP1 protein in the worm. The polyclonal antibody raised to CeHIP1 recognized a single band of approximately 104 kDa in Westerns of whole worm extracts (figure 3.11). This is the size of the predicted CeHIP1 protein.

Immunofluorescence with a CeHIP1 polyclonal antibody showed a pattern of protein localization that was in agreement with the spatial and temporal expression of the *CeHIP1::GFP* reporter constructs. CeHIP1 protein was observed in the pharynx in young animals, and in the spermatheca and vulval muscles of adult animals (figures 3.12 and 3.13). Protein could not be detected in the anal depressor muscles. This suggests the GFP expression in the anal depressor muscles may be artefactual. Staining was detected also in the gonad of hermaphrodites. The intensity of the staining was weaker relative to that of the somatic gonad. The intensity of staining was greatly improved upon dissection of the gonads from the hermaphrodites (figure 3.14).

Staining of male animals revealed CeHIP1 protein localization in the pharynx as well as the vas deferens and cloaca (figure 3.14). Staining could be detected from just prior to hatching for the pharynx, and from later larval stages (L4) for the vas deferens and cloaca. No staining was observed with preimmune sera, and staining could be extinguished with the inclusion of CeHIP1 protein in immunostaining experiments (data not shown).

Figure 3.10 *CeHIP1* Expression.

Transgenic strains expressing a *CeHIP1::GFP* reporter construct were examined. **A.** DIC image of the head of an adult hermaphrodite. **B.** GFP fluorescence can be observed in the pharynx. **C.** Merged image of A and B. **D.** DIC image of the tail of an adult male. **E.** GFP fluorescence can be observed in the vas deferens and cloaca. **F.** Merged image of D and E. **G.** Fluorescence image of a young adult hermaphrodite. GFP can be detected in the spermathecae (large arrowheads), vulval muscles (small arrow), and the anal depressor muscles (barbed arrow). Scale bar is 50 μm .

3.5 PCR Mapping of Deficiencies

Our laboratory possesses a number of lethal mutations mapping approximately to the same area as *CeHIP1* on LGIII. I decided to use complementation analysis to test if any of these mutations mapped to *CeHIP1*. The first step was to identify deletions that uncovered *CeHIP1*, which would subsequently be used for mapping experiments against the lethal point mutations in our collection. None of the deficiencies tested deleted the *CeHIP1* locus. Except for *nDf17*, the deficiencies tested behaved in accordance with the genetic mapping data. Analysis of *nDf17* reveals that it is not a contiguous deletion, but a complex rearrangement containing coding sequence for *CeHIP1*. I was able to place the left breakpoint of *sDf110* to somewhere between *CeHIP1* and *sma-2*, a region of approximately 30 kb. The results of the PCR mapping of homozygous deficiency embryos are presented in figures 3.15–20, and table 3.2.

The data suggest that it may not be possible to maintain a strain with a deletion of the *CeHIP1* region.

Figure 3.12 CeHIP1 Protein Localization in Developing Embryos.

Polyclonal CeHIP1 antibody was used to stain developing embryos. CeHIP1 protein can be detected in the mature pharynx. Embryo ages are given after Sulston, 1983.

1A. Immunofluorescence of a 700 minute embryo stained with CeHIP1. CeHIP1 can be detected in a pharynx that is nearing maturation. The pharyngeal bulbs are indicated with arrows. **1B.** Nucleic acid staining of embryo in 1A with propidium iodide.

2A. 800 minute embryo on the left, 525 minute embryo on the right (visible in 2B). CeHIP1 protein in a mature pharynx. The pharyngeal bulbs are indicated with arrows.

2B. Nucleic acid staining of embryo in 2A with propidium iodide. Scale bar is 10 μm .

Figure 3.13 CeHIP1 Protein Localization in the Adult Hermaphrodite.

Polyclonal CeHIP1 antibody was used to stain an adult hermaphrodite.

- A. DIC image of the head of an adult hermaphrodite.
- B. Immunofluorescence of a same animal as in (A) stained with a CeHIP1 antibody. CeHIP1 is present in the pharynx.
- C. Immunofluorescence image of CeHIP1 staining in the spermatheca
- D. Immunofluorescence image of CeHIP1 staining in the vulva.

Figure 3.14 CeHIP1 Protein Localization in the Adult Hermaphrodite and Male Gonad.

CeHIP1 antibody was used to stain dissected hermaphrodite gonads in **A - C**. **A**. Immunofluorescence image of CeHIP1 antibody staining, which in the gonad appears to be non-nuclear and may be specific to developing oocytes. **B**. DNA staining of the gonad in **A**. **C**. Merged image. CeHIP1 antibody was used to stain males **D - F**. **D**. CeHIP1 staining can be observed in the vas deferens and cloaca of the male gonad. **E**. DNA staining of the gonad in **D**. **F**. Merged image. Scale bar is 20 μm .

3.6 Reverse Genetic Screen

As it was not possible to map existing mutations to *CeHIP1*, I decided to use a reverse genetics approach to produce a mutation. Three libraries with a total of 1.6×10^6 F1 progeny were screened with 4 *CeHIP1* primer sets. 31 putative deletions were identified in first round screening, 4 of which faithfully resampled. No worms could be isolated bearing these deletions through sib selection. Three of the deletion bands were sequenced: deletion 203 removed 3174 nucleotides, deletion 573 removed 262 nucleotides, and deletion 831 removed 2956 nucleotides. These data are presented in figure 3.21. These deletions were predicted to result in premature stop mutations.

3.7 Overexpression Analysis

The previous data suggested that it may not be possible to recover a null, or hypomorphic mutation of *CeHIP1*. An alternate approach was to engineer a dominant mutation. Overexpression of *CeHIP1* was studied with strain KR3793 that contains the full length *CeHIP1* cDNA behind the heat shock promoter hsp16-2 (Jones, 1989; Stringham, 1992). Upon heat shock, the animals ($40\% \pm 12$) would fail to thrive, and subsequently die. The animals appeared sickly and often contained vacuoles (figure 3.22). Control animals included: heat shocked N2, CB907 *dpy-5*, and a strain carrying the β -galactosidase gene behind the hsp16-2 promoter, did not display any adverse effects. Thus, *CeHIP1* may be a dose sensitive locus, with negative effects on viability of the expression level is perturbed.

LGIII

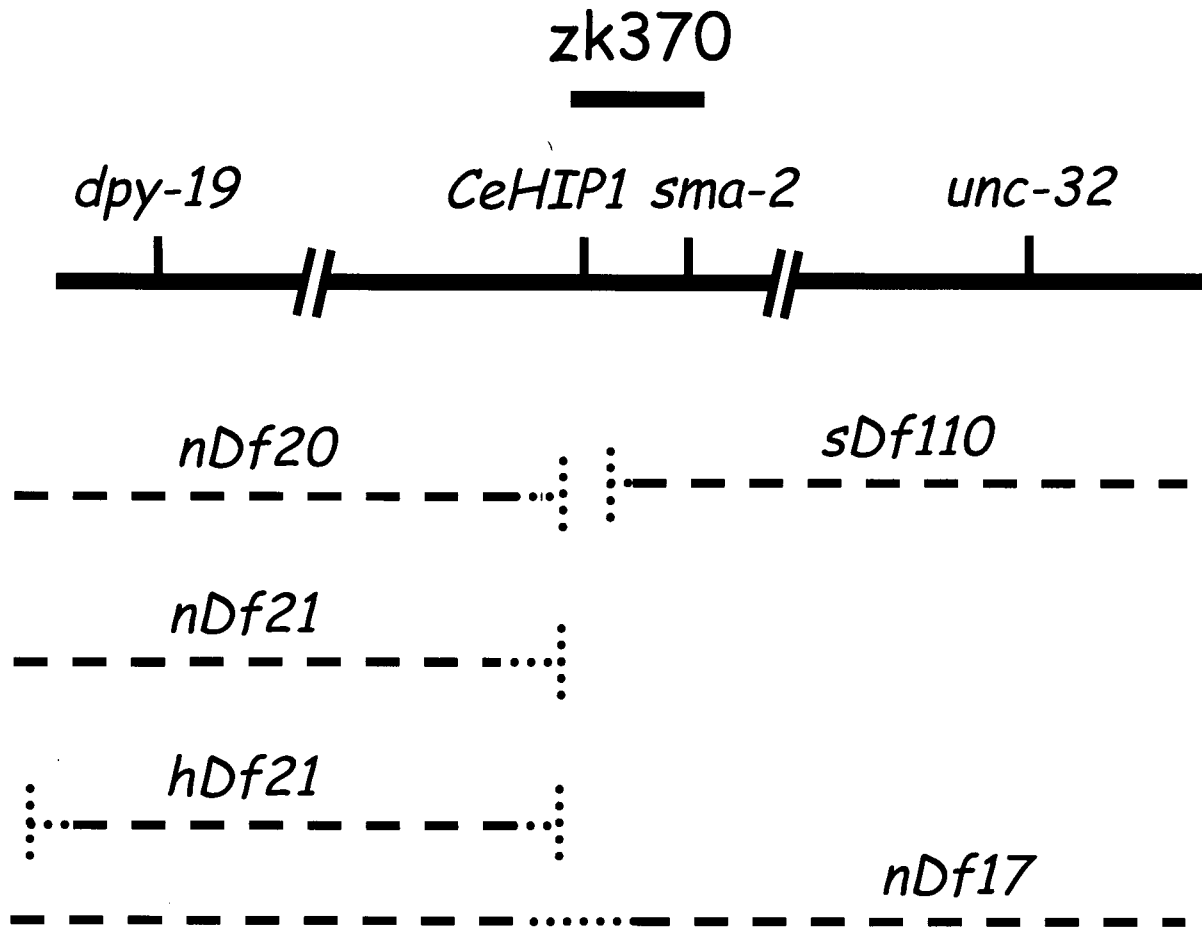


**Figure 3.15 Map of Deficiency Breakpoints
in Relation to *CeHIP1*.**

A map of the endpoints of the deficiencies studies in the PCR mapping experiments is presented. The thick black line represents genomic DNA. DNA deleted by a deficiency is indicated by a dashed line, with dotted lines indicating DNA not deleted by the deficiency.

Primers	Deficiency				
	<i>hDf21</i>	<i>nDf17</i>	<i>nDf20</i>	<i>nDf21</i>	<i>sDf110</i>
KRp 47/94 bli-4 LGI	✓	✓	✓	✓	✓
KRp 112/113 rad-3 LGI	✓	✓	✓	✓	✓
KRp 176/177 dpy-19 LGIII	✓	X	X	X	✓
KRp 178/179 sma-2 LGIII	✓	X	✓	✓	X
KRp 300/301 CeHIP1 LGIII	✓	✓	✓	✓	✓
KRp 347/348 unc-32 LGIII	✓	X	✓	✓	X

Table 3.2 PCR Deficiency Mapping Data.

The results of the mapping of deficiency homozygotes with several primer sets is presented.

✓ indicates amplification, X indicates no amplification

3.8 RNA Interference Analysis

RNAi is a method that allowed for cursory examination of a predicted null phenotype of *CeHIP1*. There is evidence that the method of dsRNA delivery into the worm can affect the efficiency of RNAi (Fraser, 2000; Tavernarakis, 2000; Timmons, 1998). Late acting, and especially neuronally expressed genes, are often resistant to dsRNA injection methods. Methods that allow for the delivery of dsRNA to later stages of development can alleviate this resistance. Several RNAi approaches were used to determine the function of *CeHIP1*. The methods used included the injection of dsRNA into young adult animals, soaking young animals in dsRNA, and creating an inducible transgene capable of producing dsRNA *in vivo*.

The administration of dsRNA by injection and soaking was less successful than transgene expression in generating phenotypes. The presence of a greater than average number of unfertilized oocytes was the only phenotype common to all three approaches (summarized in table 3.3). Additional phenotypes were observed using the transgene-generated dsRNA. This method was used for the analysis of *CeHIP1* function.

Figure 3.22 Overexpression of *CeHIP1*.

Overexpression of *CeHIP1* was studied with transgenic strain KR3793, containing the full length *CeHIP1* cDNA behind the hsp 16-2 promoter. L4 hermaphrodites were heat shocked at 30°C for 60 minutes and let recover for 12-24 hours at 20°C before examination.

40% (\pm 12%) of heat shocked KR3793 animals would fail to thrive and would often die. **A.** This worm appears sickly and contains vacuoles.

B. Close-up of **A.** Vacuoles are indicated with arrowheads.

C. The head of an adult hermaphrodite, vacuoles are also present.

Control animals included: heat shocked N2, CB907 *dpy-5*, and a strain carrying the β -galactosidase gene behind the hsp16-2 promoter, displayed no adverse effects. Scale bar is 50 μ m.

3.8.1 Fertilization Effects

RNAi treated animals displayed an increase in the number of unfertilized oocytes laid, which is summarized in table 3.3. This effect is most pronounced approximately 48 hours after the first egg is laid.

Immunostaining of wild type animals shows CeHIP1 protein is localized to the spermatheca. CeHIP1 antibody does not stain sperm. RNAi treated animals show a loss of CeHIP1 staining in the spermatheca, and have a decreased sperm count, with fewer sperm residing in the spermatheca. Control animals have staining of the spermatheca, and a normal sperm count. Additionally, staining of the hermaphrodite germline is also lost after RNAi treatment (figure 3.23).

The appearance of unfertilized oocytes often indicates a sperm defect. In efforts to identify the nature of the fertilization error, several outcross experiments were conducted. If the hermaphrodite sperm were defective, then outcrossing should rescue the unfertilized oocyte phenotype. Partial, or no rescue would occur if the hermaphrodite oocytes were defective. Mating of *CeHIP1* RNAi treated hermaphrodites with wild type and *CeHIP1* RNAi treated males rescued the unfertilized oocyte phenotype. Thus, male sperm is capable of fertilizing the oocytes of RNAi treated animals. The defect resides in some aspect of hermaphrodite sperm function (table 3.4).

Gene Disruption Approach	Unfertilized oocytes	Number of trials
KR3761 hsp16-2 _p CeHIP1 (IR) transgene + heat shock	68 ± 13	10
KR3792 hsp16-2 _p CeHIP1 (IR) integrated + heat shock	67 ± 11	5
dsRNA CeHIP1 injection	13 ± 5	8
dsRNA dpy-5 injection	80 ± 10	4
dsRNA CeHIP1 soaking	8 ± 4	6
dsRNA dpy-5 soaking	64 ± 13	4

Controls		
1× IM Buffer injection	3 ± 1	4
1× IM Buffer soaking	2 ± 1	4
KR3761 hsp16-2 _p CeHIP1 (IR) transgene - heat shock	3.0 ± 0.5	4
KR3792 hsp16-2 _p CeHIP1 (IR) integrated - heat shock	2.0 ± 1.5	4
N2 + heat shock	15 ± 6	4
CB907 (<i>e907</i>) + heat shock	20 ± 8	4
hsp16-2 _p β-galactosidase + heat shock	8 ± 2	4

Table 3.3 Comparison of RNA Interference Methods; Injection, Soaking and *in vivo*.

Unfertilized oocytes laid are given as percentage of total progeny.

The Dpy-5 phenotype was scored for *dpy-5* RNAi. For heat shock experiments, L1 to L3 larvae were heat shocked at 35°C for 4 hours.

After heat shock, animals were allowed to recover overnight at 20°C, and transferred every day and assayed for various defects. 10-15 animals were used per trial.

Mating Condition	Percentage Unfertilized Oocytes	Number of trials
KR3761 hsp16-2 _p <i>CeHIP1</i> (IR) transgene + heatshock × N2 males - heatshock	2 ± 1	3
KR3761 hsp16-2 _p <i>CeHIP1</i> (IR) transgene + heatshock × N2 males + heatshock	3 ± 1	3
KR3792 hsp16-2 _p <i>CeHIP1</i> (IR) integrated + heatshock × KR3792 males - heatshock	2 ± 1	3
KR3792 hsp16-2 _p <i>CeHIP1</i> (IR) integrated + heatshock × KR3792 males + heatshock	2 ± 1	3

Table 3.4 Outcrossing of *CeHIP1* RNAi Hermaphrodites.

CeHIP1 RNAi treated hermaphrodites were mated to either N2 or KR3792 males (\pm heatshock) and scored for the presence of unfertilized oocytes, presented here as a percentage of progeny laid. Heatshock conditions: L1 to L3 animals were heat shocked at 35°C for 4 hours and allowed to recover at 20°C until the males reached sexual maturity. 15-20 separately RNAi treated hermaphrodites were plated with an excess of males (~ 3 males for every hermaphrodite) over several NGM dot plates and incubated overnight at 20°C to allow for mating. Hermaphrodites were transferred individually to new NGM plates and subsequently transferred every 16-24 hours and scored for the unfertilized oocyte phenotype.

Figure 3.23 The Effect of RNAi on CeHIP1 Protein Localization in the Gonad.

To assess the effects of *CeHIP1* RNAi, L1 to L3 hermaphrodites transgenic KR3792 animals were heatshocked at 35 °C for 4 hours and let recover at 20 °C until mature.

The spermathecae in A through F were fixed and stained as described in 2.15.4. The gonads in G through L were dissected, fixed and stained as described in 2.15.5. A. Wild type spermatheca stained with CeHIP1 antibody. B. DNA staining of sperm nuclei with propidium iodide. C. Merged image. D. Spermatheca of a RNAi treated animal stained with CeHIP1 antibody. E. DNA staining of sperm nuclei with propidium iodide. F. Merged image. G. Wild type hermaphrodite gonad stained with CeHIP1 antibody. H. DNA staining of germline nuclei with propidium iodide. I. Merged image. J. Gonad staining of a RNAi treated animal with CeHIP1 antibody. K. DNA staining of germline nuclei with propidium iodide. L. Merged image.

To determine if the loss of CeHIP1 after RNAi treatment was due to depletion of CeHIP1 protein or a loss of the spermatheca, treated animals were stained with a polyclonal antibody to HSP25. HSP25 is a small heat shock protein that is associated with the dense bodies of *C. elegans* muscle, the lining of the pharynx and to the junctions between cells of the spermathecal wall of adult animals (Ding and Candido, 2000). Staining of RNAi treated animals with the HSP25 polyclonal antibody shows that the spermatheca is still present (not shown). The loss of CeHIP1 staining is due to RNAi treatment and not to a failure in the development of the spermatheca.

3.8.2 Egg Laying Deficiency Observed after *CeHIP1* RNAi

Another phenotype observed after RNAi treatment of young hermaphrodites is an egg laying deficiency, which is summarized in table 3.5. The animals retain a greater number of embryos than in either wild type or controls. Embryos are not retained indefinitely and larvae have not been observed to hatch within the hermaphrodite. Immunostaining of wild type animals shows CeHIP1 protein localization in the vulval muscles, shown in figure 3.24, which is subsequently lost in RNAi treated animals (not shown). Control animals do not display an egg laying phenotype or a loss of vulval staining.

3.8.3 *CeHIP1* RNAi Deforms the Mature Pharynx

The pharynxes of RNAi treated animals are malformed, which is summarized in table 3.5. The pharynxes are often recurved and show a loss of structural integrity. They do not display the typical smooth, dual bulbs. Instead, they appear rough and loose. This phenotype can be observed through DIC optics, and is readily apparent through immunostaining (figure 3.25). This phenotype is not observed in any of the controls.

Gene Disruption Approach	Phenotype scored	Frequency Observed	Trials
KR3761 hsp16-2 _p <i>CeHIP1</i> (IR) transgene + heat shock	Egg laying defect	58 +/- 7	5
KR3761 hsp16-2 _p <i>CeHIP1</i> (IR) transgene - heat shock	Egg laying defect	10 +/- 2	4
N2 + heat shock	Egg laying defect	8 +/- 2	4
CB907 (<i>e907</i>) + heat shock	Egg laying defect	8 +/- 3	4
hsp16-2 _p β-galactosidase + heat shock	Egg laying defect	6 +/- 2	4
KR3761 hsp16-2 _p <i>CeHIP1</i> (IR) transgene + heat shock	Malformed pharynx	54 +/- 12	7
KR3761 hsp16-2 _p <i>CeHIP1</i> (IR) transgene - heat shock	Malformed pharynx	0	4
N2 + heat shock	Malformed pharynx	0	4
CB907 (<i>e907</i>) + heat shock	Malformed pharynx	0	4
hsp16-2 _p β-galactosidase + heat shock	Malformed pharynx	0	4

Table 3.5 Additional Phenotypes of *CeHIP1* RNAi.

Phenotypes observed are given as percentage of animals tested. L1 to L3 hermaphrodites were heat shocked at 35°C for 4 hours and let recover overnight at 20°C. The animals were transferred every 12-16 hours and examined for defects. 10-15 animals were used per trial.

Figure 3.24 The Effect of *CeHIP1*

RNAi on Egg Laying.

L1 to L3 hermaphrodites were heat shocked at 35°C for 4 hours and allowed to recover overnight at 20°C. The animals were transferred every 12-16 hours and examined for retention of embryos.

A. Heatshocked N2 hermaphrodite. This animal does not display any defects.

B. RNAi treated animal. This animal displays an egg laying deficiency as it is retaining a greater of embryos than wild type. Scale bar is 100 μm .

Figure 3.25 RNAi Effects on Pharyngeal Morphology.

To assess the effects of *CeHIP1* RNAi, L1 to L3 hermaphrodites transgenic KR3792 animals were heatshocked at 35 °C for 4 hours and let recover at 20 °C until mature. The animals in A and B were examined with DIC optics (2.3). The animals in D through I were fixed, stained, and examined as described in 2.3 and 2.15.4.

A. Wild type pharynx of a N2 adult hermaphrodite. B. The deformed pharynx of a *CeHIP1* RNAi treated adult hermaphrodite. The dashed line outlines the pharynx. C. Diagram of a wild type pharynx. D. Immunofluorescence image of a wild type pharynx stained with *CeHIP1* antibody. E. DNA staining of cell nuclei with propidium iodide. F. Merged image of D and E. G. Immunofluorescence image of a *CeHIP1* RNAi treated animal stained with *CeHIP1* antibody. H. DNA staining of cell nuclei with propidium iodide. I. Merged image of G and H.

3.9 Testing for CeHIP1 Interaction with Human Huntingtin

I wanted to determine if CeHIP1 was functionally equivalent to human HIP1 its ability to bind huntingtin. A two-hybrid system was used to test for a potential interaction between CeHIP1 and human huntingtin. CeHIP1 does not interact with human huntingtin (figure 3.26).

3.10 Yeast Two-Hybrid Screen

When this experiment was conducted, the *C. elegans* genome sequence was not complete. There existed the possibility of the nematode possessing a version of huntingtin. A yeast two-hybrid screen was conducted to identify interacting protein partners of CeHIP1. A *C. elegans* huntingtin homologue was not found. To date, the various sequencing projects have shown that huntingtin may be an evolutionary addition to vertebrates alone.

Approximately 5×10^5 clones of a *C. elegans* cDNA library were screened for interacting protein partners of CeHIP1. Seventeen positive clones were isolated from the screen. Upon retransformation and partial sequencing, 2 positive clones were identified (figure 3.27). The first clone corresponds to ORF F45E12.2 (represented twice). F45E12.2 maps to LGII, spanning 2558 nucleotides, with 7 exons coding for a 2280 nucleotide message and a 759 amino acid protein. It shows homology to TFIIB, a member of the class of general transcription initiation factors (Conaway, 1999).

The second clone represents ORF T05C12.10 (isolated nine times). T05C12.10 spans 4859 nucleotides of genomic DNA, and contains 12 exons coding for a 3624 nucleotide transcript and a 1207 amino acid protein. A portion of the protein shares

homology with the autocatalytic domain of *Drosophila hedgehog* protein (Hammerschmidt, 1997). T05C12.10 is a member of a large family of genes in the nematode with homology to *hedgehog* (Aspöck, 1999; Burglin, 1996).

The interaction between CeHIP1 and the interacting proteins was mapped to the carboxy terminus of CeHIP1 (figures 3.28 and 3.29).

3.10.1 Mutants Obtained

There were no known mutations mapping to the two ORFs. As a result, the two ORFs were submitted to the *C. elegans* Gene KO Consortium for gene knockout. Two strains were isolated bearing deletions of the ORFs. Strain VC28 *gk17* contains a 1333 nucleotide deletion of F45E12.2. Animals homozygous for this mutation arrest in the second larval stage. The second strain, VC42 *gk32* contains a deletion of 119 nucleotide of T05C12.10. Homozygous deletion animals arrest in the second larval stage.

Chapter IV

Discussion

4.1 Introduction

The goal of this thesis was to determine the function of the *HIP1* related gene *CeHIP1* in a simple animal system. Through understanding the role of *CeHIP1* in *C. elegans*, it may be possible to understand what human *HIP1* does, and to determine its relationship to Huntington disease.

In this thesis I have presented evidence supporting the following conclusions that *CeHIP1* may be a dose sensitive locus and that *CeHIP1* has multiple functions in the nematode, including roles in fertilization, egg laying, and promoting pharyngeal morphology. In this discussion I will examine the basis of these conclusions. I will finish with an examination of the knowledge gained from this thesis and its contribution to the study of the related genes in other species.

4.2 CeHIP1 and the Nematode

CeHIP1 appears to have multiple roles in the nematode. It is not ubiquitously expressed like mHIP1R, but is found in distinct tissue types and appears more similar to HIP1 in this respect. As *CeHIP1* is found in different tissues, and has multiple effects as assayed through RNAi, I will examine each function in turn.

4.2.1 *CeHIP1* and Fertilization

CeHIP1 protein can be detected in the germline and somatic structures of the *C. elegans* gonad. Staining can be observed in developing oocytes, where CeHIP1 is found to be non-nuclear. CeHIP1 is abundant in the spermatheca, a structure that houses mature sperm and facilitates ovulation and fertilization. In males, CeHIP1 can be observed in the vas deferens and the cloaca.

Among other things, *CeHIP1* RNAi hermaphrodites have a decreased sperm count, and lay a large number of unfertilized oocytes. It would appear that the coordination of events is perturbed when CeHIP1 protein has been depleted from the gonad. I will present a brief overview of *C. elegans* germline development and fertilization.

4.2.1.1 Anatomy of the Adult Gonad

The adult hermaphrodite reproductive system is composed of two tubular ovotestes, anterior and posterior. They are joined centrally by two spermathecae and a uterus. The uterus opens mid-ventrally to the exterior through the vulva (figure 3.8). The adult male reproductive system consists of a tubular testis that is connected to the cloaca through the seminal vesicle and vas deferens (figure 3.9). The hermaphrodite ovotestis and the male testis are essentially U-shaped tubes possessing distal and proximal arms. The distal-proximal axis refers to the relative position along the tubular gonad. A distal structure is defined as being further from the gonadal opening than a proximal structure. The gonadal opening is the vulva in hermaphrodites, and the cloaca in males (Hirsh et al., 1976; Kimble et al., 1979; Klass et al., 1976).

The distal arm, for both sexes, is composed primarily of immature germline tissue. The germline nuclei of the distal arm are composed of mitotic nuclei most distally and meiotic nuclei more proximally. The nuclei in meiosis progress from leptotene distally through diplotene of meiotic prophase I proximally. In both sexes, gametogenesis occurs in the proximal arm. For hermaphrodites, a somatic contractile sheath, or oviduct encapsulates the germline of this arm. In males, the germline is partially ensheathed by the distal cells of the seminal vesicle (Kimble and White, 1981; Wolf et al., 1978).

Sperm are generated continuously in males, whereas they are produced only briefly in hermaphrodites. Approximately 150 sperm are produced at the proximal edge of the proximal arm of each ovotestis. Once this is done, germ cell differentiation switches to oogenesis, thereafter only oocytes are produced (Klass et al., 1976).

Oocyte maturation, ovulation and successful fertilization require careful coordination of the somatic gonad and the germ cells to ensure that proper embryonic development occurs. Oocytes in mature wild type hermaphrodites mature in an assembly line manner, and undergo several stereotyped events (McCarter et al., 1999). The first noticeable change in the oocyte is breakdown of the nucleolus. As the oocyte moves to the proximal region of the gonad, its volume increases and the nucleus moves distally. Just prior to ovulation, the oocyte nuclear membrane breaks down, and the gonadal sheath cells increase their contractions. Ovulation now occurs and the spermathecal valve dilates and the oocyte passes into the spermatheca where it is fertilized (McCarter et al., 1999).

Oocytes will arrest at diakinesis of prophase I if there are no sperm present for fertilization. This occurs normally in older hermaphrodites that have exhausted their supply of sperm, or in mutant animals that are feminized and produce no sperm. The rate of ovulation for a worm lacking sperm is 1:40 of that of a worm containing sperm (McCarter et al., 1999). Oocytes can be released from arrest by the introduction of sperm through mating; the oocyte will complete maturation, ovulate and be fertilized. The signals to mature and ovulate occur independently of fertilization. It may be that the signal to arrest maturation and ovulation is mediated through the somatic gonad.

Depletion of CeHIP1 from the hermaphrodite gonad results in a fertilization error. A number of oocytes are not fertilized and escape the signal to arrest, and instead pass through the uterus and are laid. RNAi treated hermaphrodites also appear to contain fewer sperm within the spermatheca when compared to control animals. As CeHIP1 protein is found in both germline and somatic structures, there are multiple interpretations of the RNAi phenotype. Depletion of CeHIP1 protein may result in an impairment of cytoskeletal or endocytic functioning. I will examine each of these components in turn.

4.2.1.2 The Spermatheca

The 24 cells that make up the spermatheca are born in the middle of the fourth larval stage. The cells form two groups: 8 distal cells aligned in two rows form a narrow corridor to the gonad arm, while 16 proximal cells form a wider bag-like chamber (Hirsh, 1976; Kimble, 1979). Sperm become located within the spermatheca adjacent to its inner membrane. The structure has a constriction at the distal end connecting the oviduct, and a complex valve at the proximal end connecting to the uterus. When an oocyte matures

in the oviduct, it is pushed up against the constriction by contractions of the oviduct sheath, and is ultimately pushed through by stronger contractions from the sheath. Multiple sperm make contact with the oocyte as it enters the spermatheca, but only one sperm penetrates and fertilizes the egg (Ward and Carrel, 1979). Fertilization of the egg can be recognized by a sudden increase in granule movement in the egg cytoplasm followed by formation of the eggshell. The fertilized egg remains in the spermatheca for several minutes. To enter the uterus, the egg must pass through an elaborate valve at the proximal end of the spermatheca. The valve consists of a single cell with 4 nuclei. The cytoplasm of this cell contains an annulus of filamentous material, which has elaborate folds of plasma membrane on the inside surface of the plasma membrane (Hirsh et al., 1976; Kimble and Hirsh, 1979). The valve opening expands to several times its diameter as an egg passes through. Often, a few sperm are swept along with the egg through to the uterus. These sperm usually migrate back through the valve and resume lodging within the spermatheca (Hirsh et al., 1976; Ward and Carrel, 1979).

Spermathecal cells contain actin, but myosin, however, has not been detected (Strome, 1986). The microfilaments of the cells are predominantly circumferential, which is suited to the task of dilation during ovulation, rather than longitudinal contraction (as exhibited by the sheath cells, whose microfilaments run longitudinally).

4.2.1.3 Fertilization Errors

A number of oocytes that are made in aged hermaphrodites depleted of sperm, or in mutants with defective sperm, undergo partial maturation as they pass through the spermatheca. The oocytes lose their nuclear membrane and resume meiosis. No eggshell is formed, and the characteristic movements of the cytoplasmic granules are reduced or absent, implying that sperm contact is required for these processes (McCarter et al., 1999). Upon entering the uterus, the oocyte undergoes nuclear division without cytokinesis or karyokinesis to produce a highly polyploid cell, which is expelled through the vulva. The appearance of such oocytes from young hermaphrodites is often an indication of a sperm defect (L'Hernault et al., 1988).

A related phenotype, Emo (endomitotic in the gonad arm) is an indication of defective ovulation. Mutants with polyploid oocytes due to endomitosis arise frequently in recessive sterile screens and are now beginning to be characterized. Some Emo mutants include: *ceh-18 (mg57)* which encodes a POU-domain homeobox (Greenstein et al., 1994), certain alleles of *emo-1* which encodes a homolog of Sec61 γ (Iwasaki et al., 1996), *lin-3* which encodes a protein similar to the EGF family (Hill et al., 1992; Katz et al., 1995), *let-23* which encodes an EGF-receptor class tyrosine kinase (Aroian et al., 1991; Aroian et al., 1994), and *mup-2* which encodes a troponin T homolog (Myers et al., 1996). The Emo phenotype can arise from germ-line or somatic defects; mosaic analysis of *emo-1* indicates a germ-line focus, where CEH-18 is found in the sheath cell nuclei. Laser ablation of certain cells of the somatic gonad can result in the Emo phenotype. Ablation of cells in mid L4 of the fourth and fifth pairs of sheath cells, and of the distal spermathecal cells results in an Emo phenotype (McCarter et al., 1997).

These results indicated that the cells along the narrow corridor linking the oviduct to the spermatheca are essential to prevent Emo sterility into L4 and possibly adulthood. A current hypothesis is that the maturing oocyte signals the surrounding sheath and spermathecal cells to trigger ovulation. Failure of this process traps the mature oocyte in the gonad where it undergoes mitotic cycling (McCarter et al., 1997; McCarter et al., 1999).

4.2.1.4 Receptor Mediated Endocytosis in the Oocyte

CeHIP1 protein can be detected in developing oocytes in the gonad. The localization is non-nuclear but it is difficult to determine the cellular localization beyond that. The role of CeHIP1 in the oocyte is unclear, but it may have a structural role as suggested from its cytoskeletal contribution in other systems (Engqvist-Goldstein et al., 2000; Holtzman et al., 1993).

Receptor mediated endocytosis has recently been described as an important mechanism of yolk-protein uptake in oocytes (Grant et al., 1999). *C. elegans* yolk is secreted from the intestine into the pseudocoelomic space and is ultimately taken up into vesicles within the developing oocytes (Kimble and Sulston, 1983; Sharrock et al., 1983). A combination of GFP tagged proteins and RNAi was used to demonstrate the role of orthologs of several proteins involved in the secretory and endocytic pathways of other organisms. These included homologs of the clathrin heavy chain, dynamin, adaptins, and subunits of the adaptor complex AP2. A screen was developed using transgenic strains expressing vitellogenin::GFP to monitor yolk endocytosis, and several mutants were isolated. Vitellogenins are one of the most abundant proteins in developing embryos

(Sharrock et al., 1983). One mutant identified was *rme-2*, a new member of the low-density lipoprotein receptor superfamily which is the *C. elegans* yolk receptor (Grant et al., 1999).

CeHIP1 may contribute to a receptor mediated endocytosis pathway to coordinate signaling necessary for fertilization. The effect of CeHIP1 RNAi may have several components that add up to the laying of unfertilized oocytes as a phenotype. The amount of sperm present in the spermatheca is depleted, which would ordinarily result in a signal to halt ovulation. This signal is missing, and oocytes continue to mature but are not fertilized and are expelled from the animal. As CeHIP1 protein is present in the spermatheca and developing oocytes, it may be a component of this signaling pathway to promote fertilization.

4.2.1.5 Sperm Depletion

The reason for the reduction in the number of sperm housed in the spermatheca is not understood. One possibility is that the sperm are not crawling back into the spermatheca after they have been swept into the uterus by a passing fertilized egg. These sperm would be ultimately lost as they are expelled through the vulva as eggs are laid.

Hermaphrodite and male spermatozoa both crawl to locate themselves properly in the spermatheca. The signal that attracts the sperm to the spermatheca is unknown. There are several mutants (*spe-8* and *spe-12*) in which sperm are rapidly displaced from the spermatheca into the uterus by passing oocytes, and have great difficulty returning to the spermatheca afterwards (L'Hernault et al., 1988). CeHIP1 may be involved in presenting and maintaining the signal on the spermathecal membrane. This is not without

precedent, as SLA2 had been identified as Mop2p, a protein essential for the presentation and maintenance of an ATPase on the surface of the plasma membrane (Na et al., 1995). Thus, it is possible that the signal which would ordinarily direct spermatozoa to the spermatheca, and retain them, is depleted in *CeHIP1* RNAi animals. As fertilized oocytes pass through the spermatheca, a number of sperm would be swept into the uterus. The signal for the sperm to return to the spermatheca may be compromised, and as a result over successive rounds of ovulation, fertilization and egg laying, the normal number of hermaphrodite sperm could be reduced. As well, the signal to halt ovulation may also be damaged with the end result being the laying of unfertilized, endomitotic oocytes. A model for the fertilization error is presented in figure 4.1.

4.2.1.6 Outcrossing Rescues the RNAi Phenotype; Therefore, Not a Sperm Defect

An experiment that lends support to this model is the outcrossing of RNAi treated hermaphrodites. Successful mating with both wild type and *CeHIP1* RNAi treated males rescues the unfertilized oocyte phenotype. A new batch of sperm is introduced, and can now fertilize the oocytes. Male sperm is functionally, but not morphologically distinct from hermaphrodite sperm (LaMunyon et al., 1995).

When a male copulates with a hermaphrodite, the sperm is deposited through the vulva among the fertilized eggs in the uterus. The sperm then crawl among the eggs the length of the uterus, navigate past the valve and into the spermatheca. Male sperm will outcompete any hermaphrodite sperm present and preferentially fertilize the oocytes

Figure 4.1 Depletion of CeHIP1 from the Gonad Results in the Production of Unfertilized Oocytes.

A model for the series of events that leads to the appearance of unfertilized oocytes after CeHIP1 RNAI treatment is presented. **A.** A maturing oocyte is pushed into the spermatheca by sheath contractions. **B.** Multiple sperm contact the oocyte, one of which will successfully fertilize the oocyte. **C.** The proximal spermathecal valve opens and the fertilized oocyte moves into the uterus and number of sperm are swept along with it. **D.** The spermathecal valve closes and the sperm within the uterus that would ordinarily swim back to the spermatheca, fail to do so. **E.** The sperm within the uterus are swept out of the animal as the eggs are laid. **F.** After successive rounds of fertilization and egg laying, the normal complement of hermaphrodite sperm is depleted. This would normally result in a halting of ovulation. This does not occur, perhaps because of the loss of a CeHIP1 mitigated signal. Ovulation continues and the oocytes are pushed through into the spermatheca. **G.** The lack of sperm results in a failure to fertilize. **H.** The unfertilized oocyte is pushed into the uterus. **I.** A number of unfertilized oocytes are laid.

(LaMunyon et al., 1999). Predominantly outcross progeny are produced until the male sperm are depleted, at which time self-progeny will appear. The basis of male sperm competitive superiority is unknown; fertilization is not required, but motility is (Singson et al., 1999).

The male sperm may follow a different signal, which allows them to take up a more favorable position in the spermatheca. Male sperm are not affected by the loss of CeHIP1 in RNAi hermaphrodites, and rescue the unfertilized oocyte phenotype. The phenotype recurs upon the depletion of male sperm.

Additionally, the integrity of the spermatheca may be compromised; it can no longer hold maturing oocytes back, and they are pushed through the spermatheca by continued sheath contractions and into the uterus.

4.2.1.7 *CeHIP1* Promotes Fertilization in *C. elegans*

CeHIP1 has a role in the somatic gonad to facilitate signaling required for coordination of the events necessary to produce an embryo. In this case, CeHIP1 would be responsible for presenting, maintaining, and recycling the appropriate signals and receptors. This would explain why there are several, apparently separate consequences of the removal of CeHIP1. Mature sperm may not faithfully recognize the spermatheca, resulting in their random loss. The oocytes may not receive the signal that the system is in error, and continue maturation and ovulation, and after fertilization has failed may be subsequently ejected as endomitotic oocytes.

4.2.2 Egg Laying and *CeHIP1*

Egg laying is a complex behavior that is controlled by 16 specialized muscle cells: 8 uterine muscle cells and 8 vulval muscle cells. The uterine muscles are aligned circumferentially around the uterus and presumably squeeze eggs toward the vulva. The vulval muscle cells are arranged in a cross and contract to expand the uterus and open the vulva, facilitating egg laying (Hirsh et al., 1976; Kimble and Sulston, 1979; Sulston and Horvitz, 1977).

Two types of neurons synapse onto the sex muscles: the two HSN cells and the six VC motor neurons. Laser ablation of both HSN neurons results in animals that fail to lay eggs. The eggs are retained in the uterus and the animals become severely bloated (Trent et al., 1983). Dominant mutations of the *egl-1* gene cause the HSN's to undergo programmed cell death in hermaphrodites, causing an egg-laying defect (Conradt et al., 1998). Ablation of the six VC, or just one of the HSN neurons does not result in any noticeable effect on egg laying.

Numerous stimuli can affect the rate of egg laying, including the presence of food; hermaphrodites will lay more eggs in the presence of bacteria. Several pharmacological agents have been identified that stimulate egg laying in the absence of food. These include acetylcholine, octopamine, and serotonin. Cholinergic activity stimulates egg laying, and octopamine inhibits egg laying. Serotonin stimulates egg laying, as does imipramine, a drug that potentiates endogenous serotonin by preventing serotonin reuptake (Horvitz et al., 1982). The source of the endogenous serotonin activity is likely the HSN neurons. The HSN neurons stain with an antiserotonin

antibody, and when the HSN neurons have been ablated, egg laying can be reestablished in response to serotonin, but not imipramine.

RNAi treated animals display an egg laying (Egl) defective phenotype. The animals retain a greater number of embryos than either wild type or controls. Embryos are not retained indefinitely and larvae have not been observed to hatch within the hermaphrodite. CeHIP1 protein can be observed in the vulval muscles through immunostaining. This staining is subsequently lost in RNAi treated animals. It is likely that CeHIP1 has a role in vulval muscle contraction to promote proper egg laying. When CeHIP1 protein is depleted the animals display a hindered egg laying behavior. It may be that the embryos are simply pushed out when there are too many within the uterus. Egg laying is a redundant process, and it is obvious that RNAi of *CeHIP1* does not shut the process down, but results in an inefficiency.

Numerous egg laying defective mutants in the three basic components of the egg-laying system (vulva, sex muscles, and neurons) have been identified from various screens (Trent et al., 1983). CeHIP1 seems to be present in the vulval muscles. At this point it is not clear what role CeHIP1 has in these cells, but the depletion of the protein can impair normal egg laying. CeHIP1 may contribute to the structural integrity of the vulval muscles, which is compromised in the RNAi animals leading to impaired muscle function. The putative endocytic function of CeHIP1 may also be important. As may be similar for the pharynx, the vulval muscles may have a requirement for endocytosis for signaling or the recycling of, as yet, unidentified molecules for proper functioning.

4.2.3 The Role of *CeHIP1* in Pharynx Development and Function

C. elegans is an obligatory predator, and it uses its pharynx to ingest anything smaller than the opening of its buccal cavity. The pharynx is a self-contained neuromuscular pump, and is a prominent feature of the *C. elegans* head (reviewed in Wood, 1988). It is composed of 80 nuclei: 5 belonging to gland cells, 18 to miscellaneous structures, 37 to muscle cells, and 20 to pharyngeal neurons (Albertson and Thomson, 1975; Avery, 1993). The cells are arranged into 4 distinct regions: the anterior procorpus, a bulb shaped metacarpus, a cylindrical isthmus, and a terminal bulb. See figure 3.25 A and C. The structural organization of the pharynx shows triradial symmetry; cross sectioning shows a central lumen with three muscles arranged around it. The entire structure is surrounded by a basement membrane, isolating it from the rest of the animal. The 20 neurons constitute the pharyngeal nervous system, which is self-contained. There is one bilaterally symmetric pair of connections between the pharyngeal nervous system and the extrapharyngeal nervous system, but this connection is dispensable for normal feeding (Avery and Horvitz, 1989; Avery, 1993). Of the 20 pharyngeal neurons, only M4 is essential for viability (Avery and Horvitz, 1989). A worm lacking the remaining 19 neurons is viable and fertile, although many do not display normal growth rates and fertility levels (Avery, 1993).

The pharynx undergoes an orchestrated set of motions to take up food, grind it, add digestive enzymes and transport the food through a valve into the intestine. The nematode feeds almost constantly during its life cycle, except during the molt, or when it enters the resistant dauer larval stage. At these times, a mechanism for the inhibition of pharyngeal pumping is required (reviewed in Riddle, 1997 and Wood, 1988).

The development of the pharynx is complex. It is not clear how multiple cell types from distinct cell lineages are specified and assembled into a functioning organ. Organogenesis depends on complex patterns of morphogenesis and differentiation, often arising from interactions between adjacent tissues. The *C. elegans* pharynx is generated by two early blastomeres, ABa and MS (Sulston et al., 1983). Each blastomere gives rise to multiple cell types within the pharynx, but they use different genetic programs. Cells from the ABa-derived pathway depend on intercellular signaling mediated by the GLP-1 (**germline proliferation**) receptor. GLP-1 is a transmembrane receptor closely related to LIN-12 (**lineage abnormal**) and *Drosophila* Notch (Berry et al., 1997; Greenwald et al., 1994). Pharynx production from MS appears to be cell autonomous. The putative transcription factors, SKN-1 (**skin**) and POP-1 (**posterior pharynx defective**), are required for the MS developmental program, including the generation of pharyngeal cells (Bowerman et al., 1993; Horner et al., 1998; Lin et al., 1995). The genetic networks involving *glp-1*, *pop-1*, and *skn-1* are beginning to be understood, but very little is known about the mechanisms that act downstream of these genes to mediate pharyngeal organogenesis (Horner et al., 1998).

A point of convergence for pharyngeal development is *pha-4* (**pharynx development abnormal**). Animals lacking zygotic *pha-4* activity fail to generate pharyngeal cells from either ABa or MS lineages. Most other cells appear to be produced normally in *pha-4* mutant embryos, including cells from ABa and MS that are non pharyngeal (Horner et al., 1998).

pha-4 encodes transcription factor of the winged helix variety, and is a forkhead/*HNF-3* homolog, that is expressed in all pharyngeal precursors and establishes

their fate (Horner et al., 1998; Kalb et al., 1998; Weinstein et al., 1994). A consensus PHA-4 binding site has been identified, and all pharyngeally expressed genes examined to date possess this sequence (Gaudet and Mango, personal communication).

GFP reporter and immunocytochemistry studies I have conducted show that *CeHIP1* is found in the pharynx. *CeHIP1* possesses two potential PHA-4 binding sites in its putative promoter region, making it a candidate for PHA-4 activity (figure 2.2).

CeHIP1 cannot be detected in early development, it is first observed in animals around the time the pharynx first starts pumping (~ 750 minutes after the first cell cleavage, after Sulston et al., 1983). *CeHIP1* can be detected in the pharynx through all subsequent stages. A reduction of *CeHIP1* message in young animals, as assayed through RNAi, results in deformation of the pharynx of older animals.

4.2.3.1 *CeHIP1* and the Cytoskeleton

CeHIP1 is necessary to maintain proper pharyngeal morphogenesis. *CeHIP1* is a putative actin binding protein, with its homologs being important for the maintenance of the cortical actin cytoskeleton among other things. The pharynx is an organ that undergoes considerable physical stress, as it is a near continuously active organ. If it stops pumping, the animals will cease to feed and will presently die. It is likely that the pharynx has to undergo considerable cellular rearrangement to facilitate continuous pumping. If a component of the cytoskeleton is depleted, the pharynx may not be able to maintain its normal shape, and will ultimately deform under the force of continuous pumping.

There are numerous mutants with defective pharyngeal morphology and function, including *pha-2*, *pha-3*, and *phm-2* (**ph**aryngeal **m**uscle abnormal, Avery, 1993). These mutations have not been cloned as of yet. The misshapen pharynxes observed as an effect of *CeHIP1* RNAi are visible under Nomarski optics and are easily observed through immunostaining. The isthmus of the deformed pharynx is not straight, it appears to curve and sometimes folds back on itself. The procorpus seems to be reduced in length, and from immunostaining it looks as if it is lost to an increase in size of the metacarpus. It sometimes appears as if the metacarpus structure is repeating itself at the expense of the procorpus. Overall, the pharynx looks as if it has lost structural integrity, and the animals look slightly starved, indicating inefficient feeding.

The RNAi phenotype is similar in some aspects to the phenotypes observed for the aforementioned mutants. *pha-2* mutants have misshapen pharynxes in which the cells of the terminal bulb and isthmus appear to have mixed; the resulting being a smaller bulb and a thicker isthmus (Avery, 1993). These animals become extremely starved adults. *pha-3* mutant animals have a deformed isthmus (Avery, 1993). The isthmus, which is normally of a constant diameter throughout its length is instead tapered from the terminal bulb becoming quite thin where it joins the metacarpus. In *phm-2* worms, the grinder is unable to move to its full forward position, and the muscle fibers of the terminal bulb appear shorter than normal (Avery, 1993).

In *C. elegans*, 5 genes encode actin, three of which, *act-1,2,3*, are arranged in a cluster on LGV (Krause et al., 1989; Landel et al., 1984). The act (*ad468 ad767sd*) double mutation was isolated in an F1 screen for dominant mutations; this turned out to be semi-dominant as many *ad468 ad767I/+* heterozygotes were slightly starved. *ad468*

ad767 homozygotes displayed a pharyngeal muscle defect, with barely detectable contractions of the pharynx. *ad468 ad767* mutants contain point mutations in *act-2* and *act-3*, and are unique among actin mutants in that the worm's motility is normal. All previously known actin mutations were isolated by their effects on body wall muscle, suggesting that *ad468 ad767* specifically affects pharyngeal muscle. *ad468* is the first known mutation of *act-2* suggesting *act-2* may function specifically in pharyngeal muscle, while *act-1* and *act-3* may function in both pharyngeal and body wall muscle (Avery, 1993).

Thus, as is demonstrated by *ad468 ad767* and *CeHIP1* RNAi, the pharynx is a structure that requires an intact cytoskeletal complex to function. Perturbation of any component can result in deformity of the pharynx. At this point it is still unclear what the specific contribution *CeHIP1* makes to maintain pharynx structure and function. *CeHIP1* does not seem to be involved in early development in the context of pharyngeal development. It may be one of a host of genes that are activated by PHA-4, and acts once the mature pharynx has been generated to maintain its structure and promote its function.

4.2.3.2 Endocytosis and Pharynx Function

It is not known what the role of receptor mediated endocytosis is in the pharynx. *CeHIP1* appears to be present in all parts of the pharynx, including the pharyngeal nervous system. Endocytic trafficking may be important to maintain the structure of the pharynx, or it could be involved in the recycling of signaling components. Several neurotransmitters are known to be active in the pharynx, including serotonin and glutamate (reviewed in Riddle, 1997). A simplified account of synaptic transmission is

as follows: Synaptic vesicles are synthesized in the soma and transported to the synaptic terminals. Along the way they are loaded with neurotransmitter synthesized from cellular metabolites. Loaded vesicles are translocated and docked at specific release sites, and become poised for fusion. Calcium influx initiates a rapid fusion of the vesicle with the plasma membrane and the neurotransmitter is released. The neurotransmitter diffuses across the synaptic cleft and interacts with receptors on the surface of the postsynaptic cell. Neurotransmission is terminated through destruction of the neurotransmitter, or the transmitter is transported back into the presynaptic cell through a transmitter uptake transporter. At this point, vesicle membrane that had been incorporated into the plasma membrane is recycled by endocytosis. Vesicular components are known to be sequestered into clathrin-coated pits, and these membrane patches bud off of the plasma membrane as coated vesicles.

Perhaps CeHIP1 is involved in this process. The *unc-101* gene codes for a clathrin adaptor protein, an ortholog of mouse AP47 (Lee et al., 1994). The distribution of CeHIP1 protein appears normal in *unc-101(m1)* animals (data not shown). This would be expected if CeHIP1 is recruited to the later stages of endocytosis, once clathrin and the accessory proteins have set up the scaffold from which the membrane will bud. Further investigation is required to determine what contribution CeHIP1 may have to endocytosis and pharynx function.

4.3 *CeHIP1*, A Dose Sensitive Gene?

Null mutations in most diploid organisms appear recessive in heterozygotes as no phenotypes are observed under cursory examination. The reduced viability of animals heterozygous for deletions of chromosomal regions can be interpreted as a deleterious effect caused by the cumulative dosage reduction of independent gene products.

Aneuploid analysis in *Drosophila* has shown several instances where relatively small deletions that are lethal in only one copy (Lefevre et al., 1972; Lindsley et al., 1972; Prado et al., 1999). Although most of the seven haplolethal regions contain a muscle or cytoskeletal protein, a direct relationship with haplolethality has only been demonstrated for *dpp* (which codes for the *Drosophila* homolog of bone morphogenic protein 2, Padgett et al., 1987) and *wupA* (which codes for troponin I, Barbas et al., 1991). Thus, haplolethality may result from an imbalance of muscle or cytoskeletal proteins.

4.3.1 *CeHIP1* and Haploinsufficiency

There are several regions and loci in *C. elegans* suspected of demonstrating haploinsufficiency. This includes mutation *ct45*, which maps between *dpy-28* and *unc-49* on LGIII (Mains and Wood, personal communication). *ct45* shows maternal effect, dominant embryonic lethality, which can be rescued by a duplication of the region (*mnDp37*). The heterochronic gene *lin-41*, which codes for a RBC (Ring finger-B box- Coiled coil) protein, is a haploinsufficient locus (Slack and Ruvkun, personal communication).

The map location of *CeHIP1* was suspicious from the outset of this work. Many well characterized deficiencies appeared to break upon either side of the region. Only

one deficiency, *nDf17*, appeared to span *CeHIP1*. None of the deficiencies tested deleted *CeHIP1*.

These data suggest that this gene may not be tolerated in one copy by the animal; the region is haploinsufficient. Additional evidence for haploinsufficiency comes from the inability to recover animals bearing deletions of *CeHIP1* from reverse genetic screens. Multiple deletions were generated, but no animals with these chromosomal alterations could be isolated. It may not be possible to recover a gene knockout of *CeHIP1* by conventional means.

CeHIP1 may be dose sensitive as it is required in large amounts in the gonad for fertilization. When this is perturbed, through RNAi or genetic lesion, fertilization will not occur and no affected progeny will be present in the next generation. *CeHIP1* has a role in late development in pharyngeal morphology and egg laying, which can only be seen in silencing the gene after fertilization.

4.3.2 Overexpression of *CeHIP1*

Evidence from other systems indicated that the overexpression of the *CeHIP1* related proteins mitigated a toxic effect in the respective systems. There are several examples of the overexpression of various genes leading to reduced viability in *C. elegans*, including gain of function and dominant negative mutations of *let-60 ras* (Sternberg and Han, 1998). High level expression of the talin-like domain of Sla2p in a *SLA2* deletion background resulted in cell death (Yang et al., 1999). Likewise, overexpression of *HIP1* in mammalian cell culture caused the cells to undergo apoptosis

(Hackam et al., 2000). Thus, this family of proteins may display dosage sensitivity, a hypothesis supported by my attempts to generate a deletion of *CeHIP1* in *C. elegans*.

Transgenic strains were generated that contained inducible *CeHIP1* expression constructs. Elevated *CeHIP1* expression resulted in animals becoming sickly, and often dying. These animals fail to thrive, and upon examination under Nomarski optic would often contain vacuoles. The toxic effect may be due to a titration of proteins away from their proper interacting partners. CeHIP1 possesses several domains predicted to bind other proteins, including an actin binding motif, an ENTH domain and several putative coiled-coil domains (Engqvist-Goldstein, 2000; Kay, 1999; Lupas, 1991; McCann, 1997; Yang, 1999). The flooding of cells with CeHIP1 may in effect mop up the normal complement of interacting proteins from fulfilling their normal function. Potential interacting proteins include filamentous actin, and endocytic machinery components such as clathrin and AP2. Massive dysregulation of the cytoskeleton and endocytic pathways may be the effect of excess CeHIP1 in the cell. This is detrimental not only to the cell, but the animal as well. Although it is enticing to consider the appearance of vacuoles as an indication of CeHIP1's supposed endocytic function, more work is necessary to confirm this. It is evident, however, that an increase in endogenous CeHIP1 hinders viability of the animal and the locus may indeed display dosage sensitivity.

It is not known if the toxic effect from the overexpression of CeHIP1 follows an apoptotic pathway, as is the case for HIP1 (Hackam et al., 2000). Apoptosis in *C. elegans* requires the caspase 3 CED-3 (Horvitz paper). It would be informative to see if the toxic effect of *CeHIP1* overexpression is *ced-3* dependent. Additionally, sick animals could be examined for markers of apoptosis.

4.4 CeHIP1 and Interacting Proteins

Several experiments were conducted to learn more about potential interacting protein partners of CeHIP1. As HIP1 was identified as a specific interacting partner of huntingtin, I addressed whether CeHIP1 displayed a similar interaction and found that CeHIP1 does not associate with huntingtin. At this point, the various sequencing projects have identified huntingtin homologues only in vertebrates. Thus huntingtin may be an addition late in evolution, coinciding with the appearance of vertebrates. In lieu of genetically identifying interacting genes of CeHIP1, a molecular approach was used. A yeast two-hybrid screen identified two clones that potentially associate with CeHIP1. These interactions have not been confirmed through independent means.

4.4.1 Yeast Two-Hybrid Screen

4.4.1.1 T05C12.10 and *C. elegans* Hedgehog-Like Genes

The first interacting protein is T05C12.10, a protein that shows sequence similarity to *Drosophila hedgehog* (*hh*). *hh* genes encode a family of secreted signaling molecules with functions in anteroposterior patterning as well as differentiation of neurons and many other cell types in flies and vertebrates (Hammerschmidt, 1997). A single member exists in *Drosophila*, whereas vertebrates possess multiple related genes. These genes all possess a highly conserved amino-terminal signaling domain that is cleaved off and anchored to a cholesterol moiety by the protein's own carboxy-terminal protease domain (Goodrich and Scott, 1998).

A survey of the *C. elegans* genome sequencing and EST projects revealed several genes that encode a *hh*-like autocleavage domain at their carboxyl terminus (Aspöck, 1999; Burglin, 1996; Porter, 1996). This domain has been termed the Hog domain, due to its sequence similarity to *hedgehog* (Aspöck et al., 1999). The part that shares similarity with intein domains of prokaryotes is also referred to as the Hint domain (Hedgehog/intein Hall). With the complete *C. elegans* genome available for scrutiny, there does not exist an obvious *hh* homolog outside of the genes containing Hog domains (Aspöck et al., 1999; Ruvkun et al., 1998). The region amino-terminal to the Hog domains of several of these genes contain novel domains, which have been termed Wart and Ground. Genes that encode these domains but lack the Hog domain have also been found. These gene families have been named *warthog* (*wrt*) and *groundhog* (*grd*) regardless of their association with a Hog domain. Greater than 50 genes in *C. elegans* have been classified under this nomenclature (Aspöck, 1999). Initial characterization of a handful of these genes has revealed a diverse expression pattern, including the hypodermis, seam cells, the excretory cell, sheath and socket cells, and different neurons.

T05C12.10 (also known as M110,(Aspöck et al., 1999)) contains a Hog domain, but its amino-terminus is unlike the related genes. It contains no *wrt* or *grd* domains, and instead possesses a large ORF upstream of the Hog domain. The first 250 residues show a unique, diverse composition, whereas the central region consists of repeated amino acids. The amino terminus matches no other proteins with any significance. T05C12.10 is considered an orphan *hog* gene.

Initial analysis of T05C12.10 has outlined a role for the gene in molting. RNAi of T05C12.10 results in larval lethality, as the animals are unable to molt effectively (Wang

and Seydoux, personal communication). In many cases a cuticular plug can be seen obstructing the mouth region, which presumably interferes with feeding. A T05C12.10::GFP reporter construct shows expression in several regions, including the hypodermis and pharynx. A T05C12.10 deletion mutant, VC42 (*gk32*) was obtained from the *C. elegans* KO Core Facility (UBC). Animals homozygous for *gk32* arrest at the second larval stage.

Postembryonically, all nematodes progress through four larval stages characterized by different cuticle structures. Molting permits growth, but is not necessary as nematodes increase in size between molts and after the final molt (Singh and Sulston, 1978). Molting is thought to be important for parasitic nematodes that need to alter their surface composition to survive changing environments, but not for most free-living species. It is likely that the molting cycle activates basic developmental programs, and the linkage between molting and development has been maintained through nematode evolution. At each molt, the animal enters a period of lethargus, lasting approximately 2 hours, during which pharyngeal pumping and movement is suppressed. Connections between the hypodermis and cuticle are broken at the beginning of lethargus and a new cuticle is formed. About 30 minutes before the old cuticle is shed (known as ecdysis), the animals can be observed to spin or flip about their axis. Just prior to ecdysis, the pharynx will begin spasmodic contractions (Singh, 1978). The cuticle lining the pharynx breaks, and the old cuticle distends around the head. The animal will repeatedly pull back to dislodge the cuticle remaining in the pharynx. The animal will continue to push with its head until the old cuticle breaks, upon which it will crawl out of the remains. The cuticle is often ingested by the animal (Albertson, 1975).

Thus, T05C12.10 seems to be essential for molting and viability. The involvement of CeHIP1 is less clear. The overlap of gene expression in the pharynx may indicate a functional interaction between the two gene products. Depletion of CeHIP1 does not result in a molting defect. The interaction between CeHIP1 and T05C12.10 maps to the carboxyl terminus of CeHIP1, containing both the large central coiled-coil domain and the talin-like region. CeHIP1 has a putative role in cytoskeletal and endocytic function. T05C12.10 may act through these pathways to initiate molting. It is difficult to interpret the significance of the interaction at this point. Additionally, the interaction of CeHIP1 and T05C12.10 has not been confirmed by independent means.

4.4.1.2 F45E12.2 and RNA Turnover in *C. elegans*

The second protein identified was F45E12.2, which shows similarity to RNA transcription initiation factor type IIB (TFIIB). TFIIB is one of a group of general initiation factors (TFIIB, TFIID, TFIIE, TFIIF, and TFIIH) which function in association with RNA polymerase II and are required for selective binding of polymerase to its promoters (Conaway and Conaway, 1999). A deletion mutant of F45E12.2, strain VC28 (*gk17*) was obtained from the *C. elegans* KO Core Facility (UBC). Animals homozygous for *gk17* arrest in the second larval stage.

A screen for factors involved in mRNA turnover in yeast identified four strains with defects in the decay of several mRNAs (Zuk et al., 1999). One of the mutations identified was allelic to *SLA2*. The mutation, *ts942*, stabilized several mRNAs that would have ordinarily decayed. The putative link between RNA stability and cytoskeletal and endocytic event is not self-evident. There is evidence for a link between the cytoskeleton

and the stability of specific mRNAs. Disruption of the cytoskeleton with cytochalasin leads to the stabilization of lymphokine mRNAs in human peripheral blood lymphocytes (Henics et al., 1997). Thus, Sla2p may have yet another role, linking the cytoskeleton to mRNA stability.

It is not known if CeHIP1 has a similar function; mRNA stability was not assayed in CeHIP1 RNAi experiments. CeHIP1 may contribute to mRNA turnover in the tissues in which it is found. It is worth considering that endogenous CeHIP1 protein may have an effect on the stability of RNA species, and what this may contribute to RNAi experiments. CeHIP1 may be involved in promoting turnover of RNA, which would hinder RNAi techniques. Further investigation is required to determine if CeHIP1 is involved with RNA stability in *C. elegans*.

4.5 Is *CeHIP1* the nematode homologue of human *HIP1*?

C. elegans does not possess a homologue of huntingtin. An obvious and important question then is whether or not CeHIP1 is the worm ortholog of HIP1, A second candidate is HIP12 (Chopra et al, 2000). CeHIP1 and HIP1 both show restricted expression, while HIP12 is widely expressed. CeHIP1 and HIP1 show dose sensitive toxic effects. Overexpression of HIP1 causes cell death through an apoptotic pathway, and this effect is wholly dependent on a novel death effector domain (DED) within HIP1 (Hackam et al., 2000). This domain is not present in HIP12, and HIP12 has no toxic effects (Chopra et al., 2000). CeHIP1 has a region with weak similarity to the DED of HIP1. The potential DED of CeHIP1 is closely related to the predicted DED's of CED-4 (CED-4 reference). A test to resolve between these two candidates would be to

determine if the toxic effects observed from overexpression of CeHIP1 follows an apoptotic mechanism. If it does, this would argue in favor of CeHIP1 being the true homologue of human HIP1. A cursory examination of the human genome reveals that humans often possess multiple versions of a gene, with lower organisms containing just one or two (human genome paper). Lastly, it cannot be ignored that perhaps F08A8.6 is not a pseudogene. Its absence from EST databases, and my inability to detect it reflecting its low abundance or specialized expression. If this is the case then there exists the possibility that F08A8.6 may contribute to the function of CeHIP1.

4.6 Conclusion

CeHIP1 encodes a gene that shares sequence identity with a family of genes in many eukaryotes, ranging from yeast to humans. Studies of these genes have ascribed numerous, seemingly disparate roles to this family of proteins. The protein has a role in maintaining the cortical actin cytoskeleton (Holtzman et al., 1993). It also has a role in endocytic events, and may represent a link between the actin cytoskeleton and endocytic events (Engqvist-Goldstein et al., 2000; Na et al., 1995; Raths et al., 1993) as well as role in RNA stability (Zuk et al., 1999). Most recently, human HIP1 has been shown to have a proapoptotic function. Cultured cells transfected with HIP1 undergo programmed cell death (Hackam et al., 2000). For the most part, the role of this protein has been described in cellular terms. The endocytic function illustrates that the cell is actively receiving input from neighbors. Thus, the protein will have functions outside of its immediate cellular environment. What is the role of this conserved gene in the context of the development of a complex, multicellular eukaryotic system?

In this thesis I have begun to answer this question. CeHIP1 is a protein that seems to have multiple functions in *C. elegans*. CeHIP1 may have a function in cytoskeletal structural integrity, as well as endocytosis and vesicle trafficking. *CeHIP1* shows tissue specific expression in the nematode, and likewise, tissue specific function. There is precedence for multiple function for a single protein. The *C. elegans* patched homolog PTC-1 is proposed to retain a signaling role in the germ line as a receptor for one of the Hh-related molecules, and has additional roles in vesicle trafficking and membrane deposition and cellular structural integrity (Kuwabara et al., 2000).

CeHIP1 possesses an ENTH domain, which has been found in proteins with endocytic and cytoskeletal functions (Kay, 1999). The I/LWEQ domain ascribes F-actin as an interacting protein (McCann and Craig, 1999). The putative coiled-coil domains of CeHIP1 suggest that it is likely to have multiple protein partners (Lupas, 1997). Thus, the function of CeHIP1 may largely depend on its local cellular context.

CeHIP1 may contribute to cytoskeleton dynamics, and thus have a structural role. This can be observed from the pharyngeal deformities observed after *CeHIP1* RNAi treatment of young animals. The depletion of *CeHIP1* message, and ultimately protein results in a loss of structural integrity of the pharynx. CeHIP1 has a role in maintaining morphology and subsequent functioning of very different organs.

An exhaustive examination of the components of the gonad for structural defects has not been conducted. These structures do show imperfect functioning however. Errors in ovulation and fertilization are contingent upon *CeHIP1* RNAi. This defect may reflect a structural deficit of the gonad, but it may also point out a signaling function. The signal to halt ovulation is lost and oocytes continue to mature even though the

system is in error. It is known that somatic structures of the gonad are required to prevent the Emo phenotype perhaps this is facilitated through *CeHIP1* (McCarter et al., 1997). The signal from the somatic gonad may be received by the oocytes through a receptor mediated endocytosis system utilizing *CeHIP1*. The reduction in the number of mature sperm housed within the spermatheca of RNAi animals may be a consequence of a loss of signaling as well. It is unknown what directs sperm to the spermatheca. *CeHIP1* may have role in presenting and maintaining molecules in the surface of the spermatheca to coordinate sperm movements to the structure.

Depletion of *CeHIP1* within the vulval muscles results in an egg-laying defect. This phenotype can be attributed to either a structural or signaling deficiency. It is easy to envisage how either situation could lead to a defect in the function of these muscles.

4.7 Model

C. elegans provides a good model to interpret the role of the human homolog, *HIP1*. The two genes, *CeHIP1* and *HIP1* show restricted expression. *CeHIP1* in the pharynx, vulval muscles and spermatheca of the worm and *HIP1* is enriched in the brain and testes of humans. The expression of *HIP1* in the brain, specifically the cortex, is one of the features which has implicated it strongly in the specific neuropathology of HD. Thus, the tissue-restricted expression of *CeHIP1* may be useful to identify the specific cellular context in which it functions.

Likewise, the two proteins also display dose sensitive toxic effects. Overexpression of human *HIP1* results in cellular death through an apoptotic pathway (Hackam et al., 2000). Overexpression of *CeHIP1* results in negative consequences in

terms of viability of the worm. It may be possible to use this system to delineate the toxic effect in nematodes, and establish genetic screens for suppression of the phenotype. These findings may reflect the situation in humans, and perhaps point out avenues of potential treatment.

The family of *CeHIP1* related genes have multiple functions, with new ones sprouting up like heads of the mythical hydra. Careful examination is revealing phenotypes not anticipated. It is an exciting family of genes to study as it is uncovering connections between previously distinct cellular pathways. The study of *CeHIP1* has been particularly informative as it has outlined the multiple roles this protein has in the development of an animal system, which in turn may shed light on the functioning of *HIP1* in the pathogenesis of Huntington disease. This thesis describes the characterization of a member of a family of genes becoming recognized for connecting different aspects of cell biology.

Bibliography

- Adams, M.D., Celniker, S. E., Holt, R. A., Evans, C. A., Gocayne, J. D., Amanatides, P. G., Scherer, S. E., Li, P. W., Hoskins, R. A., Galle, R. F., and et al. 2000. The Genome Sequence of *Drosophila melanogaster*. *Science*. 287.
- Albertson, D.G., and Thomson, J. N. 1975. The Pharynx of *Caenorhabditis elegans*. *Phil. Trans. R. Soc. Lond. B*. 275:299-325.
- Andrew, S.E., Goldberg, Y. P., and Hayden, M. R. 1997. Rethinking Genotype and Phenotype Correlations in Polyglutamine Expansion Disorders. *Hum. Mol. Genet.* 6:2005-10.
- Aroian, R.V., and Sternberg, P. W. 1991. Multiple Functions of *let-23*, a *Caenorhabditis elegans* Receptor Tyrosine Kinase Gene Required for Vulval Induction. *Genetics*. 128:251-67.
- Aroian, R.V., Lesa, G. M., and Sternberg, P. W. 1994. Mutations in the *Caenorhabditis elegans let-23* EGFR-like Gene Define Elements Important for Cell-type Specification and Function. *EMBO J*. 13:360-6.
- Aspöck, G., Kagoshima, H., Niklaus, G., and Burglin, T. R.,. 1999. *Caenorhabditis elegans* has Scores of *Hedgehog*-related Genes: Sequence and Expression Analysis. *Genome research*. 9:909-23.
- Avery, L., and Horvitz, H. R. 1989. Pharyngeal Pumping Continues after Laser Killing of the Pharyngeal Nervous System of *C. elegans*. *Neuron*. 3:473-85.
- Avery, L. 1993. The Genetics of Feeding in *Caenorhabditis elegans*. *Genetics*. 133:897-917.

- Barbas, J.A., Galceran, J., Krah-Jentgens, I., DE LA Pompa, J. L., and Canal, I. 1991. Troponin I is Encoded in the Haplolethal Region of the Shaker Gene Complex of *Drosophila*. *Genes Dev.* 5:132-40.
- Barinaga, M. 1996. An Intriguing New Lead on Huntington's Disease. *Science.* 271.
- Bassett, D.E.J., Boguski, M. S., Spencer, F., Reeves, R., Kim, S., Weaver, T., and Hieter, P. 1997. Genome Cross-referencing and XREFdb: Implications for the Identification and Analysis of Genes Mutated in Human Disease. *Nat. Genet.* 15:339-44.
- Benmerah, A., Lamaze, C., Begue, B., Schmid, S. L., Dautry-Varsat, A., and Cerf-Bensussan, N. 1998. AP-2/Eps15 Interaction is Required for Receptor-mediated Endocytosis. *J. Cell Biol.* 140:1055-62.
- Berry, L.W., Westlund, B., and Schedl, T. 1997. Germ-line Tumor Formation Caused by Activation of glp-1, a *Caenorhabditis elegans* Member of the Notch Family of Receptors. *Development.* 124:925-36.
- Blader, I.J., Cope, M. J., Jackson, T. R., Profit, A. A., Greenwood, A. F., Drubin, D. G., Prestwich, G. D., and Theibert, A. B. 1999. GCS1, an Arf Guanosine Triphosphatase-activating Protein in *Saccharomyces cerevisiae*, is Required for Normal Actin Cytoskeletal Organization *in vivo* and Stimulates Actin Polymerization *in vitro*. *Mol. Biol. Cell.* 10:581-96.
- Blumenthal, T., and Thomas, J. 1988. *Cis* and *trans* mRNA Splicing in *C. elegans*. *Trends Genet.* 4:305-8.

- Bowerman, B., Draper, B. W., Mello, C. C., and Priess, J. R. 1993. The Maternal Gene *skn-1* Encodes a Protein that is Distributed Unequally in Early *C. elegans* Embryos. *Cell*. 74:443-52.
- Brenner, S. 1974. The Genetics of *Caenorhabditis elegans*. *Genetics*. 115:71-94.
- Burglin, T.R. 1996. Warthog and Groundhog, Novel Families Related to Hedgehog. *Curr. Biol*. 6:1047-50.
- Burridge, K., and Connel, L. 1983. Talin: A Cytoskeletal Component Concentrated in Adhesion Plaques and Other Sites of Actin-membrane Interaction. *Cell Motil*. 3:405-17.
- Chen, H., Fre, S., Slepnev, V., Capua, M., Takei, K., Butler, M., Di Fiore, P., and De Camilli, P. 1998. Epsin, an EH Domain Binding Protein Implicated in Clathrin-mediated Endocytosis. *Nature*. 394:793-7.
- Chopra, V. S., Metzler, M., Rasper, D. M., Engqvist-Goldstein, A. E., Singaraja, R., Gan, L., Fichter, K. M., McCutcheon, K., Drubin, D., Nicholson, D. W., and Hayden M. R. 2000. HIP12 is a Non-proapoptotic Member of a Gene Family Including HIP1, an Interacting Protein with Huntingtin. *Mamm Genome* 11:1006-15
- Cinibo, G.D., Gamper, H. B., Isaacs, S. T., and Hearst, J. E. 1985. Psoralens as photoactive probes of nucleic acid structure and function: organic chemistry, photochemistry, and biochemistry. *Annu. Rev. Biochem.* 54.
- Clark, M.S. 1999. Comparative Genomics: the Key to Understanding the Human Genome Project. *BioEssays*. 21:121-30.
- Conaway, J.W., and Conaway, R. C. 1999. Transcription Elongation and Human Disease. *Annu. Rev. Biochem.* 68:301-19.

- Conradt, B., and Horvitz, H. R. 1998. The *C. elegans* Protein EGL-1 is Required for Programmed Cell Death and Interacts with the Bcl-2-like Protein CED-9. *Cell*. 93:519-29.
- Consortium, T.C.e.S.p.e.a.i.S.J.a.M.a.S. 1998. Genome Sequence of the Nematode *C. elegans*: A Platform for Investigating Biology. *Science*. 282:2012-2018.
- Coulson, A., Waterston, R., Kiff, J., Sulston, J., and Kohara, Y. 1988. Genome Linking with Yeast Artificial Chromosomes. *Nature*. 335:184-6.
- Coulson, A., Kozono, Y., Lutterbach, B., Shownkeen, R., Sulston, J. and Waterston, R. 1991. YACS and the *C. elegans* Genome. *Bioessays*. 13:413-7.
- Coulson, A., Huynh, C., Kozono, Y., and Shownkeen, R. 1995. The Physical Method of the *Caenorhabditis elegans* Genome. *Methods Cell Biol.* 48:533-50.
- Davies, S.W., Turmaine, M., Cozens, B.A., DiFiglia, M., Sharp, A. H., Ross, C. A., Scherzinger, E., Wanker, E. E., Mangiarini, L., and Bates, G. P. 1997. Formation of Neuronal Intranuclear Inclusions Underlies the Neurological Dysfunction in Mice Transgenic for the HD Mutation. *Cell*. 90:537-48.
- de Camilli, P., Takei, K., and McPherson, P. S. 1995. The Function of Dynamin in Endocytosis. *Curr, Opin. Neurobiol.* 5:559-65.
- DiFiglia, M., Sapp, E., Chase, K. O., Davies, S. W., Bates, G. P., Vonsattel, J. P., and Aronin, N. 1997. Aggregation of Huntingtin in Neuronal Intranuclear Inclusions and Dystrophic Neurites in Brain. *Science*. 277:1990-3.
- Ding, L., and Candido, E. P. M. 2000. HSP25, a Small Heat Shock Protein Associated with Dense Bodies and M-lines of Body Wall Muscle in *Caenorhabditis elegans*. *The Journal of Biological Chemistry*. 275:9510-7.

- Dragatsis, I., Levine, M. S., and Zeitlin, S. 2000. Inactivation of *Hdh* in the Brain and Testis Results in Progressive Neurodegeneration and Sterility in Mice. *Nature Genet.* 26:300-6.
- Drubin, D.G., Miller, K. G., and Botstein, D. 1988. Yeast Actin-binding Proteins: Evidence for a Role in Morphogenesis. *J. Cell Biol.* 144:1203-18.
- Engqvist-Goldstein, A.E., Kessels, M. M., Chopra, V. S., Hayden, M. R. and Drubin, D. G. 2000. An Actin-binding Protein of the Sla2/Huntingtin Interacting Protein 1 Family is a Novel Component of Clathrin-coated Pits and Vesicles. *J. Cell Biol.* 147:1503-18.
- Evans, D., and Blumenthal, T. 2000. *Trans* Splicing of Polycistronic *Caenorhabditis elegans* Pre-mRNAs: Analysis of the SL2 RNA. *Mol. Cell. Biol.* 20:6659-67.
- Faber, P.W., Alter, J. R., MacDonald, M. E., and Hart, A. C. 1999. Polyglutamine-mediated Dysfunction and Apoptotic Death of a *Caenorhabditis elegans* Sensory Neuron. *PNAS.* 96:179-84.
- Finney, M., and Ruvkun, G. 1990. The *unc-86* Gene Product Couples Cell Lineage and Cell Identity in *C. elegans*. *Cell.* 63:895-905.
- Fire, A. 1986. Integrative Transformation of *Caenorhabditis elegans*. *EMBO.* 5:2673-80.
- Fire, A., Xu. S., Montgomery, M. K., Kostas, S. A., Driver, S. E., and Mello, C. C. 1998. Potent and Specific Genetic Interference by Double-stranded RNA in *Caenorhabditis elegans*. *Nature.* 391:806-11.
- Francis, R., Barton, M. K., Kimble, J., and Schedl, T. 1995. *gld-1*, a Tumor Suppressor Gene Required for Oocyte Development in *Caenorhabditis elegans*. *Genetics.* 139:579-606.

- Fraser, A.G., Kamath, R. S., Zipperlen, P., Martinez-Campos, M., Sohrmann, M., and Ahringer, J. 2000. Functional Genomic Analysis of *C. elegans* Chromosome I by Systematic RNA Interference. *Nature*. 408:325-30.
- Gengyo-Ando, K., and Mitani, S. 2000. Characterization of Mutations Induced by Ethyl Methanesulfonate, UV, and Trimethylpsoralen in the Nematode *Caenorhabditis elegans*. *Biochemical and Biophysical Research Communications*. 269:64-9.
- Gietz, R.D., and Schiestl, R. H. 1995. Transforming Yeast with DNA. *Methods in Molecular Cellular Biology*. 5:255-69.
- Goodrich, L.V., and Scott, M. P. 1998. Hedgehog and Patched in Neural Development and Disease. *Neuron*. 21:1243-7.
- Grant, B., and Hirsh, D. 1999. Receptor-mediated Endocytosis in the *Caenorhabditis elegans* Oocyte. *Mol. Biol. Cell*. 10:4311-26.
- Greenstein, D.H., S., Plasterk, R. H. A., Andachi, Y., Wang, B., Finney, M., and Ruvkun, G. 1994. Targeted Mutations in the *Caenorhabditis elegans* POU Homeobox Gene *ceh-18* cause Defects in Oocyte Cell Cycle Arrest, Gonad Migration, and Epidermal Differentiation. *Genes Dev*. 8:1935-48.
- Greenwald, I. 1994. Structure/function Studies of lin-12/Notch proteins. *Curr. Opin. Genet. Devel*. 4:556-62.
- Hackam, A.S., Yassa, A. S., Singaraja. R., Metzler, M., Gutekunst. C.-A., Gan, L., Warby. S., Wellington, C. L., Vaillancourt, J., Nansheng, , and G. C., F. G. Raymond, L., Nicholson, D. W. and Hayden, M. R. 2000. Huntingtin Interacting Protein 1 (HIP-1) Induces Apoptosis via a Novel Caspase-dependent Death Effector Domain. *J. Biol. Chem.* in press.

- Hammerschmidt, M., Brook, A., and McMahon, A. P. 1997. The World According to Hedgehog. *Trends Genet.* 13:14-21.
- HDCRG. 1993. A Novel Gene Containing a Trinucleotide Repeat that is Expanded and Unstable on Huntington's Disease Chromosomes. *Cell*:971-83.
- Hemmings, L., Rees, D. J. C., Ohanian, V., Botton, S. J., Gilmore, A. P., Patel, B., Priddle, H., Trevithick, J. E., Hynes, R. O. and Critchley, D. R. 1996. Talin Contains Three Actin-binding Sites Each of which is Adjacent to a Vinculin-binding Site. *J. Cell Sci.* 109:2715-26.
- Henics, T.E., Nagy, J., and Szekeres-Bartho, J. 1997. Interaction of AU-rich Sequence Binding Proteins with Actin: Possible Involvement of the Actin Cytoskeleton in Lymphokine mRNA Turnover. *J. Cell. Physiol.* 173:19-27.
- Hill, R.J. and Sternberg, P. W. 1992. The Gene *lin-3* Encodes an Inductive Signal for Vulval Development in *C. elegans*. *Nature.* 358:470-6.
- Hirsh, D., Oppenheim, D., and Klass, M. 1976. Development of the Reproductive System of *Caenorhabditis elegans*. *Dev. Biol.* 49:200-19.
- Hirst, J.a.R., M. J. 1998. Clathrin and Adaptors. *Biochim. Biophys. Acta.* 1404:173-93.
- Holtzman, D.A., Yang, S. and Drubin, D. G. 1993. Synthetic-lethal Interactions Identify Two Novel Genes, *SLA1* and *SLA2*, That Control Membrane Cytoskeleton Assembly in *Saccharomyces cerevisiae*. *J. Cell Biol.* 3:635-44.
- Horner, M.A., Quintin, S., Domeier, M. E., Kimble, J., Labouesse, M., and Mango, S. E. 1998. *pha-4*, an *HNF-3* Homolog, Specifies Pharyngeal Organ Identity in *Caenorhabditis elegans*. *Genes & Development.* 12:1947-52.

- Horvitz, H.R., Brenner, S., Hodgkin, J., and Herman, R. K. 1979. A Uniform Genetic Nomenclature for the Nematode *Caenorhabditis elegans*. *Mol. Gen. Genet.* 175:129-33.
- Horvitz, H.R., Chalfie, M., Trent, C., Sulston, J. and Evans, P. D. 1982. Serotonin and Octopamine in the Nematode *Caenorhabditis elegans*. *Science.* 216:1012-14.
- Ikeda, H., Yamaguchi, M., Sugai, S., Aze, Y., Narumiya, S., and Kakizuka, A. 1996. Expanded Polyglutamine in the Machado-Joseph Disease Protein Induces Cell Death *in vitro* and *in vivo*. *Nature Genet.* 13:196-202.
- Iwasaki, K., McCarter, J., Francis, R., and Schedl, T. 1996. *emo-1*, a *Caenorhabditis elegans* Sec1p Gamma Homologue, is Required for Oocyte Development and Ovulation. *J. Cell Biol.* 134:699-714.
- Janke, D.L., Schein, J. E., Ha, T., Franz, N., O'Neil, N. J., Vatcher, G. P., Stewart, H. I., Kuervers, L. M., Baillie, D. L. and Rose, A. M. 1997. Interpreting a Sequenced Genome: Toward a Cosmid Transgenic Library of *Caenorhabditis elegans*. *Genome Research.* 7:974-85.
- Jansen, G., Hazendonk, E., Thijssen, K. L., and Plasterk, R. H. A. 1997. Reverse Genetics by Chemical Mutagenesis in *Caenorhabditis elegans*. *Nature Genet.* 17:119-21.
- Jones, D., Dixon, D. K., Graham, R. W., and Candido, E. P. M. 1989. Differential Regulation of Closely Related Members of the hsp16 Gene Family in *Caenorhabditis elegans*. *DNA.* 8:481-90.

- Jorgensen, E.M., Hartwig, E., Schuske, K., Nonet, M. L., Jin, Y., and Horvitz, H. R. 1995. Defective Recycling of Synaptic Vesicles in Synaptotagmin Mutants of *Caenorhabditis elegans*. *Nature*. 378:196-99.
- Kalb, J.M., Lau, K. K, Goszczynski, B., Fukushige, T., Moons, D., Okkema, P. G. and McGhee, J. D. 1998. *pha-4* is Ce-fkh-1, a Forkhead/HNF-3a,B,y Homolog that Functions in Organogenesis of the *C. elegans* Pharynx. *Devel*. 125:2171-80.
- Kalchman, M.A., Koide, B. H., McCutcheon, K., Graham, R. K., Nichol, K., Nishiyama, K., Lynn, F., Kazemi-Esfarajji, P., Metzler, M., Goldberg, Y. P., Kanazawa, I., Gietz, R. D. and Hayden, M. R. 1997. HIP1, a Human Homologue of *S. cerevisiae* Sla2p, Interacts with Membrane-Associated Huntingtin in the Brain. *Nature Genetics*. 16:44-53.
- Katz, W.S., Hill, R. J., Clandinin, T. R., and Sternberg, P. W. 1995. Different Levels of the *C. elegans* Growth Factor LIN-3 Promote Distinct Vulval Precursor Fates. *Cell*. 82:297-307.
- Kawaguchi, Y., Okamoto, T., Taniwaki, M., Aizawa, M., Inoue, M., Katayama, H., Nakamura, S., Nishimura, M., Akiguchi, I., Kimura, J., Narumiya, S., and Kakizuka, A. 1994. CAG Expansions in a Novel Gene for Machado-Joseph Disease at Chromosome 14q32.1. *Nature Genet*. 8:221-8.
- Kay, B.K., Yamabhai, M., Wendland, B., and Emr, S. D. 1999. Identification of a Novel Domain Shared by Putative Components of the Endocytic and Cytoskeletal Machinery. *Protein Sci*. 8:435-8.
- Ketting, R.F., Fischer, S. E. J., and Plasterk, R. H. 1997. Target choice determinants of the Tc1 transposon of *Caenorhabditis elegans*. *Nucleic Acids Res*. 25:4041-7.

- Ketting, R.F., Haverkamp T. H. , van Luenen H. G., Plasterk R. H. 1999. Mut-7 of *C. elegans*, Required for Transposon Silencing and RNA Interference, is a Homolog of Werner Syndrome Helicase and RNaseD. *Cell*. 99:133-41.
- Kimble, J., and Hirsh, D. 1979. The Post-embryonic Cell Lineages of the Hermaphrodite and Male Gonads in *Caenorhabditis elegans*. *Dev. Biol.* 70:396-417.
- Kimble, J. and Sulston, J. 1983. Tissue-specific Synthesis of Yolk Proteins in *C. elegans*. *Dev. Biol.* 96:189-96.
- Kimble, J. and White, J. G. 1981. On the Control of Germ Cell Development in *Caenorhabditis elegans*. *Dev. Biol.* 81:208-19.
- Klass, M., Wolf, N., and Hirsh, D. 1976. Development of the Male Reproductive System and Sexual Transformation in the Nematode *Caenorhabditis elegans*. *Dev. Biol.* 52:1-18.
- Krause, M., Wild, M., Rosenzweig, B., and Hirsh, D. 1989. Wild type and Mutant Actin Genes in *Caenorhabditis elegans*. *J. Mol. Biol.* 208:381-92.
- Krause, M. a. H., D. 1987. A *trans*-Spliced Leader Sequence on Actin mRNA in *C. elegans*. *Cell*. 49:753-61.
- Kuwabara, P.E., Lee, M. Schedl, T., and Jefferis, S. X. E. G. 2000. A *C. elegans* Patched gene, *ptc-1*, functions in germ-line cytokinesis. *Genes & Development*. 14:1933-1944.
- Kyte, J., and Doolittle, R. F. 1982. A Simple Method for Displaying the Hydrophobic Character of a Protein. *J. Mol. Biol.* 157:105-32.

- LaMunyon, C.W.a.W., S. 1995. Sperm precedence in a hermaphroditic nematode (*Caenorhabditis elegans*) is due to competitive superiority of male sperm. *Experientia*. 58:817-23.
- LaMunyon, C.W.a.W.S. 1999. Evolution of sperm size in nematodes: sperm competition favours larger sperm. *P.N.A.S.* 266:263-7.
- Landel, C.P., Krause, M., Waterston, R. H., Hirsh, D. 1984. DNA Rearrangements of the Actin Gene-cluster in *C. elegans* Accompany Reversion of 3 Muscle Mutants. *J. Mol. Biol.* 180:497-513.
- Lappalainen, P.a.D., D. G. 1997. Cofilin Promotes Rapid Actin Filament Turnover *in vivo*[published erratum appears in Nature 389:211]. *Nature*. 388:78-82.
- Lee, Y.H., Jongeward, G., and Sternberg, P. W. 1994. *unc-101*, a Gene Required for Many Aspects of *C. elegans* Development and Behavior, Encodes a Clathrin-associated Protein. *Genes Dev.* 8.
- Lefevre, G., and Johnson, T. K. 1972. Evidence for a Sex Linked Haplo Inviabile Locus in the *cut-singed* Region of *Drosophila melanogaster*. *Genetics*. 74:633-45.
- L'Hernault, S.W., Shakes, D. C. and Ward, S. 1988. Developmental Genetics of Chromosome I Spermatogenesis-defective Mutants in the Nematode *Caenorhabditis elegans*. *Genetics*. 120:435-52.
- Li, P., Zheng, Y., and Drubin, D. G. 1995. Regulation of Cortical Actin Cytoskeleton Assembly during Polarized Cell Growth in Budding Yeast. *J. Cell Biol.* 4:599-615.

- Lila, T., and Drubin, D. G. 1997. Evidence for Physical and Functional Interaction Among Two *Saccharomyces cerevisiae* SH3 Domain Proteins, an Adenyl Cyclase-associated Protein and the Actin Cytoskeleton. *Mol. Biol. Cell.* 8:367-85.
- Lin, R.L., Thompson, S., and Priess, J. R. 1995. *pop-1* Encodes an HMG Box Protein Required for the Specification of a Mesoderm Precursor in Early *C. elegans* Embryos. *Cell.* 83:599-609.
- Lindsley, D.L., Sandler, L., Baker, B. S., Carpenter, A. T. C., and Denell, R. E. 1972. Segmental Aneuploidy and the Genetic Gross Structure of the *Drosophila* Genome. *Genetics.* 71:157-84.
- Lupas, A., Van Dyke, M., and Stock, J. 1991. Predicting Coiled Coils from Protein Sequences. *Science.* 252:1162-4.
- Lupas, A. 1997. Predicting Coiled-coil Regions in Proteins. *Curr. Opin. Struct. Bio.* 7:388-93.
- Mangiarini, L., Sathasivam, K., Seller, M., Cozens, B., Harper, A., Heterington, C., Lawton, M., Trotter, Y., Lehrach, H., Davies, S. W., and Bates, G. P. 1996. Exon 1 of the HD Gene with an Expanded CAG Repeat is Sufficient to Cause a Progressive Neurological Phenotype in Transgenic Mice. *Cell.* 87:493-506.
- Matilla, A., Koshy, B. T., Cummings, C. J., Isobe, T., Orr, H. T., and Zoghbi, H. Y. 1997. The Cerebellar Leucine-Rich Acidic Nuclear Protein interacts with Ataxin-1. *Nature.* 389:974-8.
- McCann, R.O., and Craig S. W. 1997. The I/LWEQ Module: a Conserved Sequence that Signifies F-actin Binding in Functionally Diverse Proteins from Yeast to Mammals. *Proc Natl Acad Sci U S A.* 94:5679-84.

- McCann, R.O., and Craig, S. W. 1999. Functional Genomic Analysis Reveals the Utility of the I/LWEQ Module as a Predictor of Protein:Actin Interaction. *Biochem. Biophys. Res. Comm.* 266:135-40.
- McCarter, J., Bartlett, B., Dang, T., and Schedl, T. 1997. Soma-Germ Cell Interactions in *Caenorhabditis elegans*: Multiple Events of Hermaphroditic Germline Development Require the Somatic Sheath and Spermathecal Lineages. *Developmental Biology.* 181:121-43.
- McCarter, J., Bartlett, B., Dang, T., and Schedl, T. 1999. On the Control of Oocyte Meiotic Maturation and Ovulation in *Caenorhabditis elegans*. *Dev. Biol.* 205:111-28.
- Mellman, I. 1996. Endocytosis and Molecular Sorting. *Annu. Rev. Cell Dev. Biol.* 12:575-625.
- Mello, C.a.F., A. 1995. DNA Transformation. *In Methods in Cell Biology.* *Caenorhabditis elegans: Modern Biological Analysis of an Organism.* Vol. 48. H.F.a.S. Epstein, D. C., editor. Academic Press, Inc., San Diego. 451-82.
- Mello, C.C., Kramer, J.M., Stinchcomb, D., and Ambros, V. 1991. Efficient Gene Transfer in *C. elegans*: Extrachromosomal Maintenance and Integration Transforming Sequences. *EMBO.* 10:3959-70.
- Merrifield, C.J., Moss, S. E., Ballestrem, C., Imhof, B. A., Giese, G., Wunderlich, I., and Almers, W. 1999. Endocytic Vesicles Move at the Tips of Actin Tails in Cultured Mast Cells. *Nat. Cell Biol.* 1:72-4.
- Miller, D.M., and Shakes, D. C. 1995. Immunofluorescence Microscopy. *In Methods in Cell Biology.* *Caenorhabditis elegans: Modern Biological Analysis of an*

- Organism. Vol. 48. H.F.a.S. Epstein, D. C., editor. Academic Press, Inc., San Diego. 365-94.
- Morrow, D.M.T., D. A., Shiloh, Y., Collins, F.S., and Heiter, P. 1995. *TEL1*, an *S. cerevisiae* Homolog of the Human Gene Mutated in Ataxia Telangiectasia, Is Functionally Related to the Yeast Checkpoint Gene *MEC1*. *Cell*. 82:831-40.
- Moulder, G., and Barstead, R. 1998. Reverse Genetics: Isolating Deletions in PCR Screens of Mutagenized Populations.
<http://snmc01.omrf.uokhsc.edu/revgen/RevGen.html>.
- Mukherjee, S., Ghosh, R. N., and Maxfield, F. R. 1997. Endocytosis. *Physiol. Rev.* 77:759-803.
- Myers, C.D., Goh, P. -Y., Allen, T. S., Bucher, E. A., and Bogaert, T. 1996. Developmental Genetic Analysis of Troponin T Mutations in Striated and Nonstriated Muscle Cells of *Caenorhabditis elegans*. *J. Cell Biol.* 132:1061-77.
- Na, S., Hincapie, M., McCusker, J. H., and Haber, J. E. 1995. *MOP2* (SLA2) Affects the Abundance of the Plasma membrane H⁺-ATPase of *Saccharomyces cerevisiae*. *PNAS*:6818-23.
- Nasir, J., Floresco, S. B., O'Kusky, J. R., Diewert, V. M., Richman, J. M., Zeisler, J., Borowski, A., Marth, J. D., Phillips, A. G., and Hayden, M. R. 1995. Targeted Disruption of the Huntington's Disease Gene Results in Embryonic Lethality and Behavioural and Morphological Changes in Heterozygotes. *Cell*. 81:811-23.
- Niedenthal, R., Riles, L., Guldener, U., Klein, S., Johnston, M., and Hegemann, J. H. 1999. Systematic Analysis of *S. cerevisiae* Chromosome VIII Genes. *Yeast*. 15:1775-96.

- Nonet, M.L., Grundahl, K., Meyer, B. J., and Rand, J. B. 1993. Synaptic Function is Impaired but not Eliminated in *C. elegans* Mutants Lacking Synaptotagmin. *Cell*. 73:1291-1305.
- Ona, V.O., Li, M., Vonsattel, J. P. G., Andrews, L. J., Khan, S. Q., Chung, W. M., Frey, A. S., Merson-Davies, A. S., Li, X., -J., Stieg, P. E. et al. 1999. Inhibition of Caspase-1 Slows Disease Progression in a Mouse Model of Huntington's Disease. *Nature*. 399:263-7.
- Padgett, R.W., St. Johnston, R. D., and Gelbart, W. M. 1987. A Transcript from a *Drosophila* Pattern Gene Predicts a Protein Homologous to the Transforming Growth Factor-beta Family. *Nature*. 325:81-4.
- Paulson, H.L., Bonini, N. M., and Roth, K. A. 2000. Polyglutamine Disease and Neuronal Cell Death. *PNAS*. 97:12957-8.
- Plasterk, R.H., Izsvak, Z., Ivics, Z. 1999. Resident aliens: the Tc1/mariner superfamily of transposable elements. *Trends Genet*. 15:326-32.
- Ploger, R., Zhang, J., Bassett, D., Reeves, R., Hieter, P., Boguski, M., and Spencer, F. 2000. XREFdb: Cross-referencing the Genetics and Genes of Mammals and Model Organisms. *Nuc. Acid. Res*. 28:120-2.
- Porter, J.A., Young, K. E., and Beachy, P. A. 1996. Cholesterol Modification of Hedgehog Signaling Proteins in Animal Development. *Science*. 274:255-9.
- Prado, A.C., I., and Ferrus, A. 1999. The Haplolethal Region at the 16F Gene Cluster of *Drosophila melanogaster*: Structure and Function. *Genetics*. 151:163-75.
- Qualmann, B., Kessels, M. M., and Kelly, R. B. 2000. Molecular Links between Endocytosis and the Actin Cytoskeleton. *The Journal of Cell Biology*. 150:111-6.

- Raths, S., Rohrer, J., Crausaz, F., and Riezman, H. Raths, S., Rohrer, J., Crausaz, F., and Riezman, H. 1993. *end3* and *end4*: Two Mutants Defective in Receptor-mediated and Fluid-phase Endocytosis in *Saccharomyces cerevisiae*. *J. Cell Biol.* 120:55-65.
- Reddy, P.S., and Housman, D. E. 1997. The Complex Pathology of Trinucleotide Repeats. *Current Opinion in Cell Biology.* 9:364-72.
- Riddle, D.L., Blumenthal, T., Meyer, B. J., and Priess, J. R. 1997. *C. elegans* II. Cold Spring Harbor Laboratory Press, Cold Spring Harbor, NY.
- Rong, Y.S., and Golic K. G. 2000. Gene Targeting by Homologous Recombination in *Drosophila*. *Science.* 288:2013-8.
- Ross, C. 1997. Intranuclear Neuronal inclusions: a Common Pathogenic Mechanism for Glutamine-Repeat Neurodegenerative Disease? *Neuron.* 19:1147-50.
- Rothman, J.E., and Wieland, F. T. 1996. Protein Sorting by Transport Vesicles. *Science.* 272:227-34.
- Rushforth, A.M., Saari, B., and Anderson, P. 1993. Site-selected Insertion of the Transposon Tc1 into a *Caenorhabditis elegans* Myosin Light Chain Gene. *Mol. Cell Biol.* 13:902-10.
- Ruvkun, G.a.H., O. 1998. The Taxonomy of Developmental Control in *Caenorhabditis elegans*. *Science.* 282:2033-41.
- Satyral, S.H., Schmidt, E., Kitagawa, K., Sondheimer, N., Lindquist, S., Kramer, J. M., and Morimoto, R. I. 2000. Polyglutamine Aggregates Alter Protein Folding Homeostasis in *Caenorhabditis elegans*. *PNAS.* 97:5750-55.

- Saudou, F., Finkbeiner, S., Devys, D., and Greenberg, M. 1998. Huntingtin Acts in the Nucleus to Induce Apoptosis but Death does not Correlate with the Formation of Intranuclear Inclusions. *Cell*. 95:55-66.
- Schekman, R., and Orci, L. 1996. Coat Proteins and Vesicle Budding. *Science*. 271:1526-33.
- Seki, N., Muramatsu, M., Sugano, S., Suzuki, Y., Nakagawara, A., Ohhira, M., Hayashi, A., Hori, T., and Saito, T. 1998. Cloning, Expression Analysis, and Chromosomal Localization of HIP1R, an isolog of Huntingtin Interacting Protein (HIP1). *J. Hum. Gen.* 43:268-71.
- Seshagiri, S., Chang, W. T., and Miller, L. K. 1998. Mutational Analysis of *Caenorhabditis elegans* CED-4. *FEBS Lett* 22:71-4
- Sharrock, W.J. 1983. Yolk Proteins of *C. elegans*. *Dev. Biol.* 96:182-8.
- Singh, R.N., and Sulston, J. E. 1978. Some Observations on Molting in *C. elegans*. *Nemtologica*. 24:63-71.
- Singson, A., Hill K. L., and L'Hernault S. W. 1999. Sperm Competition in the Absence of Fertilization in *Caenorhabditis elegans*. *Genetics*. 152:201-8.
- Sisodia, S.S. 1998. Nuclear Inclusions in Glutamine Repeat Disorders: Are They Pernicious, Coincidental, or Beneficial? *Cell*. 95:1-4.
- Sternberg, P., and Han, M. 1998. Genetics of RAS Signaling in *C. elegans*. *Trends in Genetics*. 14:466-72.
- Stringham, E.G., Dixon, D. K., Jones, D., and Candido, E. P. M. 1992. Temporal and Spatial Expression Patterns of the Small Heat Shock (*hsp16*) Genes in Transgenic *Caenorhabditis elegans*. *Molecular Biology of the Cell*. 3:221-33.

- Strome, S. 1986. Fluorescence Visualization of the Distribution of Microfilaments in Gonads and Early Embryos of the Nematode *Caenorhabditis elegans*. *J. Cell Biol.* 103:2241-52.
- Sulston, J. E. Schierenberg, J. G., White, J. G., and Thomson, J.N. 1983. The Embryonic Cell Lineage of the Nematode *Caenorhabditis elegans*. *Dev. Biol.* 100:64-119.
- Sulston, J., Du, Z., Thomas, K., Wilson, R., Hillier, L., Staden, R., Halloran, N., Green, P., Thierry-Mieg, J., Qiu and et al. 1992. The *C. elegans* Genome Sequencing Project: A Beginning . *Nature.* 356:37-41.
- Sulston, J.E., and Horvitz, H. R. 1977. Post-embryonic Cell Lineages of the Nematode *Caenorhabditis elegans*. *Dev. Biol.* 56:110-56.
- Tavernarakis, N.W., S. L., Dorovkov, M., Ryazanov, A. and Driscoll, M. 2000. Heritable and Inducible Genetic Interference by Double-Stranded RNA Encoded by Transgenes. *Nature Genetics.* 24:180-3.
- Tebar, F., Sorkin, T., Sorkin, A., Ericsson, M., and Kirchhausen, T. 1996. Eps15 is a Component of Clathrin-coated Pits and Vesicles and is Located at the Rim of Coated Pits. *J. Biol. Chem.* 271:28727-30.
- Thompson, J.D., Higgins, D.G. and Gibson, T.J. 1994. CLUSTAL W: Improving the Sensitivity of Progressive Multiple Sequence Alignment through Sequence Weighting, Positions-specific Gap Penalties and Weight Matrix Choice. *Nuc. Ac. Res.* 22:4673-80.
- Timmons, L., Fire A. 1998. Specific Interference by Ingested dsRNA. *Nature.* 395:854.
- Trent, C., Tsung, N., and Horvitz, H. R. 1983. Egg-laying Defective Mutants of the Nematode *Caenorhabditis elegans*. *Genetics.* 104:619-47.

- Trifaro, J.-M., and Vitale, M. L. 1993. Cytoskeleton Dynamics During Neurotransmitter Release. *Trends Neurosci.* 16:466-72.
- Velier, J., Kim, M., Schwarz, C., Kim, T. W., Sapp, E., Chase, K., Aronin, N., and DiFiglia, M. 1998. Wild-Type and Mutant Huntingtins Function in Vesicle Trafficking in the Secretory and Endocytic Pathways. *Exp. Neurol.* 152:34-40.
- Wanker, E.E., Rovira, C., Scherzinger, E., Hasenbank, R., Wälter, S., Tait, D., Colicelli, J., and Lehrach, H. 1997. HIP1: A Huntingtin Interacting Protein Isolated by the Yeast Two-Hybrid System. *Hum. Mol. Genet.* 6:487-95.
- Ward, S., and Carrel J. S. 1979. Fertilization and Sperm Competition in the Nematode *C. elegans*. *Dev. Biol.* 73:304-21.
- Warrick, J.M., Paulson, H. L., Gray-Board, G. L., Bui, Q. T., Fischbeck, K. H., Pittman, R. N., and Bonini, N. M. 1998. Expanded Polyglutamine Protein Forms Nuclear Inclusions and Causes Neural Degeneration in *Drosophila*. *Cell.* 93:939-49.
- Warrick, J.M., Chan, H. Y. E., Gray-Board, G. L., Chai, Y., Paulson, H. L., and Bonini, N. M. 1999. Suppression of Polyglutamin-mediated Neurodegeneration in *Drosophila* by the Molecular Chaperone HSP70. *Nat. Genet.* 23:425-8.
- Weinstein, D.C., Ruiz, I., Altaba, A., Chen, W. S., Hoodless, P., Prezioso, V. R., Jessell, T. M., and Darnell, J. E. Jr. 1994. The Winged-helix Transcription Factor HNF-3 Beta is Required for Notochord Development in the Mouse Embryo. *Cell.* 78:575-88.
- Wendland, B., Emr, S. D., and Reizman, H. 1998. Protein Traffic in the Yeast Endocytic and Vacuolar Protein Sorting Pathways. *Curr. Opin. Cell Biol.* 10:513-22.

- White, J. G., Southgate, E., Thomson, J. N., and Brenner, S. 1986. The Structure of the Nervous System of the Nematode *C. elegans*. *Phil. Trans. R. Soc. Lond. B.* 314:1-340.
- Wilson, R., Ainscough, R., Anderson, K., Baynes, C., Berks, M., Bonfield, J., Burton, J., Connel, M., Copsey, T., Cooper, J. and et al. 1994. 2.2 Mb of Contiguous Nucleotide Sequence from Chromosome III of *C. elegans*. *Nature.* 368:32-8.
- Winzler, E.A., Shoemaker, D. D., Astromonoff, A., Liang, H., Anderson, K., Andre, B., Bangham, R., Benito, R., Boeke, J. D., Bussey, H. and et al. 1999. Functional Characterization of the *S. cerevisiae* Genome by Gene Deletion and Parallel Analysis. *Science.* 285:901-6.
- Wolf, N., Hirsh, D., and McIntosh, J. R. 1978. Spermatogenesis in Males of the Free-living Nematode, *Caenorhabditis elegans*. *J. Ultrastruct. Res.* 63:155-69.
- Wood, J.D., MacMillan, J. C., Harper, P. S., Lowenstein, P. R., and Jones, A. L. 1996. Partial Characterisation of Murine Huntingtin and Apparent Variations in the Subcellular Localisation of Huntingtin in Human, Mouse and Rat Brain. *Hum. Mol. Genet.* 5:481-7.
- Wood, W.B. 1988. The Nematode *Caenorhabditis elegans*. Cold Spring Harbor Laboratory Press, Cold Spring Harbor, NY.
- Yandell, M.D., Edgar, L. G., and Wood, W. B. 1994. Trimethylpsoralen Induces Small Deletion Mutations in *Caenorhabditis elegans*. *PNAS.* 91:1381-85.
- Yang, S., Cope, M. J. T. V., and Drubin, D. G. 1999. Sla2p Is Associated with the Yeast Cortical Actin Cytoskeleton via Redundant Localization Signals. *Mol. Biol. Cell.* 10:2265-83.

Zuk, D., Belk, J. P., and Jacobson, A. 1999. Temperature-Sensitive Mutations in the *Saccharomyces cerevisiae* *MRT4*, *GRC5*, *SLA2* and *THS1* Genes Result in Defects in mRNA Turnover. *Genetics*. 153:35-47.

Zwaal, R.R., Broeks, A., van Muers, J., Groenen, J. T. M., and Platerk, R. H. A. 1993. Target-selected Gene Inactivation in *Caenorhabditis elegans* by Using a Frozen Transposon Insertion Bank. *P.N.A.S.* 90:7431-35.